Characterizing assistive shared control through vision-based and human-aware designs for wheelchair mobility assistance

Vishnu Karakkat Narayanan

Thèse

UNIVERSITE BRETAGNE LOIRE

THESE INSA Rennes
sous le sceau de Université Bretagne Loire
pour obtenir le titre de
DOCTEUR DE L'INSA DE RENNES
Spécialité : Informatique

présentée par
Vishnu Karakkat Narayanan
ECOLE DOCTORALE : MATISSE
LABORATOIRE : IRISA/Inria Rennes - Bretagne Atlantique

Characterizing assistive shared control through vision-based and human-aware designs for wheelchair mobility assistance

Soutenance prévue à Rennes le 23.11.2016
devant le jury composé de :

François Charpillet
Directeur de Recherche, Inria Nancy Grand-Est / *rapporteur*
Philippe Martinet
Professeur, Ecole Centrale de Nantes / *rapporteur*
Ren C. Luo
Professeur, National Taiwan University / *examinateur*
Tom Carlson
Lecturer, University College London / *examinateur*
Éric Marchand
Professeur, Université de Rennes 1 / *examinateur*
Anne Spalanzani
Maître de Conférences, HDR, Université Grenoble Alpes/ Co-encadrante de thèse
Marie Babel
Maître de Conférences, HDR, INSA de Rennes/ Directrice de thèse

Characterizing assistive shared control through vision-based and human-aware designs for wheelchair mobility assistance

Vishnu Karakkat Narayanan

En partenariat avec

Our knowledge can only be finite, while our ignorance must necessarily be infinite.
- Karl Popper

Résumé

Les premiers documents attestant l'utilisation d'une chaise à roues utilisée pour transporter une personne avec un handicap datent du 6ème siècle en Chine. À l'exception des fauteuils roulants pliables X-frame inventés en 1933, 1400 ans d'évolution de la science humaine n'ont pas changé radicalement la conception initiale des fauteuils roulants. Pendant ce temps, les progrès de l'informatique et le développement de l'intelligence artificielle depuis le milieu des années 1980 ont conduit inévitablement à la conduite de recherches sur des fauteuils roulants intelligents. Plutôt que de se concentrer sur l'amélioration de la conception sous-jacente, l'objectif principal de faire un fauteuil roulant intelligent est de le rendre le plus accessible. Même si l'invention des fauteuils roulants motorisés ont partiellement atténué la dépendance d'un utilisateur à d'autres personnes pour la réalisation de leurs actes quotidiens, certains handicaps qui affectent les mouvements des membres, le moteur ou la coordination visuelle, rendent impossible l'utilisation d?un fauteuil roulant électrique classique. L'accessibilité peut donc être interprétée comme l'idée d'un fauteuil roulant adaptée à la pathologie de l'utilisateur de telle sorte que il / elle soit capable d'utiliser les outils d'assistance.

S'il est certain que les robots intelligents sont prêts à répondre à un nombre croissant de problèmes dans les industries de services et de santé, il est important de comprendre la façon dont les humains et les utilisateurs interagissent avec des robots afin d'atteindre des objectifs communs. En particulier dans le domaine des fauteuils roulants intelligents d'assistance, la préservation du sentiment d'autonomie de l'utilisateur est nécessaire, dans la mesure où la liberté individuelle est essentielle pour le bien-être physique et social. De façon globale, ce travail vise donc à caractériser l'idée d'une assistance par contrôle partagé, et se concentre tout particulièrement sur deux problématiques relatives au domaine de la robotique d'assistance appliquée au fauteuil roulant intelligent, à savoir une assistance basée sur la vision et la navigation en présence d'humains.

En ciblant les tâches fondamentales qu'un utilisateur de fauteuil roulant peut avoir à exécuter lors d'une navigation en intérieur, une solution d'assistance à bas coût, basée vision, est conçue pour la navigation dans un couloir. Le système fournit une assistance progressive pour les tâches de suivi de couloir et de passage de porte en toute sécurité. L'évaluation du système est réalisée à partir d'un fauteuil roulant électrique de série et robotisé. A partir de la solution plug and play imaginée, une formulation adaptative pour le contrôle partagé entre l'utilisateur et le robot est déduite. De plus, dans la mesure où les fauteuils roulants sont des dispositifs fonctionnels qui opèrent en présence d'humains, il est important de considérer la question des environnements peuplés d'humains pour répondre de façon complète à la problématique de la mobilité en fauteuil roulant. En s'appuyant sur les concepts issus de l'anthropologie, et notamment sur les conventions sociales spatiales, une modélisation de la navigation en fauteuil roulant en présence d'humains est donc proposée. De plus, une stratégie de navigation, qui peut être intégrée sur un robot social (comme un fauteuil roulant intelligent), permet d'aborder un groupe d'humains en interaction de façon équitable et de se joindre à eux de façon socialement acceptable.

Enfin, à partir des enseignements tirés des solutions proposées d'aide à la mobilité en fauteuil roulant, nous pouvons formaliser mathèmatiquement un contrôle adaptatif partagé pour la planification de mouvement relatif à l'assistance à la navigation. La validation de ce formalisme permet de proposer une structure générale pour les solutions de navigation assistée en fauteuil roulant et en présence d'humains.

Abstract

Earliest records of a wheeled chair used to transport a person with disability dates back to the 6th century in China. With the exception of the collapsible X-frame wheelchairs invented in 1933, 1400 years of human scientific evolution has not radically changed the initial wheelchair design. Meanwhile, advancements in computing, and the development of artificial intelligence since the mid 1980s, has inevitably led to research on *Intelligent Wheelchairs*.

Rather than focusing on improving the underlying design, the core objective of making a wheelchair intelligent is to make it more *accessible*. Even though the invention of the powered wheelchairs have partially mitigated a user's dependence on other people for their daily routines, some disabilities that affect limb movements, motor or visual coordination, make it impossible for a user to operate a common electrically powered wheelchair. Accessibility can also thus be thought of as the idea, where the wheelchair *adapts* to the user malady such that he/she is able to utilize its assistive capabilities to the fullest.

While it is certain that intelligent robots are poised to address a growing number of issues in the service and medical care industries, it is important to resolve how humans and users interact with robots in order to accomplish common objectives. Particularly in the assistive intelligent wheelchair domain, preserving a sense of autonomy with the user is required, as individual agency is essential for his/her physical and social well being. This work thus aims to globally characterize the idea of *assistive* shared control while particularly devoting the attention to two issues within the intelligent assistive wheelchair domain viz. vision-based assistance and human-aware navigation.

Recognizing the fundamental tasks that a wheelchair user may have to execute in indoor environments, we design low-cost vision-based assistance framework for corridor navigation. The framework provides progressive assistance for the tasks of safe corridor following and doorway passing. Evaluation of the framework is carried out on a robotised off-the-shelf wheelchair. From the proposed plug and play design, we infer an adaptive formulation for sharing control between user and robot. Furthermore, keeping in mind that wheelchairs are assistive devices that operate in human environments, it is important to consider the issue of human-awareness within wheelchair mobility. We leverage spatial social conventions from anthropology to surmise wheelchair navigation in human environments. Moreover, we propose a motion strategy that can be embedded on a social robot (such as an intelligent wheelchair) that allows it to equitably approach and join a group of humans in interaction.

Based on the lessons learnt from the proposed designs for wheelchair mobility assistance, we can finally mathematically formalize adaptive shared control for assistive motion planning. In closing, we demonstrate this formalism in order to design a general framework for assistive wheelchair navigation in human environments.

Contents

Préambule

Cette thèse est d'abord et avant tout une étude en robotique.

UNE ETUDE EN ROBOTIQUE commence nécessairement par les deux questions fondamentales suivantes: 'A quoi doivent ressembler les robots?' et 'Que font les robots?' [Ark98]. A la première question, la réponse peut être apportée par la description conjointe de l'apparence du robot (i.e. la structure physique et ses propriétés) et de son comportement (i.e. ses performances). La deuxième question induit naturellement une réponse qui englobe celle de la première question. Les robots qui manipulent les objets doivent être en mesure de saisir, les robots qui naviguent dans une pièce doivent avoir la capacité de percevoir l'environnement et de planifier des trajectoires, et les robots qui naviguent dans l'air et dans des conditions défavorables se doivent d'adopter des stratégies de mouvement qui facilitent les déplacements sur ces terrains, etc. Ainsi, les deux problématiques cruciales relatives à la conception des robots sont les suivantes : comprendre l'environnement dans lequel les robots opèrent et effectuer les tâches spécifiques requises.

Dans les années 1980, Rodney Brooks donna naissance à cette idée nouvelle qu'est la robotique comportementale et ouvrit par là même un vaste champ de recherches relatives à la robotique et en particulier celui de l'Interaction Homme-Robot [Bro86]. Avec l'apparition des calculateurs à fortes capacités de calcul, avec l'émergence et le large déploiement de capteurs intelligents, des robots de toutes formes et de toutes tailles ont vu le jour et ont inévitablement envahi les espaces peuplés d'humains [FND03]. De nombreuses raisons ont conduit à ce phénomène, notamment l'accroissement du niveau de productivité, l'accomplissement de tâches difficiles et/ou dangereuses pour l'opérateur humain, ou encore de façon générale la réalisation plus sûre des opérations.

Pour ce faire, il est évidemment nécessaire de mettre en place des solutions de contrôle et des stratégies de prise de décision qui permettent une collaboration sûre et sans faille entre les humains et les robots. La collaboration Humain-Robot se transforme ainsi en un domaine de recherche passionnant où l'objectif central est de permettre le travail d'équipe en toute sécurité, de proposer une interaction continue et efficace entre les humains et les robots afin d'accomplir des tâches qu'ils ne peuvent (ou sont dans l'incapacité de) faire seul [FTB03].

La coopération Homme-Robot est arrivée à maturité : un co-équipier humain aux côtés d'un bras robotisé sur une chaîne d'assemblage (à gauche), et un utilisateur de fauteuil roulant électrique *robotisé* (à droite).

Ce travail aborde la problématique de l'assistance au moyen de stratégies de contrôle partagé, mettant en oeuvre une collaboration homme-robot en général, et appliquée plus particulièrement à la navigation assistée de fauteuil roulant robotisé via des solutions basées capteur. L'idée centrale relative à l'assistance par contrôle partagé est, entre autres, que le robot (ou l'utilisateur) s'adapte aux forces/faiblesses de l'utilisateur (ou le robot), de sorte qu'une collaboration peut permettre d'effectuer une tâche de la manière la plus optimale [Fon01].

En appliquant ces principes d'assistance basée capteur à la navigation des fauteuils roulant électriques, l'objectif est de concevoir une plate-forme de fauteuil roulant intelligent capable d'assister *de façon optimale*[1] un utilisateur en situation de handicap dans des situations dangereuses. Il s'agit de proposer une assistance basée sur l'intention de l'utilisateur afin, dans un premier temps d'éviter un danger et ensuite de réduire la fatigue et le stress. Dans le cadre de l'Inria (Institut national de recherche en informatique et en automatique), l'action dénommée IPL PAL Inria Project Lab (*Personnal Assisted Living*) a notamment pour objectif l'étude des techniques à base de capteurs pour la navigation d'assistance en fauteuil roulant. Ainsi, cette application constituant le fil rouge de notre étude, nous proposons dans ce travail les contributions suivantes relatives à l'assistance par contrôle partagé.

[1] Nous détaillerons mathématiquement et préciserons ces termes dans les chapitres suivants.

Sujets abordés dans cette thèse

Pour un utilisateur souffrant de déficiences motrices, conduire un fauteuil roulant peut s'avérer une tâche difficile. Des à-coups, provoqués par des mouvements incontrôlés du joystick, sont susceptibles de produire une collision lors d'une navigation dans des couloirs. Ainsi, dans un premier temps, nous proposons dans ce document un système d'assistance basé vision, par caméra bas coût monoculaire, en vue d'une navigation sûre dans les couloirs. Pour ce faire, un asservissement de la vitesse du fauteuil, basé vision et localement asymptotiquement stable est proposé. La solution permet à un fauteuil roulant électrique de série et *robotisé* de suivre de façon autonome des couloirs et de franchir des portes. L'approche proposée s'appuie sur une extraction simple et naturelle de caractéristiques visuelles et permet de réaliser les tâches fondamentales de navigation en intérieur, à savoir le suivi de couloir, le franchissement de portes et le changement de direction en bout de couloir.

En gardant à l'esprit que la mobilité individuelle est une partie intégrante du bien-être mental, cognitif et social d'une personne en situation de handicap, il est préférable de développer des solutions de navigation semi-autonomes pour lesquelles l'utilisateur conserve le contrôle principal du mouvement du fauteuil roulant. Ainsi, nous avons conçu un système d'assistance à la navigation dans un couloir en fusionnant la commande utilisateur provenant du joystick avec le contrôle précédent lié à la navigation autonome du fauteuil et qui, à son tour, facilite un système d'assistance activé progressivement à l'approche d'un obstacle, en fonction du risque de collision perÃ§ue. Afin d'améliorer le confort de navigation, un retour de force, guidant la commande utilisateur et utilisant le schéma d'assistance précédent, est également proposé. Néanmoins, le déploiement dans le monde réel de solutions d'assistance en faveur de la mobilité en fauteuil roulant nécessite de prendre en compte le fait que les environnements naturels de navigation sont peuplés d'humains. Il est donc essentiel de développer des approches qui intègrent les contraintes sociales[2] en vue d'accroître la sécurité et l'acceptabilité de solutions robotique, ainsi que pour réduire les perturbations induites. En tirant parti de la théorie bien connue de la proxémie et des distances sociales, une loi de contrôle de vitesse, indépendante du capteur utilisé, est proposée. Appliquée à un robot social (comme un fauteuil roulant robotisé), la solution robotique permet d'aborder de façon équitable des groupes en interaction et de les rejoindre.

Finalement, au vu des résultats des études précédentes, nous proposons un système semi-autonome de navigation en milieu humain adapté au cas d'un fauteuil roulant. Le système s'appuie sur une formulation généralisée conjointe de la notion de l'estimation de l'intention utilisateur et du contrôle partagé dans le cadre de la navigation assistée en fauteuil roulant. Enfin, les enseignements tirés des analyses précédentes permettent de définir un cadre mathématique nouveau dédié à l'assistance et au contrôle partagé.

[2]Nous faisons référence ici aux contraintes relatives à la gestion des espaces physiques, et non des problématiques liées aux gestes.

Organisation de la thèse

Les contributions originales de ce travail de thèse sont structurées en trois parties. La partie I détaille l'application relative au domaine de l'assistance à la navigation dans un couloir d'un fauteuil roulant, sur la base de la vision monoculaire. Dans la deuxième partie (II), les concepts déduits de la théorie bien connue de la proxémie sont mis à profit pour proposer des systèmes de navigation en environnement peuplé d'humains pour des robots sociaux tels que des fauteuils roulants robotiques. En particulier, la question d'approcher et de se joindre à un groupe en interaction est étudiée. Enfin en partie III, une vue d'ensemble de la navigation en fauteuil roulant semi-autonome est proposée : outre une présentation de tous les résultats obtenus, de nouvelles perspectives dans le domaine de l'assistance et du contrôle partagé sont abordées.

Avant de plonger dans le cœeur de cette thèse, dans le chapitre 1 sont donnés les concepts mathématiques et robotiques fondamentaux utilisés dans ce travail.

Organisation de la Partie I - Assistance basée vision pour la navigation de fauteuil roulant

Chapitre 2 : Nous commençons par exposer le contexte relatif aux fauteuils roulants intelligents et la motivation pour investiguer des solution d'assistance basée vision pour les tâches fondamentales de mobilité en fauteuil roulant en intérieur.

Chapitre 3 : Dans ce chapitre, nous présentons les contrôleurs autonomes basés vision qui permettent à un fauteuil roulant équipé de caméras monoculaires de suivre un couloir et de passer à travers une porte ouverte / à tourner dans un couloir [**J.2**,**W.1**].

Chapitre 4 : Nous utilisons les loi de commande basées vision développées dans le chapitre précédent pour concevoir des systèmes d'assistance souples pour les tâaches respectives (i.e. suivi de couloir et passage de porte) par une fusion progressive du contrÃ´le avec la commande utilisateur par téléopération. Un nouveau formalisme pour le contrôle partagé est alors présenté. Ce formalisme facilite également l'intégration d'un retour haptique pour rendre intuitive la navigation [**J.1**].

Organisation de la Partie II - Compréhension des environnements humains pour la navigation des fauteuils roulants

Chapitre 5 : Nous passons ensuite à la problématique des fauteuils roulants intelligents (robots sociaux) opérant dans des environnements humains. Les idées issues de la sociologie sont utilisées pour appréhender les concepts de la répartition sociale et spatiale des humains en public, qui sont à leur tour utilisés pour introduire une méthode de planification en présence d'humains. Un état de l'art de la littérature dans le domaine de la navigation en présence d'humains est également présenté.

Chapitre 6 : Tout en adoptant les mêmes stratégies de conception, telles que présentées dans la partie III, nous proposons une commande robotique adaptative basée caractéristiques en vue d'aborder de façon équitable et rejoindre les humains en interaction [**C.2**,**C.3**, **P.1**].

Organisation de la partie III - Vers une assistance par contrôle partagé

Chapitre 7 : Nous abordons alors la problématique des méthodes générales de navigation semi-autonome pour l'assistance à la conduite de fauteuil roulant. Une représentation d'objectifs à court terme dans un paradigme probabiliste, et une formulation générale pour le contrôle partagé servent de première étape dans l'idée de l'assistance à la conduite de fauteuil roulant. Cette solution est testée et analysée dans le cadre d'un scénario de navigation en présence d'humains [**C.1**].

Chapitre 8 : Des fauteuils roulants aux robots d'assistance en général, nous proposons un formalisme mathématique dédié au contrôle partagé pour l'assistance. Il s'agit alors d'analyser en quoi une telle solution serait en mesure de résoudre les problèmes actuels et futurs en termes d'interaction homme-robot pour un contrôle partagé / collaboratif.

Preamble

Robotics is a technology that doesn't inherently have any good or bad effects to it. You could use a hammer to hit a nail, or you can use a hammer to hurt somebody.

S. Shyam Sundar

This thesis is first and foremost a study in Robotics.

A STUDY IN ROBOTICS begins with the following two fundamental questions. 'What should the robots be like?' and 'What should the robots do?' [Ark98]. The first question can be answered by describing the robot's appearance (i.e. physical structure and properties) and its behaviour (i.e. performance). The second question thus naturally frames an answer for the first question. Robots that manipulates objects should be able to grasp, robots that navigate in a room should have the capability of sensing the environment and planning trajectories, and robots that navigate outdoors in adverse conditions should have motion strategies that facilitates natural movement on such terrains, etc. Thus the two critical issues in designing robots are the following: understanding the environment within which it operates and performing the required specific tasks.

In the 1980s, Rodney Brooks gave birth to this very idea of Behaviour-based Robotics thus spanning a multitude of research avenues within robotics, especially, Human-Robot Interaction [Bro86]. With the explosion of computing technology since the late 1990s and the emergence of widely available electronic sensing media, robots of all forms and sizes are inevitably being deployed within human environments [FND03]. A variety of reasons, including higher productivity, safer operation, and easier accomplishment of difficult/dangerous tasks, being the driver of this phenomenon.

This evidently calls for control and decision making strategies that allows safe and seamless collaboration between humans and robots. Human-Robot collaboration is thus transforming into an exciting area of research where the central objective is to allow safe, seamless and effective teamwork between humans and robots in order to accomplish tasks that neither can (or may be able to) do alone [FTB03].

Human robot collaboration comes of age. A human worker alongside an autonomous robotic manipulator in an assembly line (left), and a user with a *robotized* powered wheelchair (right).

This work aims to then tackle the issue of *assistive shared control* within human-robot collaboration in general, applied to sensor assisted navigation using a robotic wheelchair, in particular. We can define the central idea of assistive shared control, among other objectives, that the robot (or the user) adapts to strengths/weaknesses of the user (or the robot) so that a collaborative task can be performed in the most optimal manner [Fon01].

Introducing the application of sensor-based assistive wheelchair navigation, the objective is to design an intelligent wheelchair platform that *optimally* [3] assists a user with disability in dangerous situations. We aim to provide assistance based on his/her intention, firstly, in order to evade danger and secondly, in order to reduce fatigue and stress. Within the context of the Inria (Institut national de recherche en informatique et en automatique) Project Labs *PAL (Personally Assisted Living)*, one of the many goals is to investigate sensor-based techniques for assistive navigation in wheelchairs. Thus keeping this application as the backbone, we propose the following contributions in this work towards assistive shared control.

[3] We will mathematically define and precise such terms in the following Chapters

Topics covered in the thesis

In case of a user suffering from motor impairments, steering a wheelchair can become a hazardous task. Joystick jerks induced by uncontrolled motions may lead to wall collisions when a user steers a wheelchair along corridors. Thus to begin with, we introduce a low-cost monocular vision-based assistance system for wheelchair navigation within corridors. Consequently we start by presenting locally asymptotically stable vision-based velocity controllers that allows an off-the-shelf *robotized* electrically powered wheelchair to autonomously follow corridors and pass through doorways. The proposed approach, that uses easily extractable and natural image features, allows us to perform two fundamental tasks in indoor navigation i.e. following a corridor and pass through doorways/turn about corridors.

Keeping in mind that individual mobility is an integral part of the mental and social well-being of a disabled person, it is essential to develop semi-autonomous controllers wherein the user has primary control over the wheelchair motion. We then design an assistance scheme for corridor navigation by fusing user teleoperation coming from the joystick with the proposed autonomous controllers which in turn facilitates a system, that *smoothly and progressively* assists the user if he in danger of perceived collision. An application to integrate a guiding force feedback is also proposed alongside the assistance scheme.

Nevertheless, a key issue that hinders the deployment of such solutions for wheelchair mobility in the real world is that they need to operate in human environments. Thus it is essential to develop ideas that incorporate *social*[4] constraints in order to increase safety and acceptability as well as to reduce disturbance. Leveraging a well established proxemic theory, we design a feature-based, sensor-agnostic velocity controller for a social robot (such as a robotized wheelchair) to equitably approach and join groups in interaction.

Evidently, marrying the results from the previous studies we then propose a *semi-autonomous* framework for human-aware navigation in a wheelchair. The framework introduces generalised formulations for user intention estimation and control sharing within the context of assistive wheelchair navigation. Finally we conclude with formalising a new mathematical framework for assistive shared control based on the lessons learned from previous analyses.

Outline of the thesis

This original contributions of the thesis are structured into three parts. Part I details the application in the area of monocular vision-based assistance for corridor navigation in a wheelchair. Then in Part II, concepts inferred a well established proxemic theory are leveraged to propose human-aware navigation schemes for social robots such as robotic wheelchairs. In particular the issue of approaching and joining a human interaction is addressed. Finally with Part III, the big picture is presented on semi-autonomous wheelchair navigation marrying all the results obtained along with new insights in the area of assistive shared control.

[4]Here we refer to constraints that concern only with physical space management and not gestural issues.

Before delving into the core of the thesis, in **Chapter 1** we present preliminaries for the fundamental mathematical and robotics concepts used in this work.

Organization of Part I - Vision-based assistance for wheelchair navigation

Chapter 2 : We start by providing a background on intelligent wheelchairs and the motivation to investigate vision-based assistance for fundamental indoor wheelchair mobility tasks.

Chapter 3 : Then, in this chapter we present vision-based autonomous controllers that allow a wheelchair equipped with monocular cameras in order to follow a corridor and pass through an open doorway/corridor turns [**J.2**,**W.1**].

Chapter 4 : We use the vision-based controllers developed in the previous chapter to design smooth assistance schemes for the respective tasks (i.e. corridor following and doorway passing) by progressively fusing it to user teleoperation. A new formalism is inferred for sharing control that also facilitates the integration haptic feedback for intuitive guidance [**J.1**].

Organization of Part II - Human awareness in wheelchair navigation

Chapter 5 : We then move onto the issue of (social robots) intelligent wheelchairs operating in human environments. Ideas from sociology is utilized to learn the concepts of human spatial social management in public which is in turn used to introduce a human-aware motion planner. A literature review in the area of human-aware navigation is also presented.

Chapter 6 : Keeping in line with the same design strategies as presented in Part I, we propose an adaptive feature-based controller for a robot to equitably approach and join human interactions [**C.2**,**C.3**, **P.1**].

Organization of Part III - Towards assistive shared control

Chapter 7 : We move towards a general human-aware semi-autonomous framework for wheelchair navigation assistance. A representation of short-term goals within a probabilistic paradigm, and a general formulation for sharing control serves as the first step in the idea of assistive shared control for wheelchair navigation. This framework is analysed within a human-aware navigation scenario [**C.1**].

Chapter 8 : Moving from wheelchairs to assistive robots in general, we propose a mathematical formalism for assistive shared control and analyse how such a design would be able to tackle present and future problems in human-robot shared/collaborative control.

Thesis Related Publications

Journal Articles

J.1 **Vishnu K. Narayanan**, François Pasteau, Maud Marchal, Alexandre Krupa and Marie Babel. 'Vision-based adaptive assistance and haptic guidance for safe wheelchair corridor following' *Computer Vision and Image Understanding (CVIU)*, 149, pp. 171-185, 2016.

J.2 François Pasteau, **Vishnu K. Narayanan**, Marie Babel and François Chaumette. 'A visual servoing approach for autonomous corridor following and doorway passing in a wheelchair' *Robotics and Autonomous Systems (RAS)*, 75, pp. 28-40, 2016.

Refereed Conference Papers

C.1 **Vishnu K. Narayanan**, Anne Spalanzani and Marie Babel. 'A semi-autonomous framework for human-aware and user intention driven wheelchair mobility assistance', *IEEE International Conference on Intelligent Robots and Systems (IROS)*, 2016.

C.2 **Vishnu K. Narayanan**, Anne Spalanzani, Ren C. Luo and Marie Babel. 'Analysis of an adaptive strategy for equitably approaching and joining human interactions' *IEEE International Symposium on Robot and Human Interactive Communication (RO-MAN)*, 2016 (conditionally accepted).

C.3 **Vishnu K. Narayanan**, Anne Spalanzani, François Pasteau and Marie Babel. 'On equitably approaching and joining a group of interacting humans' *IEEE International Conference on Intelligent Robots and Systems (IROS)*, 2015.

Refereed Workshop Papers

W.1 **Vishnu K. Narayanan**, François Pasteau, Marie Babel and François Chaumette. 'Lyapunov-based visual servoing for autonomous doorway passing in a wheelchair' *IEEE International Conference on Intelligent Robots and Systems (IROS W), Workshop on Assistance and Service Robotics in a Human Environment*, 2014.

Pre-Prints

P.1 **Vishnu K. Narayanan**, Anne Spalanzani, Ren C. Luo and Marie Babel. 'An adaptive motion strategy for equitably approaching and joining groups in interaction', Journal article in preparation.

Chapter 1

Preliminaries

IN THIS CHAPTER, we provide an overview of the fundamental concepts used in the thesis with the aim to provide a context for the formulations described in the later chapters. Owing to the fact that the work presented in the thesis considers, from a control theoretic point of view, a robotic wheelchair as a *non-holonomic unicycle type* robot, we start the chapter with a basics on control for unicycle type robots in Section 1.1. We then move onto a primer on Visual Servoing in Section 1.2 as it forms the backbone for the vision-based controllers to be discussed in Part I. Finally, as the final part of the work uses Bayesian probability theory and some machine learning concepts, we also illustrate some of its ideas in Section 1.3. The contents presented here are well established and researched ideas, but put together, they form a contextual prologue to the technical approaches proposed in this thesis.

1.1 Control of a Unicycle-type Robot [SSVO08]

Geometrically, a robot is a set of rigid bodies, called *links*, connected by *joints* that are possibly actuated by motors. A single sequence of $n-1$ links coupled with n joints connects the *base* (assumed to be fixed) to the *end-effector* of the robot where a tool, specific to the desired task (for example, a wheel, a gripper, a camera) is attached.

The *configuration* (i.e. the *pose* comprising of both the position and the orientation) of such a system can be characterized by an n-dimensional vector $\boldsymbol{q} = [q_1, q_2, ...q_n]^T$ of *generalized co-ordinates*. Here $\boldsymbol{q} \in \mathcal{Q}$, where $\mathcal{Q}$ is an n-dimensional smooth manifold locally diffeomorphic to the n-dimensional Euclidean space $\mathbb{R}^n$. In such a case, the *generalized velocity* at a point $\boldsymbol{q}(t) \subset \mathcal{Q}$ is the tangent vector $\dot{\boldsymbol{q}} = [\dot{q_1}, \dot{q_2}, ...\dot{q_n}]^T$.

Such a mechanical system may also be subject to a set of kinematic constraints, for example a first-order kinematic constraint represented by $\mathbf{A_K}(\boldsymbol{q}, \dot{\boldsymbol{q}}) = 0$ with $i = 1, 2, ...m$. In many cases the constraints are *Pfaffian* where it is of the form $\mathbf{A_K}^T(\boldsymbol{q})\dot{\boldsymbol{q}} = 0$. A set of Pfaffian constraints is called holonomic if it is integrable (a geometric limitation), otherwise, it is called nonholonomic (a kinematic limitation).

To make an intuitive explanation, Figure 1.1 shows a rolling disk which is a canonical example of non-holonomy. Here the generalized co-ordinates of the system can be expressed as $\boldsymbol{q} = [x, y, \theta]^T$ as shown. We can observe the *pure rolling* non-holonomic constraint $\mathbf{A_K}^T(\boldsymbol{q})\dot{\boldsymbol{q}} = 0$ where $\mathbf{A_K} = [\sin\theta, -\cos\theta, 0]$ and $\dot{\boldsymbol{q}} = [\dot{x}, \dot{y}, \dot{\theta}]^T$. Owing to the non-holonomic constraint, any desired point $[x_d, y_d, \theta_d]^T$ can be reached by:

- Rotating the disk to aim at (x_d, y_d),
- Rolling the disk to (x_d, y_d),
- Rotating the disk until the orientation has reached θ_d.

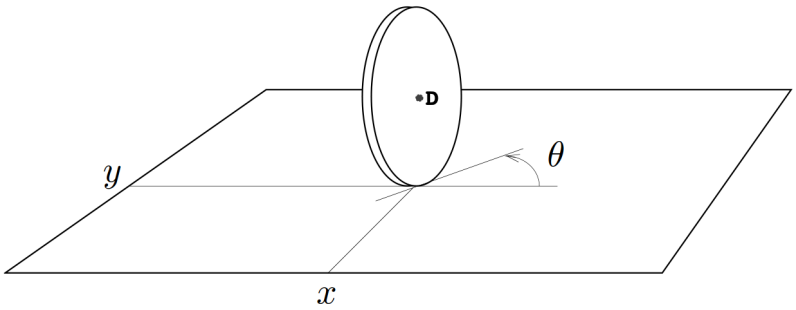

Figure 1.1: A unicycle (or a rolling disk): The quintessential non-holonomic system. We can clearly see that the unicycle cannot move sideways thus restricting the amount of independent motions the system can produce in order to reach a desired configuration.

The above analysis intuitively demonstrates that there are two *controls*, i.e. the *driving velocity* and the *steering velocity* respectively, for the 3 Degrees of Freedom (DOF) system. If the disk is *controllable* then it is called a unicycle. A variety of wheeled mobile robots are characterized as unicycles from a motion control point of view.

In order to characterize the two controls, we can define a matrix $G(\boldsymbol{q})$ whose columns span the null space of the constraint matrix $\mathbf{A_K}$ as follows:

$$G(\boldsymbol{q}) = \begin{bmatrix} \cos\theta & 0 \\ \sin\theta & 0 \\ 0 & 1 \end{bmatrix} = [g_1, g_2]. \tag{1.1}$$

Hence if $\boldsymbol{v} = [v_1, v_2]$ is a set of arbitrary real numbers, the kinematic model of the unicycle is given by

$$\dot{\boldsymbol{q}} = G(\boldsymbol{q})\boldsymbol{v} = g_1(\boldsymbol{q})v_1 + g_2(\boldsymbol{q})v_2, \tag{1.2}$$

with v_1 and v_2 being the two *controls* i.e. the *driving velocity* and the *steering velocity* respectively of the system.

Generally the end-effector linear and angular velocities say $\boldsymbol{v_e} \in \mathbb{R}^6$ can be expressed using the *robot geometric Jacobian* $\boldsymbol{J_r}(\boldsymbol{q})$ as,

$$\boldsymbol{v_e} = \boldsymbol{J_r}(\boldsymbol{q})\dot{\boldsymbol{q}}. \tag{1.3}$$

The robot geometric Jacobian $\boldsymbol{J_r}(\boldsymbol{q}) \in \mathbb{R}^{6\times n}$ is expressed in the end-effector frame, and can be computed directly using the robot kinematic model as explained in [SSVO08]. In a right handed Cartesian co-ordinate system we can then express the velocity of the unicycle end-effector (the mid point D of the disk in Figure 1.1) as

$$\boldsymbol{v_e} = [v_1, 0, 0, 0, 0, v_2]^T. \tag{1.4}$$

For all purposes we re-denote the expression as

$$\boldsymbol{v_e} = [v, 0, 0, 0, 0, \omega]^T \tag{1.5}$$

with v representing the *translational* (driving) velocity and ω representing the *angular* (steering) velocity. Similarly there are generalised kinematic (and dynamic) models for other non-holonomic systems such as a car-like robot, trailer systems, etc., we restrict the definitions here to a unicycle robot as we kinematically model the wheelchair as a unicycle.

In a real world wheeled mobile robot, the wheels are actuated by motors that apply forces/-torques on the joint links. The resulting motion produced (i.e. the velocities) is due to the robot dynamics that depend on, in addition to the kinematic parameters, a variety of dynamic parameters such as (but not limited to) mass, inertia tensor and elasticity of the robot/wheels. These dynamic parameters can be obtained using Lagrange or Newton methods as explained in [SSVO08]. Further, dynamic control techniques [CPST02] can be used to compute the motor commands (i.e. force or torque) to control the system.

But in present real world systems the presence of stable lower level feedback control loops capable of executing a desired kinematic command (such as a velocity), allows us to consider the said kinematic command as the system input. A satisfactory performance can be obtained in such a case if the kinematic command is physically admissible and does not exceed the robot motor capabilities. The control architecture of a unicycle-type robot can then be thought of as a velocity-level controller for the purpose of this thesis, as we can effectively ignore the problem of addressing the robot dynamics. Moreover, commercial robots (as well as powered wheelchairs) typically have closed architectures for lower-level control loops that do not allow a user direct control over the forces and torques applied to the motors.

1.2 Visual Servoing [CH06]

In practice, to implement a form of *intelligent control* onto a system such as wheeled mobile robots or manipulators, we need to firstly recover the current configuration of the system in relation to the control task to be performed. This is done by using sensors like joint encoders, laser scanners, sonars, cameras etc.

The concept of using computer vision data extracted from cameras in order to control robot motion (in a closed loop) is termed as *visual servoing* or *visual servo control* [CH06]. Classically, visual servoing is distinguished by its two main approaches:

- Position Based Visual Servoing (PBVS) : In PBVS, visual information is used to infer a set of 3-D parameters (such as the pose) of the *camera* (or the robot end-effector) with respect to a reference frame. Once such a localization problem is solved, the resulting control problem falls to a classical geometrical control of the robot end-effector.
- Image Based Visual Servoing (IBVS) : Whereas, in IBVS, visual information is *directly* used to control the robot motion. The robot pose is never reconstructed and the desired (or goal) configuration is specified in terms of the value the visual information assumes at the desired configuration.

Furthermore, the cameras may be mounted on the robot end-effector (*eye in hand* configuration) or they may be fixed on an external base (*eye to hand* configuration) or a mixture of both configurations may also be utilized (as in many humanoid applications).

In this thesis, as will be explained in Part I, we employ cameras on-board the wheelchair to detect and extract relevant visual features around which control schemes are designed. Therefore we provide a fundamental overview of Image Based Visual Servoing.

Image Based Visual Servoing (IBVS)

Keeping in line with the objective of a visual servoing task as proposed by [CH06], the aim is to minimize an error $\boldsymbol{e}(t)$ where

$$\boldsymbol{e}(t) = \boldsymbol{s}(\boldsymbol{m}(t), \boldsymbol{a}) - \boldsymbol{s}^*. \tag{1.6}$$

Here $\boldsymbol{m}(t)$ are the set of image measurements (for example, image coordinates of interest points, image coordinates of the centroid of an object etc.) which are used to compute a set of k features $\boldsymbol{s}(\boldsymbol{m}(t), \boldsymbol{a})$ where $\boldsymbol{a}$ is an parameter set that provides additional knowledge of the system (for example, 3D model of a perceived object). The vector $\boldsymbol{s}^*$ contains the desired value of the feature set.

In the case of IBVS, the feature set $\boldsymbol{s}$ consists of features that are directly available in the image data. Once $\boldsymbol{s}$ is selected, a simple approach would be to design a velocity controller in order to minimize the error $\boldsymbol{e}$ observed between $\boldsymbol{s}$ and $\boldsymbol{s}^*$. If the camera velocity is denoted by $\boldsymbol{v}_c = (v_c, \omega_c)$ (i.e. the instantaneous linear and angular velocities of the camera frame), then we have the following relation:

$$\dot{\boldsymbol{s}} = \boldsymbol{L}_{\boldsymbol{s}}(\boldsymbol{s}, \boldsymbol{\chi})\boldsymbol{v}_{\boldsymbol{c}}. \tag{1.7}$$

Here $\boldsymbol{L}_s \in \mathbb{R}^{k\times 6}$ is the *Interaction matrix* that encodes the variation of the features with respect to the camera velocity screw. $\boldsymbol{\chi}$ is a set of unmeasurable 3-D parameters associated with the feature set $\boldsymbol{s}$. Using Eqns. (1.6) and (1.7) we have

$$\dot{\boldsymbol{e}} = \boldsymbol{L}_{\boldsymbol{e}}(\boldsymbol{s}, \boldsymbol{\chi})\boldsymbol{v}_{\boldsymbol{c}} \tag{1.8}$$

where $\boldsymbol{L}_{\boldsymbol{e}}(\boldsymbol{s}, \boldsymbol{\chi}) = \boldsymbol{L}_{\boldsymbol{s}}(\boldsymbol{s}, \boldsymbol{\chi})$. Furthermore, relating the camera velocity screw with the robot configuration $\boldsymbol{q}$ using the general Eqn. (1.3), we have

$$\boldsymbol{v}_{\boldsymbol{c}} = {}^{\boldsymbol{c}}\boldsymbol{T}_{\boldsymbol{r}}\boldsymbol{J}_{\boldsymbol{r}}(\boldsymbol{q})\dot{\boldsymbol{q}} \tag{1.9}$$

where ${}^{\boldsymbol{c}}\boldsymbol{T}_{\boldsymbol{r}}$ is the *twist matrix* that transforms the end-effector velocities to the camera frame. The matrix ${}^{\boldsymbol{c}}\boldsymbol{T}_{\boldsymbol{r}}$ contains the constant roto-translation from the end-effector frame to the camera frame. We can thus introduce the *camera geometric Jacobian* as

$$\boldsymbol{J}_{\boldsymbol{c}}(\boldsymbol{q}) = {}^{\boldsymbol{c}}\boldsymbol{T}_{\boldsymbol{r}}\boldsymbol{J}_{\boldsymbol{r}}(\boldsymbol{q}) \tag{1.10}$$

and conclude with the *visual task Jacobian*

$$\boldsymbol{J}_{\boldsymbol{s}}(\boldsymbol{s}, \boldsymbol{\chi}, \boldsymbol{q}) = \boldsymbol{L}_{\boldsymbol{s}}(\boldsymbol{s}, \boldsymbol{\chi})\boldsymbol{J}_{\boldsymbol{c}}(\boldsymbol{q}). \tag{1.11}$$

Plugging Eqn. (1.11) in (1.8), we obtain

$$\dot{\boldsymbol{e}} = \boldsymbol{J}_{\boldsymbol{s}}(\boldsymbol{s}, \boldsymbol{\chi}, \boldsymbol{q})\dot{\boldsymbol{q}}. \tag{1.12}$$

Identifying $\dot{\boldsymbol{q}}$ as the generalized robot velocity, we would like to ensure an exponential decoupled decrease of the error as $\dot{\boldsymbol{e}} = -\lambda\boldsymbol{e}$. Thus we can finally write a velocity controller as

$$\dot{\boldsymbol{q}} = -\lambda\boldsymbol{J}_{\boldsymbol{s}}^{+}(\boldsymbol{s}, \boldsymbol{\chi}, \boldsymbol{q})\boldsymbol{e}, \tag{1.13}$$

where $\boldsymbol{J}_{\boldsymbol{s}}^{+} \in \mathbb{R}^{n\times k}$ is the Moore-Penrose Pseudo Inverse of $\boldsymbol{J}_{\boldsymbol{s}}$. All the theoretical bases of the operator are given in [CH06]. The method outlined here is for general cases and a variety of caveats may exist in order to obtain a perfect exponential decrease of the error. For a thorough understanding of the subject we refer the readers to [CH06].

1.3 Bayesian Statistics and Machine Learning [Bar12]

Classically robot control was considered from a deterministic standpoint. Probabilistic techniques for robotics, especially for motion planning were introduced in the late nineties [TBF05]. But with the surge in machine learning research in the past decade, it is invariably being implemented for improving a variety of robot control tasks. The ability of man-made systems to learn from experience and, based on that experience, to improve their performance is the focus of machine learning. We define *Adaptive Control* as the concept of designing control laws that must adapt to a system with parameters which vary, or are initially uncertain. Then we aim to achieve a specific case of adaptive control where the parameters are *learned* online.

Without going to the specific details of implementing learning for robot control, we present a background for one of the tools used to build intelligent learning systems i.e. Bayesian statistics. Since the early 2000s, Bayesian machine learning has been widely used in robot control.

For the sake of clarity, we can here define machine learning as learning models of data. Bayesian inference is then an approach to statistics and machine learning in which all forms of uncertainty are expressed in terms of probability. Bayes' rule states that

$$P(M|D) = \frac{P(D|M)P(M)}{P(D)}. \tag{1.14}$$

We can read this in the following way: "the probability ($P(M|D)$) of the model M given the data D is the probability of the data given the model ($P(D|M)$) times the prior probability of the model ($P(M)$) divided by the probability of the data ($P(D)$)". Thus the Bayesian framework for machine learning states that you start out by enumerating all reasonable models of the data and assigning your prior belief $P(M)$ to each of these models. Then, upon observing the data D, you evaluate how probable the data was under each of these models to compute $P(D|M)$. Then you multiply this likelihood by the prior and renormalizing results with the posterior probability over models $P(M|D)$ which encapsulates everything that you have learned from the data regarding the possible models under consideration. Thus, to compare two models M and M', we need to compute their relative probability given the data following $\frac{P(M)P(D|M)}{P(M')P(D|M')}$.

Moreover, in Eqn. (1.14), the denominator is usually a normalizing constant. This gives

$$P(M|D) \propto P(D|M)P(M) \tag{1.15}$$

and we can schematically write this as

$$Posterior \propto Likelihood * Prior. \tag{1.16}$$

We can also make predictions by integrating with respect to the $Posterior$. If D^* is some new data,

$$P(D^*|D) = \int P(D^*|M = m)P(M = m|D)dm. \tag{1.17}$$

Now we can see a simple example of *Bayesian machine learning*. Suppose we measure some data D such that $D = \{x_i, y_i\}$, $\forall i \in \mathbb{R}$, where x_i is in an input space and $y_i = f(x_i) + \eta_i$ is the output

where f is a *possibly non-linear* deterministic function and $\eta_i \sim \mathcal{N}(0, \sigma^2)$ is a zero mean Gaussian noise on the output y_i. The aim of Bayesian learning would be to find a model M_{MAP} within a set of models $\boldsymbol{M}$ that maximises the posterior (*maximum a posteriori*) probability given the data D i.e., the model that *fits* the data or approximates the function f.

Consequently we can write,

$$M_{MAP} = \arg\max_{M \in \boldsymbol{M}} P(M|D). \tag{1.18}$$

From Eqn. (1.15) we get,

$$M_{MAP} = \arg\max_{M \in \boldsymbol{M}} P(D|M)P(M), \tag{1.19}$$

which can be simplified when we assume a uniform prior on the models as

$$M_{MAP} = \arg\max_{M \in \boldsymbol{M}} P(D|M). \tag{1.20}$$

Thus M_{MAP} is also the model that maximises the likelihood given the data. Now based on the assumptions made before, we can rewrite Eqn. 1.20 as

$$M_{MAP} = \arg\max_{M \in \boldsymbol{M}} \prod_i P(y_i|M). \tag{1.21}$$

This probability is completely dependent on the noise model which is Gaussian. Therefore,

$$M_{MAP} = \arg\max_{M \in \boldsymbol{M}} \prod_i \frac{1}{\sqrt{2\pi\sigma^2}} \exp\left(\frac{-1}{2}\frac{(y_i - M(x_i))^2}{\sigma^2}\right). \tag{1.22}$$

If we take the natural logarithm (which is monotonic), the $\arg\max$ remain unchanged. But the above equation reduces to

$$M_{MAP} = \arg\max_{M \in \boldsymbol{M}} -\sum_i (y_i - M(x_i))^2 \tag{1.23}$$

which is nothing but

$$M_{MAP} = \arg\min_{M \in \boldsymbol{M}} \sum_i (y_i - M(x_i))^2. \tag{1.24}$$

Thus the model that maximises the likelihood given the data is the model which minimizes the sum of the squared errors.

This is a beautiful result given the assumptions we made are true. However in most real world cases it is not always the case. But since the aim of this section is to provide an introduction to Bayesian inference and to illustrate how one can effectively use Bayesian methods in machine learning, we stop with this simple example that effectively does the same.

1.4 Remark

In this chapter, we came across some basic mathematical ideas related to robotics and machine learning that form the backbone for the technical approach to be encountered in this thesis. Now we commence with Part I which is on adapting vision-based assistance to two fundamental tasks in indoor wheelchair navigation viz. following a corridor and passing through a doorway.

Part I

Vision-based assistance for wheelchair navigation

Chapter 2

Background and Objectives

INDEPENDENT MOBILITY is an important component of a person's physical and social well being. While mobility increases social opportunity and reduces dependence on others, numerous studies have equivalently shown that a decrease in mobility can lead to social disorders like depression, anxiety and a fear of abandonment [FvD03, IMDS01].

Wheelchairs are versatile assistive devices that are able to address virtually all physically disabling pathologies, and consequently aid millions of people in achieving mobility [Bra12]. But motor disabilities like Parkinson's disease or visual impairments may prevent users from steering a wheelchair effectively and independently, particularly in constrained environments like narrow corridors [KBCG+12]. For example, depending on the handicap, steering a wheelchair along a corridor can become a difficult task, especially when corridors are narrow enough to induce an uncomfortable sensation in navigation [KBCG+12, KFH+12]. In the case of severe physical or motor disability, where spasticity or athetosis is induced, it is almost impossible for a user to effectively navigate without the help of another person.

Another major reported problem by wheelchair users in the United States was *non-accessibility*, even when more than four fifths of the user population identified themselves as living in a house with all the rooms on the same level [HSK00]. In addition, the issue of security becomes an important one, where for example, a person with neuromuscular disabilities finds it difficult to steer a wheelchair, particularly in limited space environments, without the risk of collision [MGBK09]. Finally, not to mention that difficulties may also appear during long-term driving.

Thus it is essential to design *intelligent systems* that provides *optimal mobility assistance* for mobility while preserving the independent autonomy of the user. Following this goal, we can say that recent advances in robotics have facilitated the enhancement of a simple *electrically powered* wheelchair into a *smart or intelligent* wheelchair [Yan98a]. The underlying idea of an *intelligent* wheelchair is to assist a user in fundamental navigation tasks like corridor following, doorway passing and to perform local obstacle avoidance. As will be discussed later in this chapter, different projects like the TAO Project [Tak98], the NavChair [LBJ+99], European FP7 Radhar project [DEVPHDS12] and the recent SYSIASS project [KFH+12] were indeed able to design systems that take partial/full control from the user for safe and effective navigation assistance.

Keeping in line these advances, we here aim to conceptualize an *intelligent wheelchair* using low cost sensors (like monocular cameras) and robust control architectures. But the big caveat being that the wheelchair should *preserve* the mobility of the user. Therefore this chapter begins with an overview of previous intelligent wheelchair research, and ends with our motivations and objectives in the pursuit of vision-based architectures for navigation assistance. Finally we summarize our approach as a prelude to Chapter 3 wherein we start with the technical details.

2.1 Prior Work on Intelligent Wheelchairs

In 1995, Miller and Slack [MS95] proposed two initial designs for a sensor-based robotic wheelchair for assisted indoor navigation. Their prototypes could perform local obstacle avoidance and also navigate to pre-designated places on a known local map with the help of sonar range finders. The control mechanism was *semi-autonomous* as in the user had control over the selection of tasks to be performed (i.e. selecting which place in a pre-built map to navigate toward). Consequently, in the late 1990s, the NavChair from the University of Michigan [LBJ+99], the Wheelesley Robot from the Massachusetts Institute of Technology [Yan98b] and the TAO Project [Tak98] proposed very similar designs for semi-autonomous wheelchairs (see Figure 2.1) where the user had high-level control over the wheelchair navigation goal and the low-level motion planning was performed with the help of sensors (generally sonar range finders) [Sim04]. We can see from Figure 2.1 that such *robots* were either built from the ground up or realised as a chair rigidly fixed on a mobile robot base.

With the exponential rise of computational and sensing power in the last 20 years, a plethora of real world implementations started emerging within the field of intelligent wheelchairs. This was further driven by the advancement in robotic technology in terms of real world practical applicability. A majority of these works focused on the issue of increasing the safety levels of the wheelchair (and thereby decreasing the amount of human intervention). In such implementations, inspired by the initial designs, the human controlled the higher level intelligence whereas the wheelchair was responsible for the lower level tasks such as planning a safe path toward a goal. For example one can mention the European FP7 Radhar project [DEVPHDS12], the SYSIASS project [KFH+12] and the COALAS project [LWG+13], all of which were designed to provide assistance in tasks like navigating through indoor environments like corridors, basic obstacle detection/avoidance and also, in some cases [DEVPHDS12, KFH+12], autonomous passage through narrow doorways.

We observe that such behaviour-based design approaches have been proven to lead to robust systems that could be commercially implemented [LBJ+99, DEVPHDS12, B. 14, BPMR08]. However, it has to be noted that the majority of the previous works in this area used a multi-sensor system with a distributed architecture that impacts the form factor of the wheelchair (see the MIT Intelligent Wheelchair Project in Figure 2.1 (right)). While the systems mentioned above consider expensive sensors and known maps of the operating environment, there lies an open avenue of research where the solution could rely on low-cost architectures [Sim04]. Secondly,

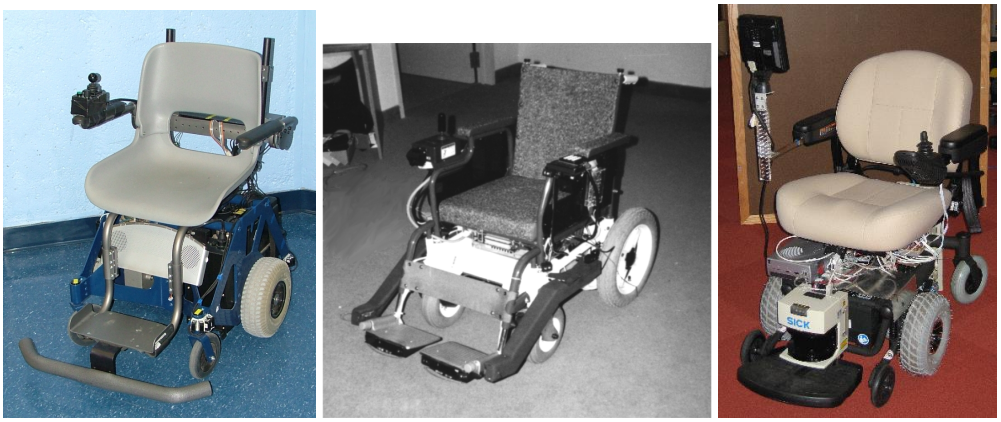

Figure 2.1: Evolution of Robotic Wheelchairs. The Wheelesley from MIT, 1996 (left), The TAO project wheelchair, 1998 (middle), and the MIT Intelligent Wheelchair Project, 2010 (right). Early intelligent wheelchair designs were robots built from the ground up or adapted by rigidly attaching a chair on a mobile robot base.

the general direction taken in intelligent wheelchair design is to propose a complete system built from the ground up. While some recent works introduce adaptable designs for increasing the *assistive* capabilities in an off-the-shelf electric wheelchair [Tak98, LBJ+99, DEVPHDS12, B. 14, BPMR08], the systems are tested and validated on specially built wheelchairs or mobile robots with the exception of a few projects which adapt existing powered wheelchairs with the requisite software or hardware [KFH+12, GNL+08, Cd13]. Therefore there also exists a hole in the research domain for plug and play assistance systems that can be adapted to commercial off-the-shelf wheelchairs.

Moving onto the issue of the *amount of control* given to the user, most intelligent wheelchair designs give the high-level control (e.g. goal selection, path selection or task selection) to the user, and the low-level control (e.g. motion control commands, obstacle avoidance) to the robot [KFH+12, Tak98, LBJ+99, DEVPHDS12, SPB02, B. 14, BPMR08]. Recently, a variety of solutions have been proposed that use non-invasive Brain-Computer Interfaces (BCI) for assessing the user intent and then augment the user intent using external sensors for safe navigation [GNL+08, Cd13, PdV+07]. Using BCIs may provide an accurate estimate of user intention (in terms of a direction towards which the wheelchair should navigate to), but the major drawback lies in the fact that the user must concentrate very hard to convey his intent. This may be a difficult task, especially for users with motor/cognitive disabilities or fatigued users. On the other hand, using voice [SL97] and/or gaze [ESL14] as user tele-operation have limited scope in terms of modularity and acceptability as well.

Therefore straightforward and modular solution would be to fuse manual control from a joystick with robot control in order to create a co-operative/collaborative system with the wheelchair user continuously monitoring with the joystick (or any adapted interface). Unless the user is severely disabled, this form of teleoperation has been reported as the most convenient and safe [Sim04, Cd13]. This simple concept was initially demonstrated by Simpson

et.al. [SPB02] where the manual control from the joystick was augmented with an autonomous controller capable of obstacle avoidance. This concept has been emplyed as a standard in the intelligent wheelchair community.

Generally for sharing control, the final wheelchair velocity was calculated using a linear blending of the form $(1-\alpha)\mathbf{v}_{op} + \alpha\mathbf{v}_r$ with $\mathbf{v}_{op}$ and $\mathbf{v}_r$ representing the user teleoperation and the corrective velocity respectively (eg. velocity coming from a motion planner). Here α henceforth termed the assistance factor represents the *amount* of control the autonomous controller has at a particular instant as it translates to an allocation weight for each contributing velocity. For example, in a work by Argall et.al. [Arg16], such a linear control blending formalism was implemented in order to fuse user and robot control for assisted doorway traversal in a wheelchair. But validation of the system was done using a mobile robot, with a user teleoperating the robot with a gaming joystick. This formalism has been researched thoroughly in the field and in majority of the studies, the assistance factor is set as a scalar (i.e all the Degrees of Freedom (DOFs) of the wheelchair respond to the same assistance factor) and is determined according to the specific needs of the control system (i.e. it is contextual) [GDA13, CD12, DEVPHDS12, Arg16]. As will be seen in the later chapters, tweaking the *assistance factor* (among other criteria) will form an important constituent for adaptive semi-autonomous teleoperation.

2.2 Exploring vision-based assistance

Evidently, in the first part of the thesis, we propose a first step in the design of *low-cost* intelligent wheelchair systems that has the user in the continuous control loop. Such semi-autonomous wheelchair systems would be helpful in conditions where physical, motor or visual impairments of the user may hinder secure and effective navigation. Alongside, we tackle an important constraint in the form of retro fitting an off-the-shelf wheelchair with the proposed control strategies.

As such, we explore two important tasks related to indoor navigation: keeping a safe and stable position while navigating corridors, and detecting and passing through doorways. We will see that this second task can also be used directly for turning between corridors. These tasks represent the fundamental capability of a wheelchair performing indoor navigation.

The motivation of our work comes partly from the fact that low cost sensors such as cameras or RGB-D sensors could be employed in designing such systems. This can ensure widespread implementation, accounting for the fact that reimbursement from government/healthcare companies typically only covers the wheelchair, and not its technological adaptations. But relevant control systems have to be designed around a vision-based paradigm which still remains a highly challenging task.

Thus in order to design vision-based *assistive control schemes*, initially we develop solutions for autonomous navigation in a wheelchair mounted with a set of monocular cameras with each camera being devoted to a particular *task*. For example, we use a front facing camera to realise the task of autonomous corridor following. The *visual tasks* can then be smoothly blended with manual control/user intention so that the user maintains a higher level control over the

wheelchair motion. Such fully vision-based setup along with a map-less design could facilitate easier commercialization, higher adaptability and widespread usage. Moreover we aim to validate the modular system on an off-the-shelf electric wheelchair. Therefore our goal is to design a robust vision-based control system that could be used in order to augment user teleoperation to derive a *semi-autonomous* solution for corridor navigation with a wheelchair.

Since the issue of retrofitting off-the-shelf wheelchairs is important, an important constraint arises when considering that the wheelchair must be able to perform in an indoor environment without any a-priori knowledge of the environment. Consequently, a solution where the semantic environmental data are not known is expected. Therefore we explore an Image-based Visual Servoing (IBVS) scheme which controls the relevant degrees of freedom (dof) of the wheelchair based on visual features directly extracted from a camera on board the wheelchair [CH06].

While specifically considering vision-based corridor following using a wheeled mobile robot, Winters et.al. [WGLSV00] provided a solution using an omni-directional camera along with a visual memory framework. Here the robot saves *keyframes* from an initial (non-autonomous) run in the environment and then replicates the motion by minimizing some *error* with respect to the selected keyframes. Furthermore, in Carelli's work [CSNF02] two vision-based control algorithms for corridor navigation were presented that exploited the geometry of a typical corridor. The first one used the optical flow measured from the corridor's lateral walls to generate an angular velocity command for the mobile robot. The second scheme found the perspective lines of the walls meeting the floor to generate the angular velocity command for the robot. Therefore, employing the geometry of a corridor in an image is a viable solution while designing vision-based algorithms around it to realise the task of corridor following. Such a vision-based system was also proposed by Faragasso et.al. [FOPV13a] that used the geometry of the corridor for humanoid corridor navigation with capability of turning at junctions.

The initial objective in any visual servoing scheme is to select features that represent visual data which in turn can be effectively exploited to perform the task at hand. With respect to the task of autonomously following a corridor, features like the vanishing point and the straight lines that represent the edges of the corridors are relevant [HAMMCne08, FOPV13a]. There are several studies which indicate the robustness of the aforementioned features (for example [TSR+ne09]). Consequently to design a stable control law that robustly achieves the objective of maintaining a stable wheelchair position in the corridor, we propose a system that employs the measure of the vanishing point and the position of the vanishing line that corresponds to the median line of the corridor (Chapter 3).

With respect to the navigation task of passing through doorways, several results have also been reported in this area for mobile/wheeled robots. A multi-sensor based algorithm for guiding a non-holonomic platform through a doorway was presented by Patel et.al.[PJO+02]. The controller used information from a camera along with a laser range finder. In the case of the previously mentioned SYSIASS project [KFH+12], a laser range finder with a PID controller was employed for doorway passing with a mobile robot. Another solution for secure navigation of a mobile robot in particular for doorway passing was proposed by Chung et.al.[CKC+09].

The framework exploited a laser-based hybrid control scheme with dynamic obstacle avoidance and path planning. We aim to realise the task of doorway passing within a purely vision-based framework. The only other fully vision-based solution for doorway passing in mobile robot was proposed by Salaris et.al. [SVSL15] *following* one of our contributions in this area where they proposed a geometrical approach that reasons among a set of paths.

When visually representing the task of passing through doorways, the features available are mostly line features that represent the position of the doorposts in the image. This is a highly challenging task while employing a monocular vision sensor especially in the case where a single doorpost is visible. Thus, we have developed a novel and robust control scheme which only uses the position of the line feature corresponding to the nearest doorpost in the image to achieve the goal. This approach is utilized since global asymptotic stability of the system can be demonstrated as will be shown in Chapter 3. Moreover, higher level constraints like the status of the door (open/closed), the decision making process of passing through the door (i.e. which door to choose from), etc, make the task non-trivial. We here focus on low level control without the help of a global planning framework. The high level attributes are left for the user to decide as the objective is to finally converge to a semi-autonomous assistive solution.

Thus our final goal is to introduce a vision-based assistance system such that the user maintains a higher level control over the wheelchair motion i.e. an adaptive assistive system in order to prevent wall collisions when a user *manually* steers a wheelchair in a corridor. As seen in the earlier section, the straightforward (and most efficient) solution would be to linearly blend manual control from a joystick with robot control where the user continuously monitors with the joystick. But we here assert that, in order to maximize the acceptability of the solution, the assistance has to be *progressively* activated only when necessary and to be deactivated as soon as the user wants to act by himself [KBCG+12].

In conjunction with automatic trajectory correction, a guiding joystick force may be necessary in the case where users suffer from visual and/or cognitive impairments and are not able to clearly observe their unsafe trajectory. It can also be seen as a communication channel between the user and the wheelchair controller for a better user experience where such an active feedback can lead to minimal interference from the automatic trajectory correction system [VDR+12]. This concept of haptic feedback for wheelchair navigation assistance has been previously explored mainly as a mechanism for obstacle avoidance where the feedback was calculated from the classical potential field method [Luo99, KKBT01, FSB04, BS07]. Recently in the context of the European FP7 Radhar project, force feedback was provided through a 2D joystick in order to achieve a bilateral guidance channel where the haptic controller relays the *intention* of the system so that the user is able to overrule actions if needed [VDR+12]. Therefore it is efficient to provide a force feedback which is *in conjunction or in proportion* with the automatic trajectory correction so that there is an intuitive form of communication with the user.

The proposed work therefore presents an image-based control schemes to integrate two autonomous visual navigation tasks with continuous user teleoperation from a joystick. The fusion aims to provide progressive assistance whenever the user is in danger of collision with

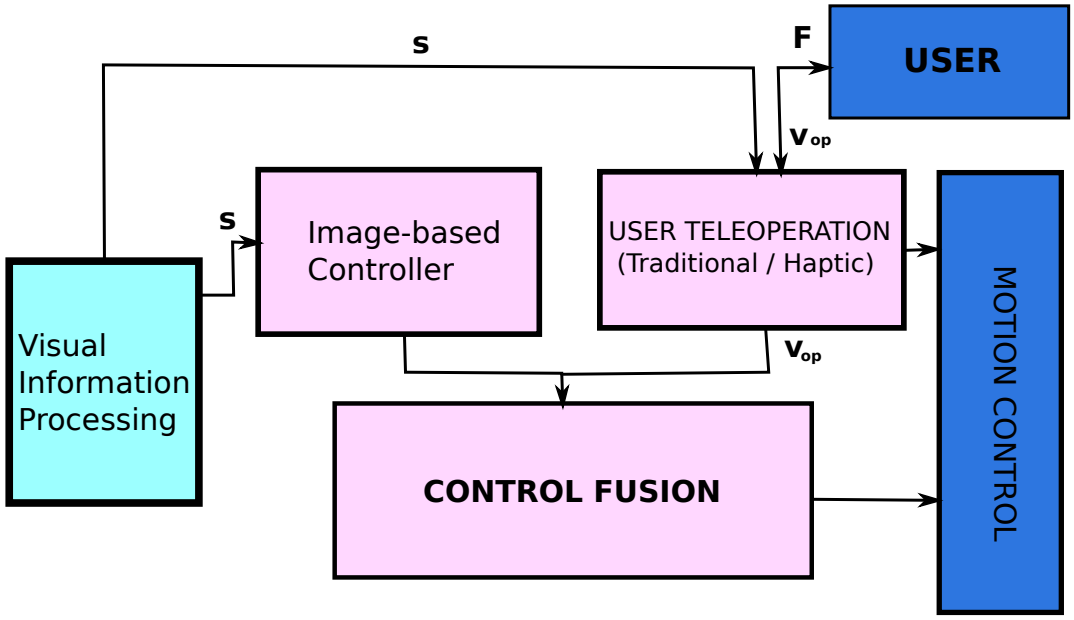

Figure 2.2: The visual feature set $\mathbf{s}$ derived from a scene is used to drive a visual controller that generates a velocity output $\mathbf{v}$. The robot output is then blended with user teleoperation from a traditional or haptic interface $\mathbf{v}_{op}$ in order to obtain a collaborative shared control system. We also illustrate a possible force feedback loop within the schematic.

walls or doorposts. In addition, we also present a formalism to integrate, a guiding force, which is also explicitly modelled from visual information, and which is applied on the joystick in order to notify the user of his/her unsafe trajectory. We then analyse the system embedded on an off-the-shelf wheelchair equipped with a monocular cameras. An schematic of the overall approach is presented in Figure 2.2.

To sum up, we initially design visual tasks using Image-Based Visual Servoing that allows a wheelchair autonomously follow corridors, pass through doorways and turn about corridors [CH06, PBS13, PKNBC15]. The visual tasks employ natural image features including the vanishing point, vanishing lines that correspond to the wall/floor boundaries, and line features that represents doorposts, as inputs. We then integrate an assistance solution, that fuses the visual tasks with user tele-operation output [PKB14]. The fusion formulation is defined in such a way that the task is progressively activated, when the wheelchair gets closer to the walls, in order to steer the wheelchair away from it. This also means that if there is no threat of collision, the user will have full control over the wheelchair motion. Finally, we design an optimal joystick force feedback in conjunction with the trajectory correction process that helps the user to understand

the dangerousness of the situation and which intuitively guides him over to a safe trajectory.

We will see in the following chapter that the proposed visual servoing schemes do not require any initialization step owing to the fact that a dedicated line detection framework was designed to detect and track the relevant line features in real time. Thus, bottleneck stage that still remains in most of the servoing schemes is avoided. In addition, as mentioned before, no a-priori environment data is required or utilized in the servoing process which further reduces the complexity of the system and in turn facilitates easier implementation.

Consequently, in Chapter 3 we present the design of the autonomous visual controllers and in Chapter 4 we finally propose the vision-based assistance and guidance system derived from the said visual controllers that assists a wheelchair user in the fundamental indoor navigation tasks of corridor following and doorway passing.

Chapter 3

Visual servoing for corridor navigation

THIS CHAPTER details the locally asymptotically optimal velocity controllers based on visual servoing, that facilitates an off-the-shelf robotized wheelchair equipped with monocular camera to autonomously navigate within corridors, i.e. perform the tasks of corridor following and doorway passing. User teleoperation can then be blended with the proposed velocity controllers in order to evolve a fully vision-based assistance solution.

The contents of this chapter has been published the scientific journal Robotics and Autonomous Systems (RAS)[**J.2**]. A part of this chapter was also presented at the workshop for Assistance and Service Robotics in a Human Enviroment at the IEEE/RSJ International Conference on Robots and Systems (IROS) in 2014[**W.1**].

3.1 Modelling

We model the wheelchair as a six wheeled robot moving on a horizontal/inclined plane as can be observed from the designs of a majority of electrically powered off-the-shelf wheelchairs. Two differentially actuated wheels located in the middle of the wheelchair provide motion along with four passive caster wheels with two each located in the front and back. The wheelchair can then be though of as a simple unicycle robot [PKay11], thus matching non-holonomic constraints. Owing to the actuated wheels, two variables can be controlled as mentioned in Chapter 2, namely the translational velocity v and the rotational velocity ω. In this Chapter, since the aim is to design a autonomous controllers that serve as the backbone of the semi-autonomous scheme, the control variable is restricted to the rotational velocity ω while a constant forward velocity v^* is maintained for motion exigency.

Three cameras located at different positions on the wheelchair are employed in order to realise the two different tasks. A front facing camera denoted as *camera 1* which is located on the left handle at a height h_1 from the floor is employed for the task of corridor following. The second and third cameras denoted as *camera 2* and *camera 3* are respectively located on the right and left handle at heights h_2 and h_3 from the floor. These cameras are used for realising the task of doorway passing: the right one to pass doors located on the right wall and the left one for doors on the left wall. These cameras are oriented in order to ensure that the doorpost stays in the camera field of view during the servoing process. For compactness, in this Chapter, we refrain the study to the camera located on the right side of the wheelchair as the solution for the left camera would be symmetric and straightforward.

Now, according to Figure 3.1, the robot frame is defined as $\mathcal{F}_r(P_O, x_r, y_r, z_r)$. The origin of the frame $\mathcal{F}_r$ is chosen as the mid-point of the line segment joining the two centres of the differential wheels. $\forall i = 1, 2, 3$, the camera frames can be defined namely as, $\mathcal{F}_{c_i}(C_i, x_{c_i}, y_{c_i}, z_{c_i})$ where C_i denotes the optical center of each camera. We finally denote the orientation of cameras i with respect to frame $\mathcal{F}_r$ as θ_i.

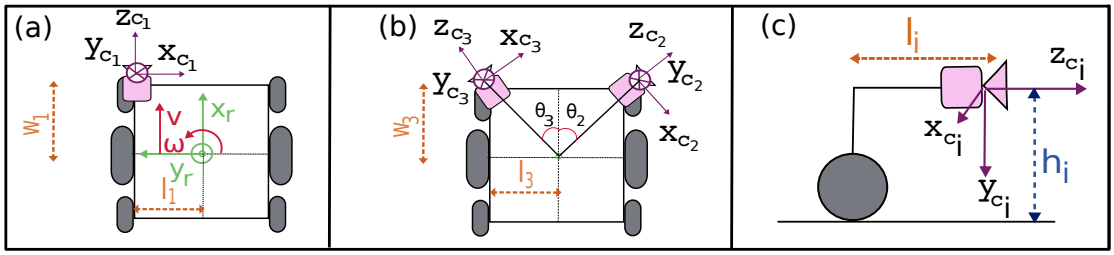

Figure 3.1: Robot and camera frame definitions (a) Top view with relative position of robot and *camera 1* frame. (b) Top view with *camera 2* and *camera 3* frames. (c) Simplified side view of the camera frames.

Consequently, the rotation matrices relative to the robot frame $\mathcal{F}_r$ and the camera frames $\mathcal{F}_{c_i}$ are given by

$$ {}^{c_i}\boldsymbol{R}_r = \begin{bmatrix} \sin\theta_i & -\cos\theta_i & 0 \\ 0 & 0 & -1 \\ \cos\theta_i & \sin\theta_i & 0 \end{bmatrix}. \tag{3.1} $$

Let ${}^f\boldsymbol{v} = (\boldsymbol{v}, \boldsymbol{\omega}) = \left({}^f v_x, {}^f v_y, {}^f v_z, {}^f \omega_x, {}^f \omega_y, {}^f \omega_z\right)$ be the velocity of a frame $\mathcal{F}_f$ expressed in $\mathcal{F}_f$, where the first three components $\boldsymbol{v}$ represent the translational velocities and the last three components $\boldsymbol{\omega}$ the rotational velocities. We have thus the velocity expressed in $\mathcal{F}_r$ as

$$ {}^r\boldsymbol{v} = (v, 0, 0, 0, 0, \omega)\,. \tag{3.2} $$

The translation ${}^r\boldsymbol{t}_{c_i}$ between the robot frame and camera frames is given by ${}^r\boldsymbol{t}_{c_i} = (l_i, w_i, 0)$. Note that for *camera 1* on the left, we have $\theta_1 = 0$, $l_1 > 0$ and $w_1 > 0$ while for *camera 2* on the right, $\theta_2 < 0$, $l_2 > 0$ and $w_2 < 0$.

By applying the well known formula

$$ {}^{c_i}\boldsymbol{v} = \begin{bmatrix} {}^{c_i}\boldsymbol{R}_r & [{}^{c_i}\boldsymbol{t}_r]_\times \, {}^{c_i}\boldsymbol{R}_r \\ 0 & {}^{c_i}\boldsymbol{R}_r \end{bmatrix} . {}^r\boldsymbol{v} \tag{3.3} $$

we obtain using (3.1)

$$ {}^{c_i}\boldsymbol{v} = ({}^{c_i}v_x, 0, {}^{c_i}v_z, 0, {}^{c_i}\omega_y, 0) \tag{3.4} $$

where

$$ \begin{cases} {}^{c_i}v_x = v\sin\theta_i - \omega(l_i\cos\theta_i + w_i\sin\theta_i) \\ {}^{c_i}v_z = v\cos\theta_i + \omega(l_i\sin\theta_i - w_i\cos\theta_i) \\ {}^{c_i}\omega_y = -\omega \end{cases} \tag{3.5} $$

3.2 Autonomous Corridor Following

As stated in Chapter 2, the task of autonomously following a corridor is modelled as an IBVS problem. The objective is to devise a control law which minimises the error between a set of observed visual features and the set of their desired values. A discriminative representation of the relevant image features in a corridor scene (as can be observed using a front facing monocular camera) is given in Figure 3.2. Here we can ascertain some of the visual features that could be exploited for realising the task. Importantly, the desired feature set should facilitate the performance the task of following a corridor without collision with the walls. More precisely the system should aim position the optical axis of camera parallel to the wall and at the middle of the corridor. To design such a system, we can select two visual features.

3.2.1 Visual Features - Definition and Extraction

We select the x-coordinate x_f of the vanishing point $f_t = (x_f, y_f)$ at an instant t (shown in Figure 3.3) as the first feature. When the robot is positioned parallel to the wall, looking forward, this

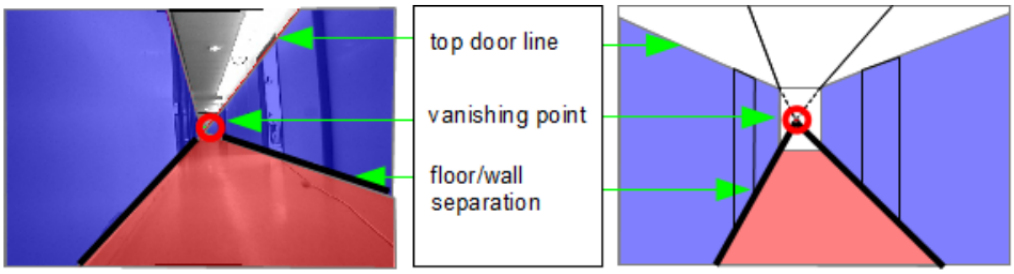

Figure 3.2: Corridor geometrical structure with floor and wall planes

feature reduces to zero. As the second feature, we select the angle θ_m made by the z-axis of the camera with the median line of the corridor (see Figure 3.3). When the position of the camera is in the middle of the corridor, this feature is also equal to zero.

Since the median line is not visible in the image, this feature can be computed from the orientations θ_l and θ_r of the straight lines in the image related to the intersection of the walls and the floor of the corridor. The median of the corridor is projected onto the image as a straight line parametrized by (ρ_m, θ_m) where

$$\rho_m = x_f \cos\theta_m + y_f \sin\theta_m. \tag{3.6}$$

Geometrically, in the 3D world, the lines related to the wall and the median of the corridor are parallel and coplanar. As a consequence, the corresponding lines in the image intersect at the vanishing point while respecting

$$\theta_m = \arctan\left(\frac{\tan\theta_l + \tan\theta_r}{2}\right). \tag{3.7}$$

Also, the lateral distance between the camera and the median of the corridor is given by $y = h_1 \tan(\theta_m)$, where h_1 is the distance between the front facing *camera 1* optical centre and the floor (see Figure 1). Therefore, we get $y = 0$ when $\theta_m = 0$.

Estimation of x_f

Estimating the vanishing point robustly and in real time is still an open area of research in computer vision. In the case of a robot equipped with a monocular camera navigating through a corridor, the vanishing point corresponds to the point where a significant number of straight lines, in the corresponding image acquired by the camera, may intersect. We use the classical Gaussian sphere projection framework [Rot00, BBP06] to estimate the vanishing point. The idea is to project onto this sphere the set of detected non-vertical lines in the image. Then the vanishing point is chosen as the point which has accumulated the maximum number of votes.

For extracting the straight lines in the image, a Line Segment Detection (LSD) algorithm is used [R. 12]. It is based on local gradient orientations in the image, from which major segments

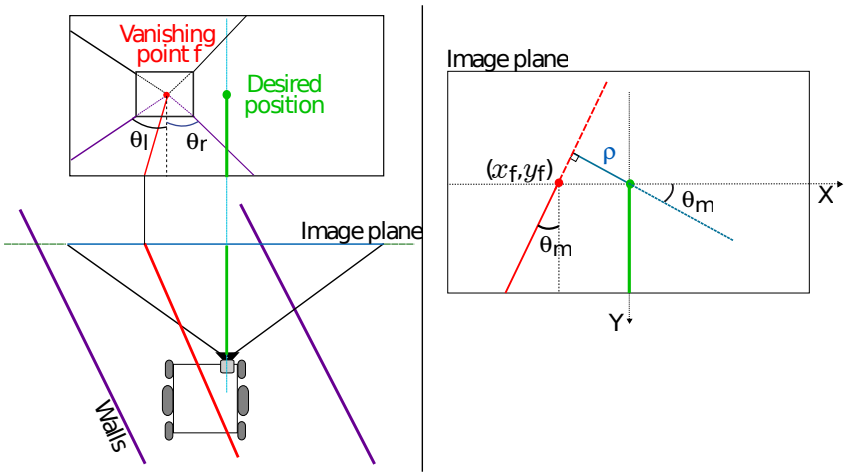

Figure 3.3: x_f and θ_m visual features

are detected. The detected segments are then classified into vertical lines and non-vertical lines. The latter is used for estimating the vanishing point.

However, the main issue of the LSD algorithm is the cutting off of one line when the direction of the observed gradient changes. Thus, to increase the robustness, a dedicated merging process is applied to a group of segments that can be considered as a single straight line. For two segments, this process is done by taking into account the slope and extremities, and if they are close enough, they are merged to form a unique line. More details are given in [SPB+13].

Since the vanishing point f_t is estimated at each frame during a sequence, we introduce a factor $\alpha_f \in]0, 1[$ for temporal filtering as

$$f_t = \alpha_f f_{t-1} + (1 - \alpha_f) f_t \tag{3.8}$$

in order to ensure a smooth variation of the resulting estimated vanishing point in the current frame. The value of α_f is empirically tuned and chosen as $\alpha_f = 0.1$. It can be postulated that since the temporal variation of the vanishing point is not very high as a wheelchair with a front facing camera moves forward in a corridor, the filtering process will be robust to variations in the factor α_f.

Estimation of θ_m

The angles θ_l and θ_r can be easily calculated if we have an accurate estimate of the wall/floor boundaries. A variety of techniques have been proposed in the area of wall/floor boundary detection. For example, wall/floor features are defined by the corners corresponding to the intersection of a vertical line and the floor plane in [OTD12]. Whereas in [DLN06], floor boundary is estimated by a dynamical Bayesian network model which is applied on each column of the image.

In our proposed scheme, a set of non-vertical lines are searched for along the image that correspond to the wall/floor boundary. The search is conducted based on two criteria: the first one being that they contribute to the vanishing point and, the second one being that they cross the bottom extremities of most number of vertical lines. In order to minimize false positives, a maximal distance between the vertical line extremity and the vanishing line is defined.

Then, from the angles θ_l and θ_r, the value of θ_m can be directly obtained using Equation (3.7).

3.2.2 Robustness of Feature Extraction

Since the autonomous control scheme to be detailed in the following Section is driven by the visual features x_f and θ_m, the estimation of the features should be fairly robust with respect to different conditions occurring in a indoor corridor driving scene. We present a small driving sequence in Figure 3.4 with a variety of disturbances occurring in the scene. On each camera frame output the vanishing point is represented by the red cross (the intersection of all the lines in the image) and the median line of the corridor is represented by the red line. The wall/floor boundaries are shown in purple. It can be observed in all the examples that the estimation of the features is quite accurate. Even when there is a direct occlusion with persons moving in front of the camera, the vanishing point position and the median line is correct. At the end of the corridor when there is very little composite wall/floor boundary the estimation is consistent, owing partly to the temporal filter used in the estimation of x_f.

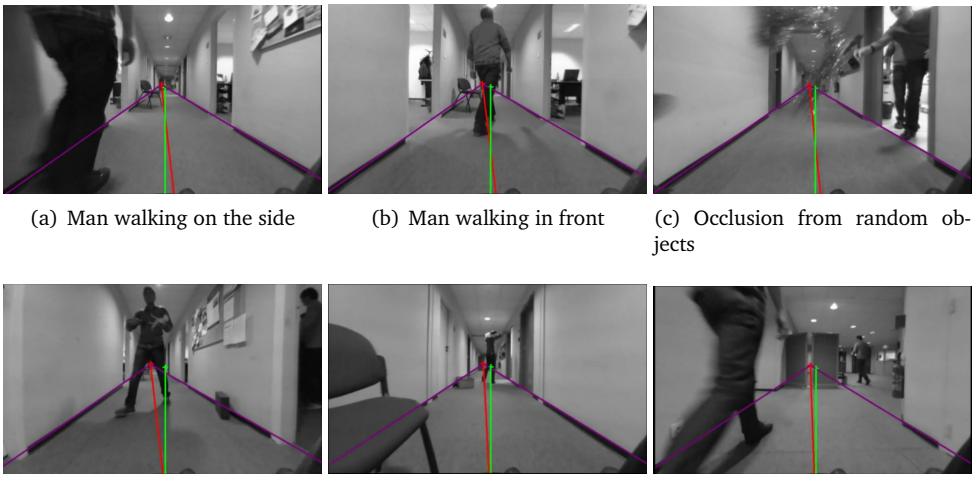

(a) Man walking on the side (b) Man walking in front (c) Occlusion from random objects

(d) Man walking in front (e) Furniture in the scene (f) End of corridor with man walking

Figure 3.4: The robustness of the feature extraction process with respect to different conditions and occlusions.

3.2.3 Image-based Visual Servoing (IBVS) for corridor following

As explained in Chapter 1, visual servoing is a classical approach to control robot motion from visual data [CH06]. The design of the kinematics controller is based on modelling the variation $\dot{\boldsymbol{s}}$ of the visual features $\boldsymbol{s}$ with respect to the camera velocity $\boldsymbol{v}_c$. More precisely, when the observed environment is static, we have

$$\dot{\boldsymbol{s}} = \boldsymbol{L}_{\boldsymbol{s}} \boldsymbol{v}_c \tag{3.9}$$

where $\boldsymbol{L}_{\boldsymbol{s}}$ is the Interaction matrix (see Section 1.2).

In the present case, when we have $\boldsymbol{s} = (x_f, \theta_m)$, the analytical form of $\boldsymbol{L}_{\boldsymbol{s}}$ is derived in [ECR92] and [AR08] respectively as

$$\mathbf{L_s} = \begin{bmatrix} 0 & 0 & 0 & x_f y_f & -1 - x_f^2 & y_f \\ \lambda_{\theta_m} & \lambda_{\theta_m} \sin\theta_m & -\lambda_{\theta_m} \rho_m & -\rho_m \cos\theta_m & -\rho_m \sin\theta_m & -1 \end{bmatrix}, \tag{3.10}$$

where $\lambda_{\theta_m} = (A \sin\theta_m - B\cos\theta_m)/D$ wherein $AX + BY + CZ + D = 0$ defines a plane to which the median line belongs. In the present case, this line belongs to the floor plane which is defined by $Y = h_1$. Therefore $A = C = 0$ and we obtain

$$\lambda_{\theta_m} = \cos\theta_m / h_1. \tag{3.11}$$

Plugging in (3.4) in (3.9), we obtain the variation of the task function $\boldsymbol{e} = \boldsymbol{s} - \boldsymbol{s}^*$ (where $\boldsymbol{s}^* = (0, 0)$) as

$$\dot{\boldsymbol{e}} = \dot{\boldsymbol{s}} = \boldsymbol{J}_\omega \omega + \boldsymbol{J}_v v$$

where

$$\boldsymbol{J}_\omega = \begin{bmatrix} 1 + {x_f}^2 \\ \frac{\cos\theta_m}{h_1} \left(\cos\theta_1 (w_1 \rho_m - l_1) - \sin\theta_1 (w_1 + l_1 \rho_m)\right) + \rho_m \sin\theta_m \end{bmatrix} \tag{3.12}$$

and

$$\boldsymbol{J}_v = \begin{bmatrix} 0 \\ \frac{\cos\theta_m}{h_1} \left(\sin\theta_1 - \rho_m \cos\theta_1\right) \end{bmatrix}. \tag{3.13}$$

Following the same strategy as in [CCO11], designing a locally asymptotically stable control scheme that tries to exponentially regulates $\boldsymbol{e}$ to 0 (i.e. such that $\dot{\boldsymbol{e}} = -\lambda \boldsymbol{e}$ where $\lambda > 0$) leads to

$$\omega = -\boldsymbol{J}_\omega^+ (\lambda \boldsymbol{e} + \boldsymbol{J}_v v^*) \tag{3.14}$$

where $\boldsymbol{J}_\omega^+$ is the pseudo-inverse of $\boldsymbol{J}_\omega$ and v^* the constant forward velocity required for motion exigency.

From the control law given in (3.14), one can observe that $\boldsymbol{J}_\omega$ is always of full rank, but for two singular degenerate configurations. They occur when the vanishing point lies at either side of the image plane (i.e if the wheelchair is perpendicular to the corridor wall), wherein $x_f = \pm\infty$ and the first row of $\boldsymbol{J}_{\boldsymbol{\omega}}$ tends to $\pm\infty$. In such a case the robot cannot decide by itself where to move (i.e. the human should make the decision, or we need to devise a shared control assistive framework which is in part one of the objectives of the work). Moreover, if $x_f = \infty$,

the vanishing point will not be detected by the feature extraction process. Another important caveat to consider is that the control law aims to center the *camera* in the middle of the corridor. Therefore, in order to center the wheelchair in the middle of the corridor, a non-zero value should be tuned for the desired value of θ_m as soon as $w_1 \neq 0$ (see Section 3.4).

3.2.4 Simulation Results

We here report two simulated cases meant to illustrate the convergence of the velocity control law and to validate it as a suitable system for the task of corridor following. The two initial conditions assessed were as follows.

- Case I: Initially $x_f = 0.15$m and $\theta_m = 0.55$rad which represents a situation where the robot is closer to the right corridor wall while facing the right corridor wall. The extrinsic parameters l_1, w_1 were set to zero in order to asses the control law in an ideal case.
- Case II: Initially $x_f = -1$m and $\theta_m = -0.85$rad which represents a case where the robot is closer to the left corridor wall and facing the left side. The extrinsic parameters were set at $l_1 = 0.5$m and $w_1 = 0.5$m. The desired value of θ_m was tuned to -0.3 rad so that the *wheelchair (i.e. the robot)* is centred within the corridor. The performance of this case was compared to the performance when there exists some calibration errors with l_1 having an error of 0.15m, w_1 an error of -0.15m and h_1 an error of $+0.2$m in order to assess the robustness of the velocity control law.

The translational velocity v^* was set as 0.2 ms^{-1} while the height h_1 as 0.5m. The results of the simulation can be observed in Figures 3.5 and 3.6 where the evolution of the visual features x_f, θ_m, ω and also the distance of the camera from the center of the corridor are shown.

We can observe that the rotational velocity ω decreases in a pure exponential way and that the visual features converge to their desired values $x_f^* = 0$ and $\theta_m^* = 0$ (Case I) or 0.3rad (Case II) in both the cases. The convergence of x_f is not completely exponential owing to the fact that two visual features are controlled with 1 DOF only. We can see that x_f tends to a value close to 0 which in turn allows θ_m to converge. This data is corroborated by the fact that the wheelchair distance from the center of the corridor moves to zero as θ_m converges to θ_m^*.

Moreover the inclusion of calibration errors in the camera extrinsic parameters does not affect the convergence of the system as seen in Figure 3.6. The only effect of such errors in modelling is an offset in the position of the wheelchair in the corridor corresponding to the modelling error: the wheelchair naturally overshoots the center of the corridor by 0.15m due to the calibration error encountered in w_1.

Based on the above results, it can be concluded that the proposed formulation for corridor following in a wheelchair is a viable solution for implementation in a real-time system. Experimental results will be shown in Section 3.4. In the next section, we present a similar vision-based velocity controller for the task of doorway passing which also represents a fundamental ability for corridor navigation.

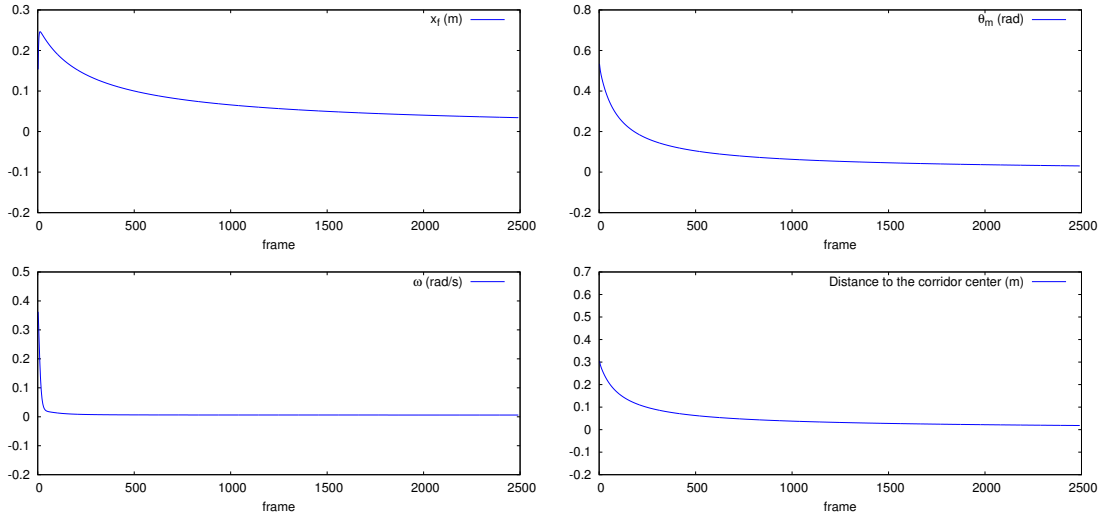

Figure 3.5: Evolution of x_f, θ_m, ω and camera distance to the corridor center - Case I

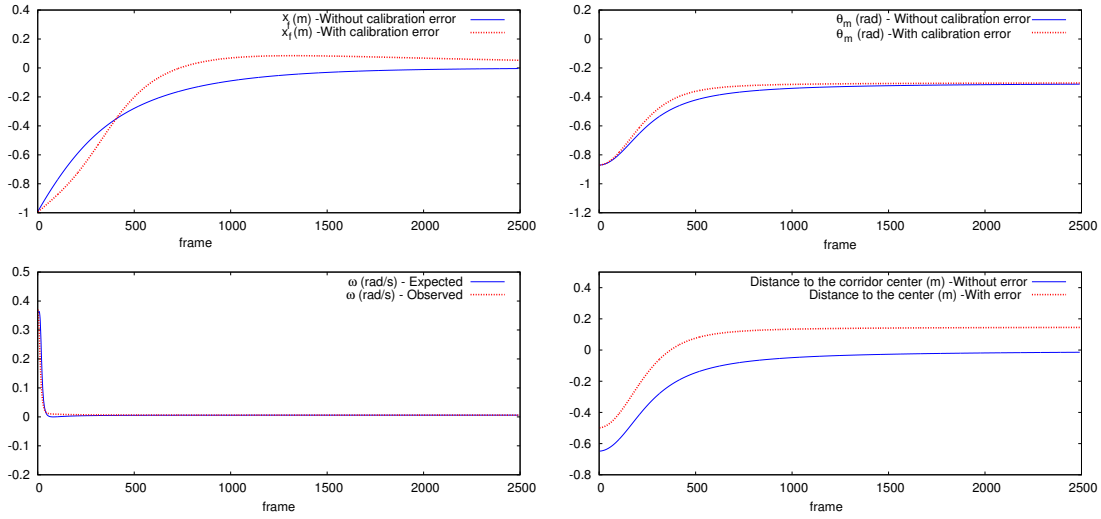

Figure 3.6: Evolution of x_f, θ_m, ω and camera distance to the corridor center - Case II with no calibration errors (blue) and with calibration errors (red)

3.3 Autonomous Doorway Passing

The task of autonomously passing through a doorway once it is detected is a non-trivial task owing to the fact that there are a lot of high level constraints to be taken care of. For example, whether the door is open or closed, and/or, is the width of the door sufficient enough to let the wheelchair through, etc remain unknown. However, these attributes either can be left for the user to set (i.e. human in the control loop), or left to a home automation system (which can work directly with the wheelchair) that manages these high level parameters.

Here the aim is to design a robust low-level velocity controller that achieves an adequate and safe wheelchair motion given a detected doorway. Thus we propose a novel Lyapunov-based velocity control scheme which exploits the position of the line feature representing the initial doorpost of the door (i.e. the doorpost closer to the robot) in the camera image as the visual feature.

3.3.1 Doorpost detection and tracking

There are several methods for detecting and representing doors in an indoor navigation scenario [AKPT04, CB08]. But, in the present case, the representations have to be simple and generic enough so that effective features can be extracted for visual servoing. Also, detections have to be robust as well as fast enough to process frames in real time at a reasonable speed.

Consequently, we use a door recognition and tracking framework specifically developed for indoor navigation tasks [SPB+13]. This framework uses a set of information including the vanishing point to estimate a 3-D geometrical structure of the corridor. This structure then defines a search space in which trapezoidal shapes representing doors are extracted. To realize this aim we consider that the doorposts are nearly verticals in the image. Furthermore, for tracking the detected doorposts, a 2-D edge tracker inspired from the $Moving\ Edges$ (ME) algorithm [Bou89, BBCJ98] is applied on the doorposts. The implementation of this framework on a generic corridor is shown in Figure 3.7.

It has to be noted that the doorpost at the far end of the door will not be present in the field of view of the camera as the wheelchair tries to position itself in front of the door (in order to pass through the doorway). Consequently we have to design a solution which uses the position of a single (i.e. the initial) doorpost as the input to the system.

3.3.2 Visual Feature - Definition and Extraction

Observing Figure 3.8, if the foot of the doorpost is represented by the point D then $D = (x_d, h_2, z_d)$ in frame $\mathcal{F}_{c_2}$. In polar coordinates point D can be represented by

$$r = \sqrt{x_d^2 + z_d^2} \quad \text{and} \tag{3.15a}$$

$$\phi_d = \arctan(x_d/z_d). \tag{3.15b}$$

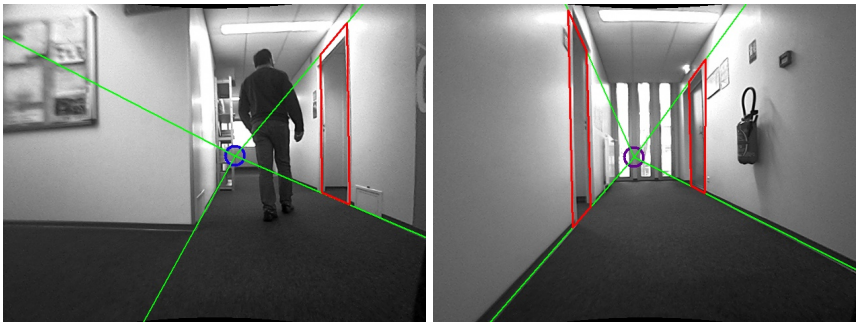

Figure 3.7: Door detection and tracking framework applied to a generic corridor scene

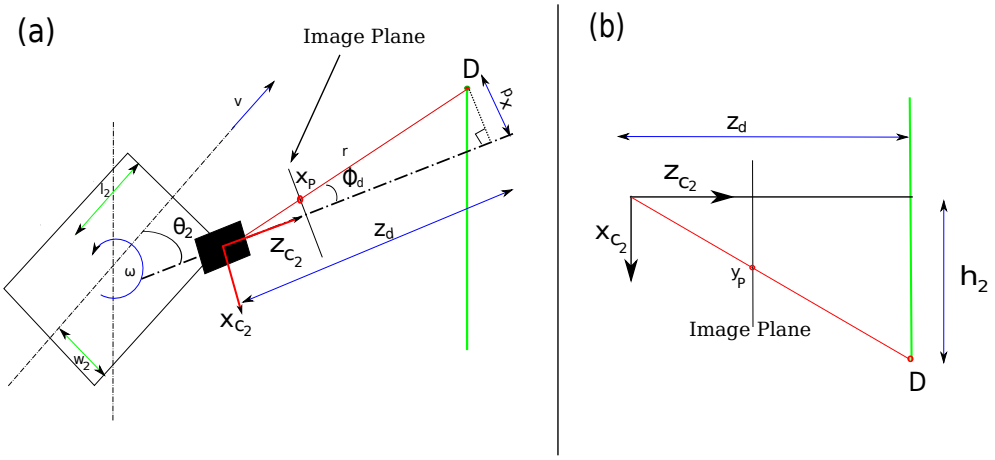

Figure 3.8: Geometrical constraints while considering doorway passing (top view (a), front view (b)). All metrics are illustrated with respect to *camera 2*.

If the point D projects in the image at point $P = (x_P, y_P)$, then owing to a calibrated camera, the perspective projection equations reduce to

$$x_P = \frac{x_d}{z_d}$$

and

$$y_P = \frac{h_2}{z_d}.$$

To perform a successful doorway passing maneuver, the wheelchair needs to avoid the closest doorpost with a predefined margin m. To do so we formally define the visual feature as the angle ϕ_d, since it can be easily estimated from the measure of the position of the doorpost. Indeed from x_P coordinate, we immediately obtain using (3.15b) that

$$\phi_d = \arctan(x_P). \tag{3.16}$$

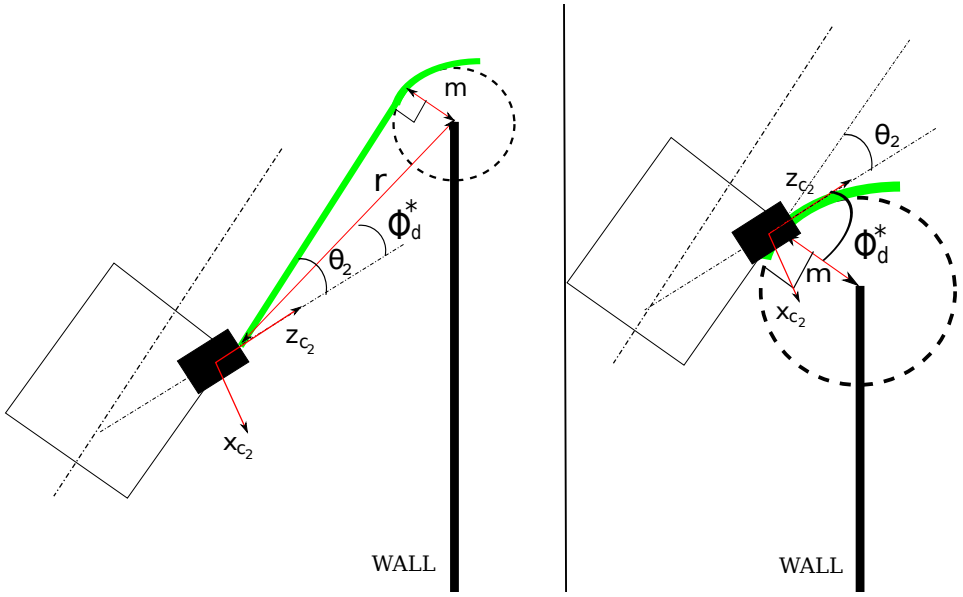

Figure 3.9: The desired camera trajectory shown in green. (a) when $r > m$ and (b) when $r < m$.

Similarly from y_P coordinate of D, the distance r between the camera and the doorpost is given by

$$r = \frac{h_2}{y_P . \cos(\phi_d)}, \tag{3.17}$$

since we get $z_d = r\cos(\phi_d)$ from Figure 3.8b.

3.3.3 Lyapunov-based controller

The visual feature ϕ_d must evolve in a certain way so that the wheelchair takes up a trajectory that realises the task. To assign a desired value ϕ_d^* which must be achieved by ϕ_d for task completion, we have to first assess this trajectory.

Desired trajectory

We specify the desired trajectory that the wheelchair should follow for a successful doorway passage as presented in Figure 3.9. This trajectory has been chosen since the wheelchair must be able to position itself in front of the doorpost with a tolerance of m no matter what its starting position and orientation are. Consequently, the wheelchair must ideally take a tangential path towards an imaginary circle centred at the doorpost (with radius m) and when the camera distance to the doorpost r is equal to m, it must take up a smooth circular trajectory about the doorpost. Note that this trajectory implicitly allows wall collision avoidance against both sides of the corridor.

The trajectory can be decomposed into two parts: an initial tangential motion towards the circle (when $r > m$) and the final circular motion about the doorpost (when $r \leq m$). The characteristic of the tangential motion toward the circle is that ideally the value of $\theta_2 - \phi_d$ (see Figure 3.9) should be equal to $\arcsin(\frac{m}{r})$. Therefore the desired value of $\phi_d (= \phi_d^*)$ for this trajectory is:

$$\phi_d^* = \theta_2 + \arcsin(\frac{m}{r}) \quad \text{if} \quad r > m. \tag{3.18}$$

As r gets closer to m, the wheelchair must switch to the circular motion about the doorpost. For such case it is clear from Figure 3.9 that the desired value of the visual feature ϕ_d^* must be equal to $\frac{\pi}{2} - \theta_2$. Therefore, we can state that

$$\phi_d^* = \theta_2 + \frac{\pi}{2} \quad \text{if} \quad r \leq m. \tag{3.19}$$

Control law formulation

We here propose a novel approach for the design of the velocity controller compared to standard visual servoing schemes (see Section 1.2). To design a globally asymptotically stable system, we select a Lyapunov candidate function

$$V = \frac{1}{2}(\phi_d - \phi_d^*)^2. \tag{3.20}$$

Of course we have $V = 0$ when $\phi_d = \phi_d^*$. Then, we have to design a control scheme so that $\dot{V} < 0$. We have

$$\dot{V} = (\phi_d - \phi_d^*)(\dot{\phi_d} - \dot{\phi_d^*}). \tag{3.21}$$

First by deriving (3.15b) we obtain

$$\dot{\phi_d} = \frac{z_d \dot{x_d} - x_d \dot{z_d}}{x_d^2 + z_d^2}, \tag{3.22}$$

which can be re-written as (see Appendix A),

$$\dot{\phi_d} = \omega + \frac{1}{r}\left[\sin(\phi_d - \theta_2)v + (l_2 \cos(\phi_d - \theta_2) - w_2 \sin(\phi_d - \theta_2))\omega\right]. \tag{3.23}$$

In addition, from (3.18) we obtain when $r > m$

$$\dot{\phi_d^*} = \frac{d}{dt}\left(\arcsin\left(\frac{m}{r}\right)\right) = \frac{-\dot{r}m}{r\sqrt{r^2 - m^2}} \tag{3.24}$$

which can be re-written as (see Appendix A)

$$\dot{\phi_d^*} = \frac{\sin(\phi_d^* - \theta_2)\left[\cos(\phi_d - \theta_2)v - (l_2 \sin(\phi_d - \theta_2) + w_2 \cos(\phi_d - \theta_2))\omega\right]}{r \cos(\phi_d^* - \theta_2)} \tag{3.25}$$

Finally from (3.19) we have when $r \leq m$

$$\dot{\phi_d^*} = 0. \tag{3.26}$$

By substituting the resulting expressions for $\dot{\phi}_d$ and $\dot{\phi}_d^*$ into (3.21), we obtain a new form of the derivative of V as (see Appendix)

$$\dot{V} = (\phi_d - \phi_d^*)\left(vA(r,\phi_d) + \omega(1 + B(r,\phi_d))\right) \tag{3.27}$$

where, when $r > m$

$$\begin{cases} A(r,\phi_d) = \dfrac{\sin(\phi_d - \phi_d^*)}{r\cos(\phi_d^* - \theta_2)} \\ B(r,\phi_d) = \dfrac{l_2\cos(\phi_d - \phi_d^*) - w_2\sin(\phi_d - \phi_d^*)}{r\cos(\phi_d^* - \theta_2)}. \end{cases} \tag{3.28}$$

and when $r \leq m$ in which case we recall that $\dot{\phi}_d^* = 0$,

$$\begin{cases} A(r,\phi_d) = \dfrac{\sin(\phi_d - \theta_2)}{r} \\ B(r,\phi_d) = \dfrac{l_2\cos(\phi_d - \theta_2) - w_2\sin(\phi_d - \theta_2)}{r}. \end{cases} \tag{3.29}$$

Thus in both cases, if we choose ω such that

$$\omega = \frac{-k(\phi_d - \phi_d^*) - A(r,\phi_d)v^*}{1 + B(r,\phi_d)}, \tag{3.30}$$

where k is a positive gain factor, we verify that $\dot{V} < 0$. This ensures that the system is globally asymptotically stable and the visual feature ϕ_d will converge asymptotically to the desired value ϕ_d^*. Furthermore, when $r > m$, it can also be shown that $\omega = 0$ when $\phi_d = \phi_d^*$ thus providing a straight tangential motion towards the circle. Finally, as soon as $\phi_d = \phi_d^* = \theta_2 + \frac{\pi}{2}$ (when $r \leq m$) from (3.29) we have $A = \frac{1}{r}$ and $B = -\frac{w_2}{r}$ from which we deduce $\omega = \frac{-v^*}{r - w_2}$. This naturally corresponds to a circular motion when $r = m$ whose radius is equal to $m - w_2$. Note also that the switching has to be performed as $r \to m$ so that A and B in (3.28) does not reach a very high value due to numerical constraints.

3.3.4 Simulation Results

To validate the framework formulated above, we present two simulated trials. The aim of the simulations were to assess the trajectory taken by the wheelchair during the task, particularly the control law switch. The switch occurs as $r \approx m$ which facilitates the wheelchair to take up a circular trajectory about the doorpost. Thus we switch the control law at $r = m + 0.01$m.

For both cases the doorpost was fixed at the origin of a Cartesian door frame say $\mathcal{F}_d$ with the wheelchair starting at a relative position (x_{door}, y_{door}) with respect to $\mathcal{F}_d$ with $x_{door} = -1.5$m and $y_{door} = -1.5$m. The camera was initially aligned parallel to the corridor wall. The margin m was set at 0.2m, the height h_2 to 0.5m and v^* was set to 0.1 ms^{-1}. Finally the gain k was set to 2.

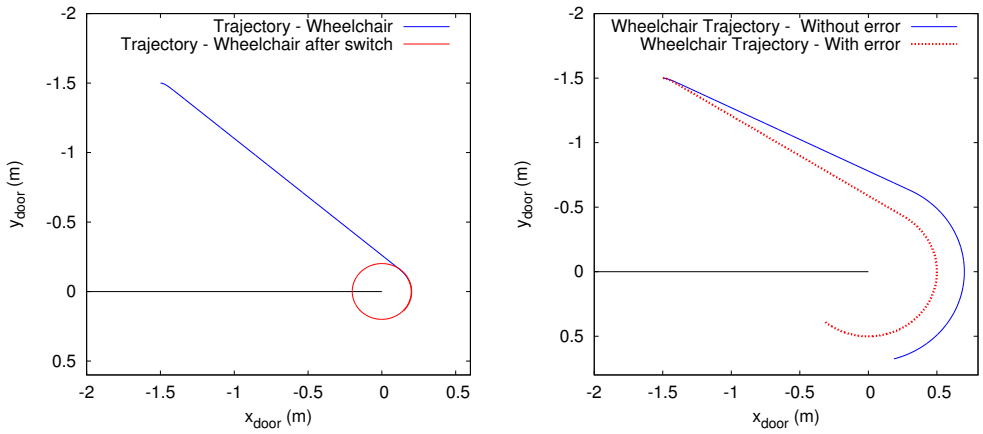

Figure 3.10: The trajectories: Case I (left) and Case II - without error in blue and with error in red (right)

- Case I represents an ideal case where the factors l_2, w_2 and θ_2 representing the extrinsic parameters were set to 0.

- Case II represents a real world situation where the extrinsic parameters were set to non-zero so that $l_2 = 0.5$m, $w_2 = -0.5$m and the angle $\theta_2 = -0.8$rad. Moreover, calibration errors were induced in this case in order to evaluate the robustness of the control law. Errors of 0.2m, -0.2m and -0.15m were respectively added to l_2, w_2 and h_2. Also an error of $+0.2$ rad was added on θ_2. It has to be noted that these errors are very high compared to the dimensions of a real wheelchair.

The trajectories taken by the wheelchair are shown in Figure 3.10. It can be observed that in both cases, the wheelchair takes up a straight line and tangential motion towards a circle centered at the doorpost. As $r \approx m$, the control law switch allows the robot to take up a circular trajectory around the doorpost. We can observe the evolution of r, ϕ_d^*, the feature error $\phi_d - \phi_d^*$ and ω in Figures 3.11 and 3.12. The point where the control law switches is illustrated in the respective figures.

As for case I, the visual feature ϕ_d converges to ϕ_d^* in a few iterations as shown by the evolution of the feature error. As the the control law switches at $r \approx 0.2$m, the error increases due to the change in behaviour of ϕ_d^* but again moves to zero exponentially. Furthermore, it is clear that the distance from the camera to the doorpost r decreases constantly and stays near to the margin $m = 0.2$m. During the task, the rotational velocity ω is initially high but converges rapidly to 0. It then reacts to the control law switch and converges to the expected value for realizing the circular trajectory. In practice, in order to avoid a sudden increase in ω at the start (which may induce discomfort for the user), a method ensuring the continuity of the control law, such as the one proposed in [MC07] could be used.

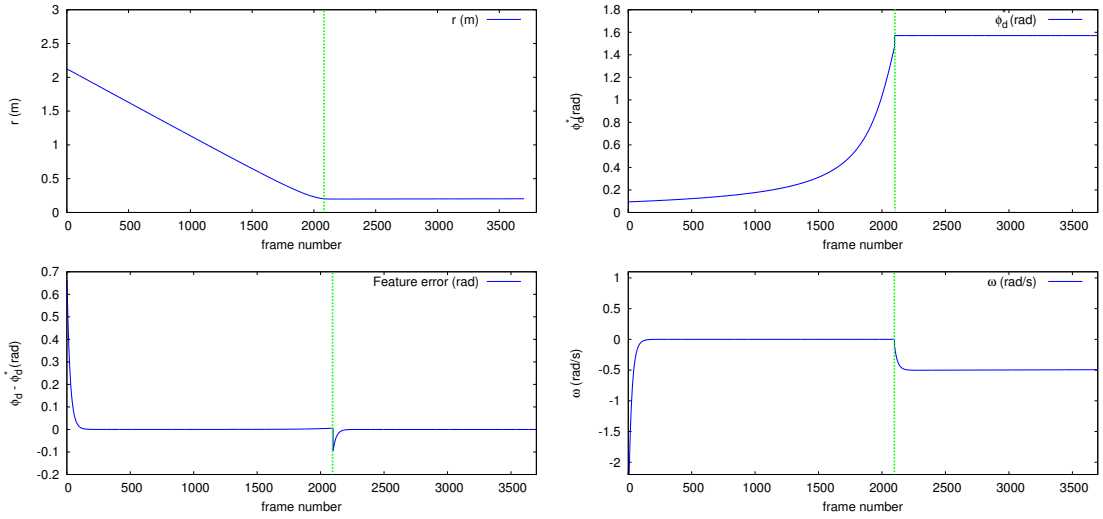

Figure 3.11: Evolution of r, ϕ_d^*, $\phi_d - \phi_d^*$ and ω - Case I. The point where the control law switches, is marked.

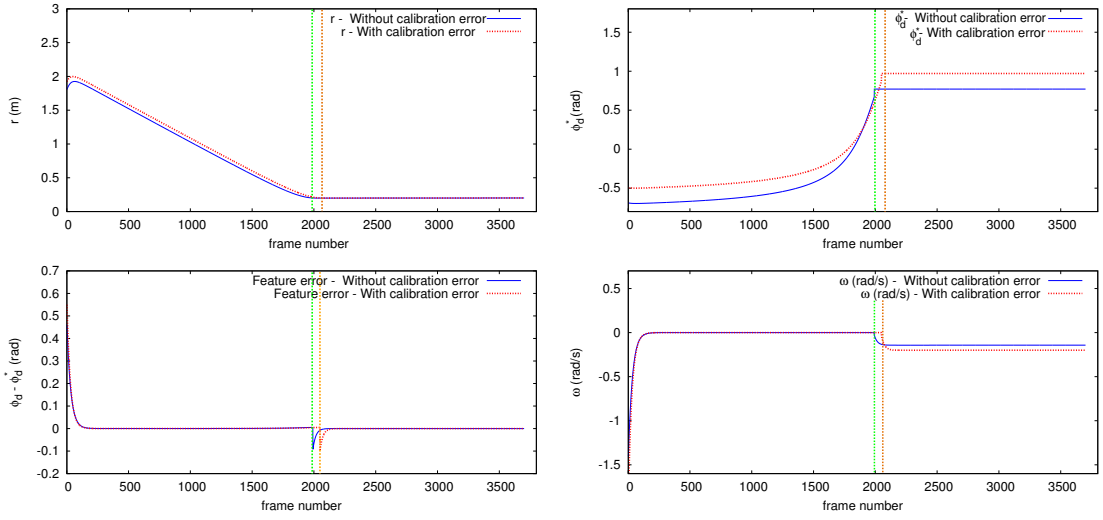

Figure 3.12: Evolution of r, ϕ_d^*, $\phi_d - \phi_d^*$ and ω - Case II. The points where the control law switches, is marked for each test.

The addition of the real world dimensions to the controller does not affect the system dynamics at all. As shown in Figure 3.10 the trajectory taken up by the wheelchair respects the dimensions of the wheelchair in the case with perfect calibration. Moreover, errors in calibration do not have an impact on the convergence of the control law as can be seen from the evolution of the feature error in Figure 3.12. But since there is an error in the angle θ_2, this affects the value of ϕ_d^*. Also, the error in w_2 naturally affects the trajectory of the wheelchair corresponding to the error since the radius of the circular motion is equal to $m - w_2$ according to the proposed control law. We can however note that the feature error $\phi_d - \phi_d^*$ remains small, demonstrating the robustness of the control scheme with respect to large calibration errors.

3.4 Experimental Analysis

3.4.1 Test Setup

In order to validate the proposed autonomous controllers in the real world, we *robotized* an off-the-shelf Penny and Giles wheelchair using ROS middleware [QCG+09b]. The wheelchair was then equipped with two Raspberry PI [pf12] camera modules with 100° field of view. The video stream from the camera ran at 15 frames per second and corresponded to a frame width of 808 pixels and a frame height of 480 pixels. The *camera 1* was coarsely calibrated with $l_1 = 0.38$m, $w_1 = 0.32$m and $h_1 = 0.64$m while *camera 2* was calibrated with $l_2 = 0.0$m, $w_2 = -0.32$m and $h_2 = 0.5$m with respect to $\mathcal{F}_r$. *Camera 2* was aligned at an angle of $\theta_2 = -50^\circ \sim -0.88$rad with respect to the robot frame. Finally, the margin for doorway passing m was set at 0.2m. Also, prior to the feature extraction, images were rectified against the distortions due to the camera lens. As the aim is to validate the control schemes, human intervention is needed only for turning the visual servoing process on/off and to select a doorway to pass through.

Remark Extraction of the visual features as well as the computation of the control laws were performed using the ViSP software [MSC05]. Computation was performed on a Core i7 laptop connected to the wheelchair using Ethernet network. The results presented here pertain to the one realised in one of the corridors of the Inria building 12C in Rennes, France. For all the experimental results provided in this thesis, the above remark applies unless otherwise specified.

3.4.2 Experimental Procedure

1 The wheelchair starts at an unknown position in the corridor and the servoing process is activated in order to follow the corridor.

2 As soon as a turn arrives, the user interacts with the system to select the end of the corridor to turn about using the doorway passing control scheme.

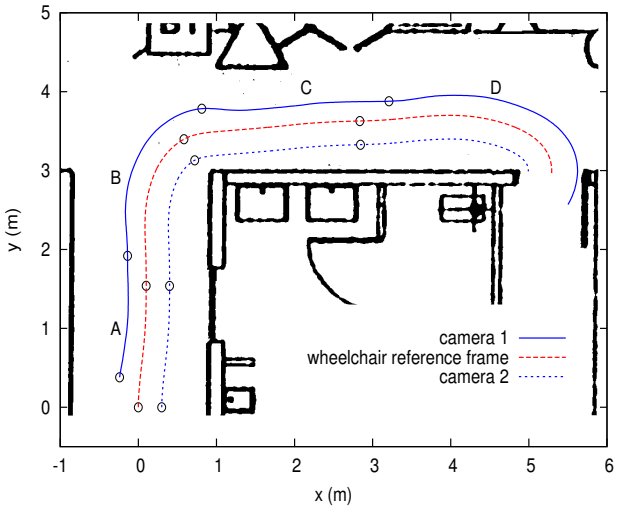

Figure 3.13: Trajectory taken by the wheelchair with respect to a frame fixed at the initial position

3 After the wheelchair has turned about the corridor, the servoing process for following the new corridor switches on automatically when both $\phi_d^* = \frac{\pi}{2} + \theta_2$ and a vanishing point is detected.

4 While the wheelchair is still following the corridor the user interacts again, this time to select a doorway to pass through.

5 The servoing process is switched off once the wheelchair manages to pass through the specific doorway.

Figure 3.13 shows the trajectory taken by *camera 1*, *camera 2* and the wheelchair during the experiment process. It is reproduced in a global frame with the wheelchair starting position taken as the origin. Odometry had only been used to reconstruct the trajectory on a map of the environment for visualization. It has to be noted that neither odometry nor the environment map is employed in the servoing process.

3.4.3 Analysis

The trajectory is decomposed into four parts. During part A, the wheelchair performs corridor following in order to position itself in the middle of the corridor while controlling the two visual features x_f and θ_m. It can be noted that the wheelchair starts relatively in a central position and the correction is done as soon as the servoing starts. As the wheelchair moves to the end of the corridor, the user selects the wall partition to turn right. Consequently, part B is activated where the wheelchair manages to judge the wall partition as a doorpost and turn about it. Thus we can observe that the framework for doorway passing can be employed for turning within corridors.

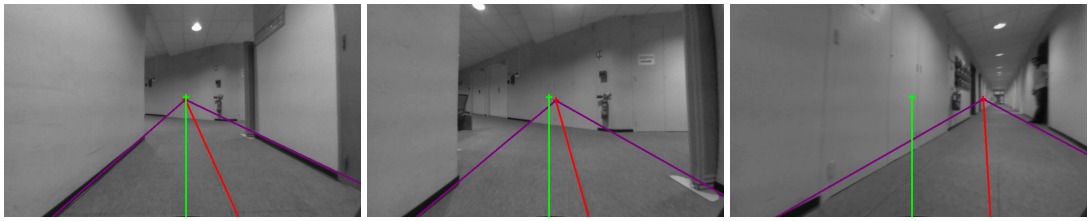

(a) Frame 23 (b) Frame 111 (c) Frame 241

(d) Frame 392 (e) Frame 590

Figure 3.14: The *camera 1* frame at points A,B,C,D at the end of the navigation respectively. The vanishing point and the median line of the corridor are represented by the red cross and red line respectively. Their desired positions in the image are shown in green.

After the wheelchair successfully turns, the corridor following task (part C) is automatically activated once $\phi_d = \frac{\pi}{2} + \theta_2$ and a vanishing point is detected. Again the control scheme acts to position the wheelchair in the middle of the corridor. Finally, the user selects a doorway to pass through to start (part D) while the wheelchair manages to turn about the doorpost for a successful doorway passing maneuver. The servoing process is stopped as soon as the wheelchair is positioned in front of the doorway.

At critical points of the servoing process, the camera views can be seen in Figures 3.14 and 3.15 for *camera 1* and *camera 2* respectively. Figures 3.14(a) and 3.15(a) represent the start of the servoing process. The user selects the wall partition in the frames shown in Figures 3.14(b) and 3.15(b) which marks the transition from A to B. A new vanishing point is obtained in frame 241 (Figures 3.14(c) and 3.15(c)) with the visual feature $\phi_d \sim \frac{\pi}{2} + \theta_2$. Then frame 392 (Figures 3.14(d) and 3.15(d)) marks the start of doorway passing and a transition onto part D. Finally, frame 590 (Figures 3.14(e) and 3.15(e)) shows the frames at the end of the navigation.

Figure 3.16 shows the behaviour of visual features x_f and θ_m during the servoing process. Since the front facing *camera 1* is located at $w = 0.32$m from the centre of the wheelchair reference frame, the desired value of θ_m was set at -0.3rad. This was done in order to facilitate the wheelchair in the middle of the corridor rather than the camera. During part A, we can observe the convergence of the features to their desired values $x_f = 0$ and $\theta_m = -0.3$ rad as the wheelchair centres itself in the corridor. The features evolve till the vanishing point is not detected anymore during the corridor turning part B. As part C starts, the features are detected again and we can observe the exponential decrease of x_f to zero. Also, θ_m converges gradually to -0.3rad as observed in simulation. Again, the features are correctly extracted during part

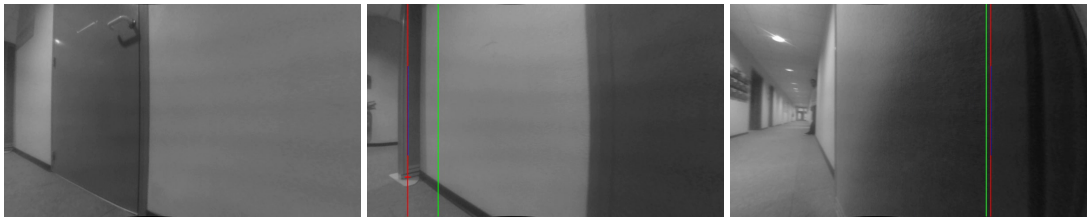

(a) Frame 23 (b) Frame 111 (c) Frame 241

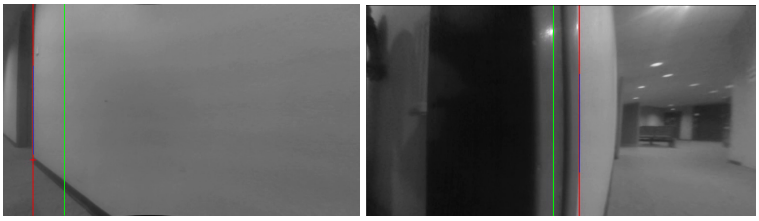

(d) Frame 392 (e) Frame 590

Figure 3.15: The *camera 2* frame at points A,B,C,D and at the end of the navigation respectively.

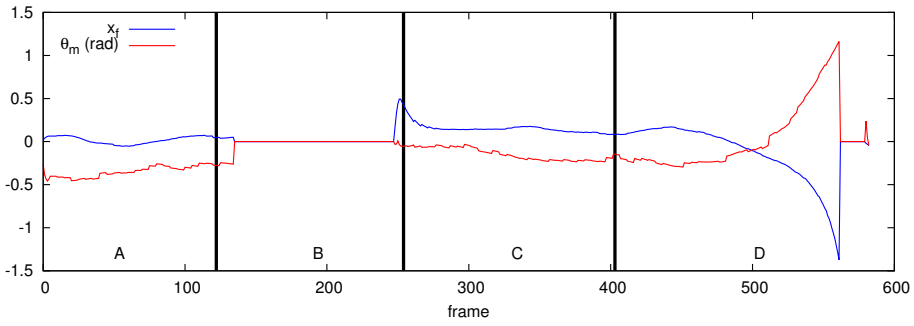

Figure 3.16: The evolution of the corridor visual features x_f and θ_m

D owing to the fact that the vanishing point is detected until the wheelchair makes a complete turn. Thus, the behaviour of x_f and θ_m during parts A and C validates the control scheme for autonomous corridor following for use in a real time system.

Figures 3.17 and 3.18 present the evolution of the visual feature ϕ_d as well as the distance r from the camera to the doorpost/wall partition during the experiment. The values are naturally equal to zero in part A and C as the controller for doorway passing is not activated. It is activated as soon as the user selects the wall partition to turn about. We can observe that ϕ_d manages to follow ϕ_d^* very closely and reaches $\frac{\pi}{2} + \theta_2 = 0.69$ rad. The perturbations in ϕ_d can be attributed to the low dynamics of the wheelchair, the wheelchair's caster wheels and to visual tracking errors. But we can observe that the control scheme manages to servo the feature to its desired value. A similar behaviour of ϕ_d can be reported while in part D. The visual feature manages to follow the desired value during the servoing process. There is a small discrepancy at the end which is again

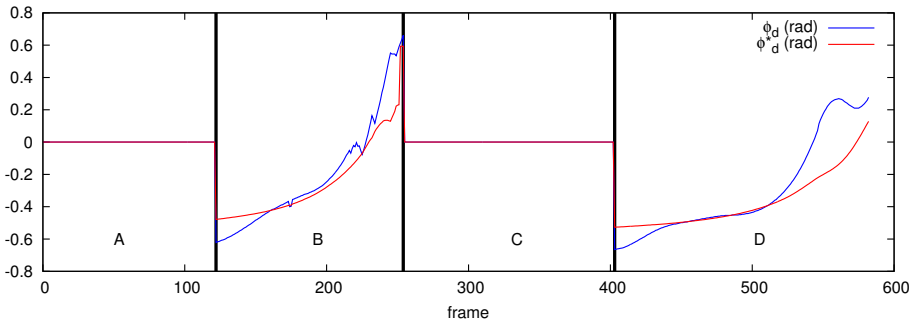

Figure 3.17: The evolution of the visual feature ϕ_d

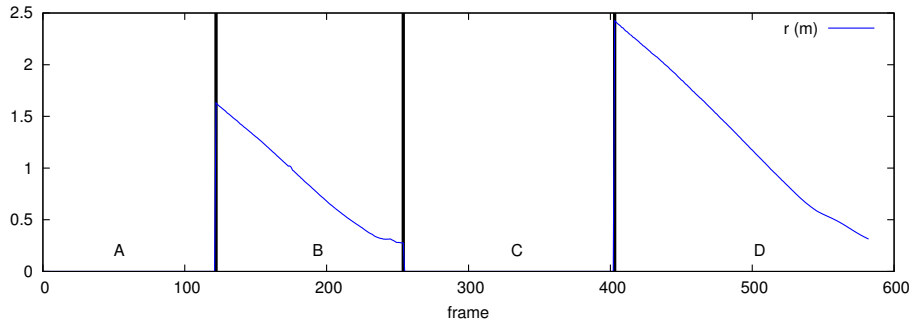

Figure 3.18: The evolution of the distance to the doorpost r

due to some tracking errors even though ϕ_d converges to ϕ_d^* at the end. The final desired value of 0.69 rad is not reached since the servoing is stopped as soon as the wheelchair is positioned in front of the doorway.

When considering r, we can observe an almost constant decrease to the margin $m = 0.2$m. Then the value of $r = m$ remains almost constant till the task switch occurs. This behaviour is critical for the purpose of doorpost collision avoidance and for the requirement that the wheelchair is able to position in front of the doorway no matter what its initial position.

A final important point to mention is that the cameras are coarsely calibrated with respect to the intrinsic parameters as well as their position with respect to the wheelchair. The robust performance of the controller in such a case demonstrates that the impact of modelling errors is minimal on the system (as already seen in the simulation results of Section 3.2.4.

3.5 Conclusion and Remarks

In this Chapter, we proposed a visual servoing approach for autonomously following a corridor as well as pass though doorways and turn about corridors in an electric wheelchair. The task of corridor following was realised by exploiting two visual features, namely the vanishing point and the angle obtained from the projection of the median line of the corridor onto the image. A control law was designed to servo the features onto their desired values by taking into account the kinematics of the wheelchair. The doorway passing (and corridor turning) task employed the position of a single doorpost in the image as an input to a Lyapunov-based control scheme which allows the wheelchair to take up a desired trajectory about the doorpost. This trajectory avoids collision with the wall and guarantees that the wheelchair positions itself in front of the doorway regardless of its initial position.

Results in simulation demonstrated the convergence and robustness of both control schemes. Experiments conducted on an off-the-shelf robotic wheelchair platform indicated the validity of applying the proposed low-level control system on a commercial assistive wheelchair.

In the next Chapter, we aim to enhance the system to account for the human-in-the-loop condition where the wheelchair user would have considerable presence in the control loop thus modifying the system into a *semi-autonomous assistive system*.

Chapter 4

Vision-based Assistance

THIS CHAPTER demonstrates the design of vision-based *semi-autonomous* controllers that allow a robotized wheelchair (such as the one described in Section 3.4) to be safely driven by the user along and within corridors.

If we denote the filtered user output from a teleoperation interface (traditionally a joystick) as $\mathbf{v}_{op} = (v_{op}, \omega_{op})$, and utilizing the same kinematic modelling for the system as described in Section 3.1, a minimal objective of the assistance scheme would be to *augment* the user teleoperation in such a manner, that it ensures that the user is the primary controller and that assistance is provided only when required. Therefore, we also assert that if the user is not in danger, it is preferable to assign full control to the user.

Thus, the velocity controllers demonstrated in the previous Chapter for the tasks for autonomous corridor following and doorway passing can be employed in order to formulate the necessary *semi-autonomous* solutions. In the first Section of this Chapter, we design an assistance framework for the task of corridor following using a bottom-up approach, i.e. we constrain the controller 3.14 so that it is *activated* only when there is danger of wall collisions. This allows us to stack user teleoperation onto the constrained controller using a redundancy formalism. We also provide a solution to integrate haptic force feedback for providing intuitive guidance to the user.

From the final *assistive* controller that we obtain, we can infer a control sharing formalism for effectively assisting the user based on the most important consideration that assistance should be provided only when needed. We then use this inference, in a top-down manner, in order to design a similar assistive controller for the task of doorway passing in the second Section of this Chapter.

The contents of this chapter has been partially published in the scientific journal Computer Vision and Image Understanding (CVIU)[**J.1**].

4.1 Assisted Corridor Following

In the case of a user with disabilities steering a wheelchair along a corridor, joystick jerks induced by uncontrolled motions may lead to wall collisions, and wall collisions do represent the fundamental danger in corridor following. Evidently, we aim to design a solution where the user has primary control over the wheelchair motion, with the system taking part of the control *only to avoid wall collisions*. We propose a bottom-up approach in the design of the design of the assistance solution where we initially design a wall collision avoidance visual task that *progressively* corrects the wheelchair trajectory as it comes closer to the walls. User teleoperation can then be fused with the said task in order to derive a semi-autonomous solution.

The following subsection summarizes a wall collision avoidance system, that is derived from the autonomous visual servoing task described in Section 3.2. This task can then be fused with the user teleoperation output $\mathbf{v}_{op}$ in order to create a solution where the user will have primary control over the wheelchair motion for the specific task of corridor following.

4.1.1 Wall collision avoidance via Visual Servoing

Recall that in Section 3.2, we designed a visual servoing scheme that uses two features namely the vanishing point (x_f) and the angle of the image projection of the corridor median line (θ_m), that allowed us to perform autonomous corridor following. In order to design a corridor wall collision avoidance scheme, we propose to gradually activate the regulation of the visual features $\mathbf{s} = (x_f, \theta_m)$ to the desired values $\mathbf{s}^* = (0, 0)$ when they leave a *pre-fixed safe interval*, namely $x_f \in [x_f^{s-}, x_f^{s+}]$ and $\theta_m \in [\theta_m^{s-}, \theta_m^{s+}]$, so that they go back inside these safe intervals.

This concept of an interval that triggers the visual servoing was introduced in [KC11] and used in [LKK12] to ensure the visibility of an organ section during remote ultrasound teleechography. Let $\mathbf{H} = \text{Diag}(h_{x_f}, h_{\theta_m})$ be a diagonal matrix that weights the visual error where $h_{x_f} \in [0; 1]$ and $h_{\theta_m} \in [0; 1]$ are varying weights respectively associated to the visual features x_f and θ_m. Owing to this definition we can propose the following control law that sets the system velocity (say $\mathbf{v_r} = (v_r, \omega_r)$) aimed at keeping the visual features inside their interval and thus allowing wall collision avoidance:

$$\mathbf{v_r} = -\lambda(\mathbf{H}\mathbf{J}_s)^{+}\mathbf{H}\mathbf{e}, \tag{4.1}$$

where $\lambda > 0$ is the control gain, $\mathbf{e} = \mathbf{s} - \mathbf{s}^*$ is the visual error and $\mathbf{J}_s$ is the image Jacobian that links the variation of the visual features to the robot control input such that $\dot{\mathbf{s}} = \mathbf{J}_s\mathbf{u}$, and $(\mathbf{H}\mathbf{J}_s)^{+}$ is the Moore-Penrose pseudo-inverse of $(\mathbf{H}\mathbf{J}_s)$.

The image Jacobian $\mathbf{J}_s$ was determined in subsection 3.2.3 of the previous chapter and was formulated as follows (please refer to 3.2.3 to identify all the parameters of $\mathbf{J}_s$):

$$\mathbf{J}_s = \begin{bmatrix} 0 & 1 + x_f^2 \\ -\lambda_{\theta_m}\rho_m & -\lambda_{\theta_m} l\cos(\theta_m) + \lambda_{\theta_m} w\rho_m + \rho_m \sin(\theta_m) \end{bmatrix} = \begin{bmatrix} \mathbf{J}_{x_f} \\ \mathbf{J}_{\theta_m} \end{bmatrix}. \tag{4.2}$$

In the definition of the weighting function $\mathbf{H} = \text{Diag}(h_{x_f}, h_{\theta_m})$, a zero weight means that the related visual feature is not regulated by the visual servoing task. The matrix $\mathbf{H}$ allows then to add or remove any visual feature in the control law when desired, and can totally deactivate the visual servoing task when $\mathbf{H}$ is null. In order to gradually activate the wall avoidance task when a visual feature leaves its pre-set safe interval, we propose to define the weight related to x_f by the following smooth function:

$$h_{x_f}(x_f) = \begin{cases} (1 - \cos(\pi \frac{x_f - x_f^{s-}}{x_f^- - x_f^{s-}}))/2 & \text{if } x_f^- \leq x_f \leq x_f^{s-} \\ 0 & \text{if } x_f^{s-} < x_f < x_f^{s+} \\ (1 - \cos(\pi \frac{x_f - x_f^{s+}}{x_f^+ - x_f^{s+}}))/2 & \text{if } x_f^{s+} \leq x_f \leq x_f^+ \\ 1 & \text{otherwise} \end{cases} \tag{4.3}$$

where $[x_f^{s-}, x_f^{s+}]$ is a safe interval within which the visual servoing task is fully deactivated (for the feature x_f). Whereas $[x_f^-, x_f^{s-}] \cup [x_f^{s+}, x_f^+]$ represent the unsafe intervals whose fixed limits (i.e., x_f^- and x_f^+ respectively) should never be overcome owing to the visual servoing scheme. A similar expression for h_{θ_m} can also be proposed. The corresponding function evolution is shown in Figure 4.1. We can note that each weight is zero in the safe interval and increases up to 1 if the related feature comes close to the tolerated interval limits. In this way, the wall avoidance task is gradually activated when the weight related to the visual feature increases.

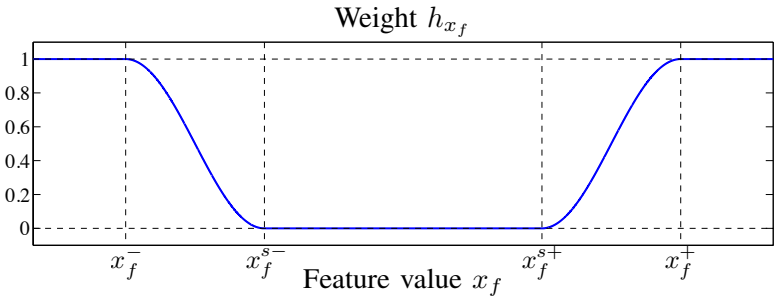

Figure 4.1: Weighting function h_{x_f} defined for feature x_f. The weight is zero in the safe interval and increases smoothly up to 1 at the borders of the unsafe values of x_f^- and x_f^+ (a similar function is used to define the weight h_{θ_m} with intervals $[\theta_m^-, \theta_m^+]$ and $[\theta_m^{s-}, \theta_m^{s+}]$).

The three conditions to obtain a continuous behaviour of the control law (4.1) are that $\mathbf{J}_s$, $\mathbf{H}$ and the pseudo-inverse of $\mathbf{H}\mathbf{J}_s$ remain continuous. The first two conditions are valid according to the form of (4.2) and the definition of the weight (4.3). However, the pseudo-inverse of $\mathbf{H}\mathbf{J}_s$ is not continuous since the rank of $\mathbf{H}\mathbf{J}_s$ could switch from zero, if all features are in their safe intervals, to 1 when only one feature leaves its interval or even 2 (full rank) when the two features are outside their safe intervals. Therefore, in order to avoid discontinuities in the control we propose to replace the Moore-Penrose pseudo-inverse operator $^+$ by the continuous pseudo-inverse operator $\oplus^{\mathbf{H}}$ introduced in the framework of varying-feature-set [MRC09].

This operator allows the inversion of a matrix say $\mathbf{J}$ weighted by a diagonal matrix say $\mathbf{H}$

by applying the following definition:

$$\mathbf{J}^{\oplus\mathbf{H}} = \sum_{\mathcal{P}\in\mathfrak{B}(k)} \left(\prod_{i\in\mathcal{P}} h_i\right)\left(\prod_{i\notin\mathcal{P}} (1-h_i)\right)\mathbf{J}_{\mathcal{P}}^{+} \tag{4.4}$$

where $\mathbf{J}$ is a matrix of size $(k \times n)$, $\mathbf{H}$ is a diagonal activation matrix of size $(k \times k)$ whose components $(h_i)_{i\in[1\ldots k]}$ are included in the interval $[0, 1]$. $\mathfrak{B}(k)$ is the set of all the combinations formed by the integers belonging between 1 and k (for example $\mathfrak{B}(2) = \{\emptyset, \{1\}, \{2\}, \{1, 2\}\}$). $\mathcal{P}$ is any element of this set and $\mathbf{J}_{\mathcal{P}} = \mathbf{H}_0\mathbf{J}$ with $\mathbf{H}_0$ being a $(k \times k)$ diagonal matrix whose diagonal component (i, i) is equal to 1 if $i \in \mathcal{P}$ and equal to 0 otherwise. All the theoretical bases including the proof of continuity of this inversion operator are presented in [MRC09]. In our case, applying this operator (with $k = 2$), the continuous inversion of the image Jacobian $\mathbf{J}_s$ activated by the weight matrix $\mathbf{H}$ can be obtained as

$$\mathbf{J}_s^{\oplus\mathbf{H}} = h_{x_f}(1-h_{\theta_m})\begin{bmatrix}\mathbf{J}_{x_f}\\ \mathbf{0}_{1\times 2}\end{bmatrix}^{+} + (1-h_{x_f})h_{\theta_m}\begin{bmatrix}\mathbf{0}_{1\times 2}\\ \mathbf{J}_{\theta_m}\end{bmatrix}^{+} + h_{x_f}h_{\theta_m}\mathbf{J}_s^{+}. \tag{4.5}$$

We can note that if both the weights of $\mathbf{H}$ are equal to 1 (full activation of the wall avoidance task) then the matrix $\mathbf{J}_s^{\oplus\mathbf{H}}$ is exactly equal to $(\mathbf{H}\mathbf{J}_s)^{+}\mathbf{H}$ and we have the same equality if all the weights are zero (deactivation of the wall avoidance task).

Hence the control law (4.1) can be replaced by the following control law ensuring a wall avoidance visual task with a continuous behaviour:

$$\mathbf{v_r} = -\lambda\mathbf{J}_s^{\oplus\mathbf{H}}\mathbf{e}. \tag{4.6}$$

4.1.2 Fusion of User and Robot Control for Semi-autonomous Navigation

In order to create a *semi-autonomous* system that prevents the user from hitting the lateral walls while he/she is manually driving the wheelchair, manual control has to be fused with the proposed wall collision avoidance task. The wall collision avoidance visual task constraints only the DOFs that regulate the *activated* (i.e. non zero) features into their safe interval. It is then possible to control the remaining DOFs using the well established *redundancy formalism* [SEB91]. Therefore when both the features have returned to their safe intervals, all the DOFs are fully available for the manual control since the visual task is fully deactivated.

This also means that the desired features $\mathbf{s}^*$ will never be reached. This is not a problem since our objective is only to bring them back within their safe intervals. The wall avoidance task (i.e. $\mathbf{v_r} = -\lambda\mathbf{J}_s^{\oplus\mathbf{H}}\mathbf{e}$) can therefore be blended with user teleoperation output $\mathbf{v}_{op}$ from the user as follows:

$$\mathbf{v} = \mathbf{P}_{\oplus}\mathbf{v}_{op} - \lambda\mathbf{J}_s^{\oplus\mathbf{H}}\mathbf{e} \tag{4.7}$$

where $\mathbf{P}_{\oplus} = \mathbb{I}_2 - \mathbf{J}_s^{\oplus\mathbf{H}}\mathbf{J}_s$ is the projection operator presented in [MC07]. The projection operator $\mathbf{P}_{\oplus}$ projects the components of $\mathbf{v}_{op}$ (which is the desired user teleoperation velocity output) onto the null space of the wall collision avoidance task so that manual control does not

disturb the visual task which has higher priority *only when in danger of wall collisions*. Thus when both features are in their safe intervals, the visual task is fully deactivated and the user has full control as $\mathbf{P}_{\oplus} = \mathbb{I}_2$. We then obtain a smooth and progressive trajectory correction framework that is only activated in case of danger (i.e. as the wheelchair is in danger of colliding with the corridor wall).

4.1.3 Discussion

From the assistive velocity controller (4.7) that we designed in a bottom-up manner, we can infer a linear formalism for sharing control. Here one can observe that the projection operator $\mathbf{P}_{\oplus} = \mathbb{I}_2 - \mathbf{J}_s^{\oplus\,\mathbf{H}}\mathbf{J}_s$ represents the *amount or level* of control the user possesses at a particular instant.

Naturally, if all the visual features are in their safe intervals, $\mathbf{J}_s^{\oplus\,\mathbf{H}}\mathbf{e}$ is null which makes $\mathbf{P}_{\oplus} = \mathbb{I}_2$, and the system does not realize any automatic control. At this point the user has full control over the motion (as there is no risk of collision). As soon as the features leave their safe intervals, $\mathbf{J}_s^{\oplus\,\mathbf{H}}$ becomes non-zero and the system *progressively* takes up some control over the motion. When both the features are constrained by the visual task we have $\mathbf{J}_s^{\oplus\,\mathbf{H}}\mathbf{J}_s = \mathbb{I}_2$ and at this point the system has full control.

4.1.4 Integrating Haptic Guidance

Such a semi-autonomous assistive system which provides a progressive assistance in the form of wall collision avoidance is an extremely helpful tool for wheelchair users. But in the case of users suffering from severe motor disabilities and visual/cognitive impairments, automatic trajectory correction may reduce the quality of experience, mainly if the user is not able to immediately perceive the danger. In order to *communicate the objective of the system* to the user and to notify the user of his unsafe trajectory, we propose to design an *active* joystick force feedback mechanism that intuitively guides the user out of his/her unsafe trajectory. Thus we have to set an optimal mapping function that maps the assistance provided to the force fed back for guidance.

We assume a 2-DOF haptic joystick having the capability of assigning forces in the x_F and y_F directions with $\mathbf{F} = (f_x, f_y)^T$ as illustrated in Figure 4.2(a).

As we have seen in the previous subsection, $\mathbf{P}_{\oplus} = \mathbb{I}_2 - \mathbf{J}_s^{\oplus\,\mathbf{H}}\mathbf{J}_s$ represents the *amount* of control that the user has at a particular configuration. Thus if the maximum exertable force at nominal position by the haptic joystick is denoted by f_{max} (expressed for example, in Newtons), we can determine the force feedback $\mathbf{F}$ as

$$\mathbf{F} = \alpha_{\mathbf{F}}\mathbf{J}_s^{\oplus\,\mathbf{H}}\mathbf{J}_s\mathbf{F}_{\mathbf{max}} \tag{4.8}$$

where $\mathbf{F}_{\mathbf{max}} = (\pm f_{max}, \pm f_{max})^T$ and $\alpha_{\mathbf{F}}$ is a factor required to normalize the force so that it can be handled by the user (or a factor that can be parametrized depending on the user's

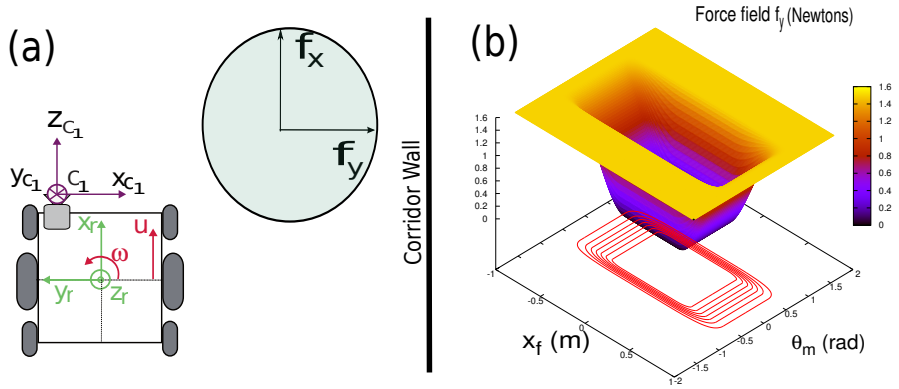

Figure 4.2: (a) The haptic joystick frame with respect to the geometric model of the wheelchair as defined in Section 3.1. (b) Model variation in the absolute value of f_y with respect to the variation in visual features x_f and θ_m. Generated using $x_f^{s-} = -0.3$m, $x_f^{s+} = 0.3$m, $x_f^- = -0.9$m, $x_f^+ = 0.9$m, $\theta_m^{s-} = -0.5$rad, $\theta_m^{s+} = 0.5$rad, $\theta_m^- = -0.8$rad, $\theta_m^+ = 0.8$rad. The upper bound f_{max} was set at 1.5 N and α at 1. We can observe the progressive increase in force from 0 to 1.5 as the visual features leave their safe interval.

capabilities). The sign of the x_F and y_F components in $\mathbf{F_{max}}$ depends on the visual features x_f and θ_m at a particular instant. We have

$$\mathbf{F_{max}} = \begin{cases} (-f_{max}, -f_{max})^T & \text{if } x_f \leq x_f^* \text{ and } \theta_m > \theta_m^* \\ (-f_{max}, f_{max})^T & \text{if } x_f \leq x_f^* \text{ and } \theta_m \leq \theta_m^* \\ (f_{max}, -f_{max})^T & \text{if } x_f > x_f^* \text{ and } \theta_m > \theta_m^* \\ (f_{max}, f_{max})^T & \text{if } x_f > x_f^* \text{ and } \theta_m \leq \theta_m^* \end{cases} \tag{4.9}$$

Therefore, when $\mathbf{J}_s^{\oplus \mathbf{H}}$ is null, no force is applied on the joystick. As the matrix becomes non-zero and eventually reaches rank 2, the force $\mathbf{F}$ increases progressively and reaches $\alpha_{\mathbf{F}}\mathbf{F_{max}}$. At this point the control system has full control and a maximum force is applied on the joystick to notify the user of his dangerous trajectory. A model force variation in the absolute value of f_y is shown in Figure 4.2 with respect to variations in the visual features.

It has to be noted that the force applied modifies the position of the joystick at a particular configuration (in a direction which safely corrects the motion of the wheelchair) thereby affecting $\mathbf{v}_{op}$. Thus we can define it as an active feedback scheme. This does not affect the system stability since the user output is explicitly considered in the control design. This also ensures that a minimal automatic correction will be required from the system for collision avoidance thus leading to a higher quality of experience.

But it is also possible to design a system that *passively* guides the user by taking into account the force fed back $\mathbf{F}$ as well as the force applied by the user $\mathbf{F_{op}}$ against the feedback force. In that case, we have

$$\mathbf{v} = \mathbf{P}_{\oplus}(\mathbf{v}_{op} - \mathbf{v}_f) - \lambda \mathbf{J}_s^{\oplus \mathbf{H}} \mathbf{e} \tag{4.10}$$

where $\mathbf{v}_f$ represents the velocity that would be transmitted to the wheelchair motion control system as a result of the feedback force $\mathbf{F}$ and the user force $\mathbf{F_{op}}$. In this study we refrain to

active feedback as the preliminary tests have concluded that it is more intuitive and helpful in guiding a user than a passive feedback scheme.

4.1.5 Experimental Analysis

Test Setup

We performed an extensive analysis in order to assess the effectiveness of the assistive mechanism (4.7) and the feedback guidance scheme (4.8) as a modular and efficient tool for safe corridor navigation.

An off-the-shelf wheelchair manufactured by You-Q which was robotised using the ROS middleware [QCG+09a] was used for the tests. A front facing Raspberry Pi camera module with an 85° field of view (fov) was rigidly fixed on the left handle as shown in Figure 4.3. It was also coarsely calibrated with $h = 0.8$m, $w = 0.32$m and $l = 0.4$ m. A traditional joystick as well as a Phantom Omni haptic device were connected to the wheelchair control system in order to compare the proposed control scheme with and without force feedback. The haptic joystick had a maximum exertable force $f_{max} = 3.3$N at nominal position. Keep in mind that this device is not designed to drive a wheelchair, nor is it adapted to handicapped people. The aim here is to evaluate the proposed concept of providing *a force feedback that is directly proportional to the assistance*. We are currently designing an adapted haptic joystick.

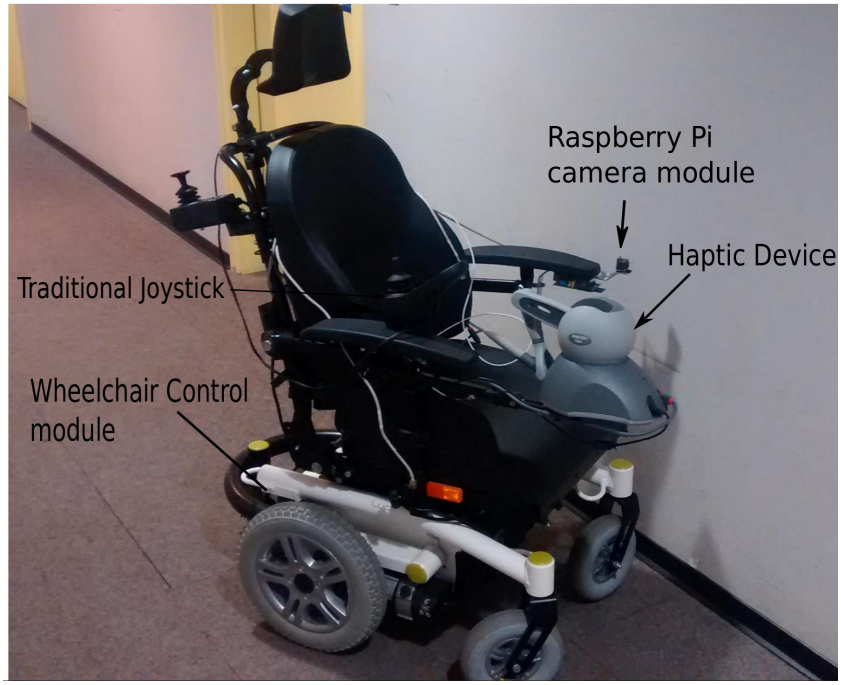

Figure 4.3: Wheelchair test platform

Prior to the feature extraction process the images were rectified against distortions from the camera lens. For ground truth estimation and visualisation purposes, the wheelchair was equipped with a laser range finder. This laser range finder was used neither in the visual feature extraction process nor in the control law. It only acted as a validation tool.

In order to perform experiments using the control law proposed in the present work, the parameters to be determined are: the boundaries of the activation intervals (i.e x_f^+, x_f^{s+}, x_f^-, x_f^{s-}, θ_m^+, θ_m^{s+}, θ_m^- and θ_m^{s-}), the control gain λ and the factor α (see Eqn. (4.8)).

x_f^+, x_f^{s+}, x_f^-, x_f^{s-} are directly dependent to the field of view (fov) of the camera. In our setup, the maximum and minimun possible values of x_f are respectively equal to $\tan(fov/2) \approx 0.916$ and $-\tan(fov/2) \approx -0.916$. Under these constraints, we chose $x_f^+ = 0.9$ and $x_f^- = -0.9$ to ensure the visibility of the vanishing point. As the visual feature extraction algorithm needs to detect both floor/wall boundary lines, we chose $x_f^{s+} = 0.3$ and $x_f^{s-} = -0.3$, to ensure the visibility of these features.

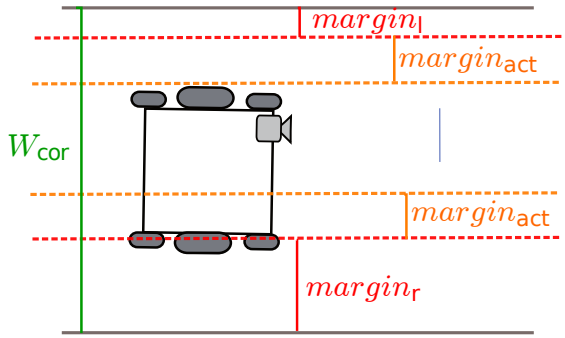

Figure 4.4: Margin definition

θ_m^+, θ_m^{s+}, θ_m^- and θ_m^{s-} are directly dependent to the width of the corridor used during the experimentation. The width of the corridor W_{cor} can be estimated online during the feature extraction process using $W_{cor} \approx h\,(tan(\theta_l) + tan(\theta_r))$. Thus one can say that the assistance scheme could automatically adapt to new corridors. Then we define $margin_l$ and $margin_r$ as the approximate margin between the walls and the camera. $margin_{act}$ is defined as depicted in Figure 4.4. We can then determine

$$\theta_m^+ = \arctan\left(\frac{W_{cor} - 2margin_r}{h}\right) \qquad (4.11)$$
$$\theta_m^{s+} = \arctan\left(\frac{W_{cor} - 2margin_r - 2margin_{act}}{h}\right)$$

$$\theta_m^- = \arctan\left(\frac{2margin_l - W_{cor}}{h}\right) \qquad (4.12)$$
$$\theta_m^{s-} = \arctan\left(\frac{2margin_l + 2margin_{act} - W_{cor}}{h}\right)$$

In our experiments, we chose $margin_l = 0.15$m, $margin_r = 0.60$m and $margin_{act} = 0.30$m, and W_{cor} is estimated using the camera at initialisation and is kept constant for the rest of the experiments. This is done in order to negate the effects of a varying θ_m interval. Finally the gain λ was empirically determined and set at 0.3 and the normalizing factor $\alpha_{\mathbf{F}}$ at 0.7 so that the maximum force experienced by the user is capped at 2.2N [NAS95].

For analysing the full potential of the control system, a non-disabled user was asked to steer the wheelchair along corridors. Initial tests were carried out using a traditional joystick with no feedback in order to assess the efficacy of the assistance scheme for wall collision avoidance. Later tests were carried out using the haptic joystick in order to gauge the effects of force feedback on trajectory correction and user experience. The visual task is activated as soon as the wheelchair starts the motion and it is switched off as the user reaches the end of the corridor.

Semi-autonomous navigation without force feedback

As the user drives the wheelchair manually in the corridor, Figures 4.8 and 4.9 respectively show the variation of the visual features x_f and θ_m plotted along with their activation factors h_{x_f} and h_{θ_m}. Figure 4.7 presents the evolution of the user teleoperation ($\mathbf{v}_{op}$) and final system velocities ($\mathbf{v}$) during the experimentation with the corresponding translational components v and v_{op} (top) and the angular components ω and ω_{op} (bottom).

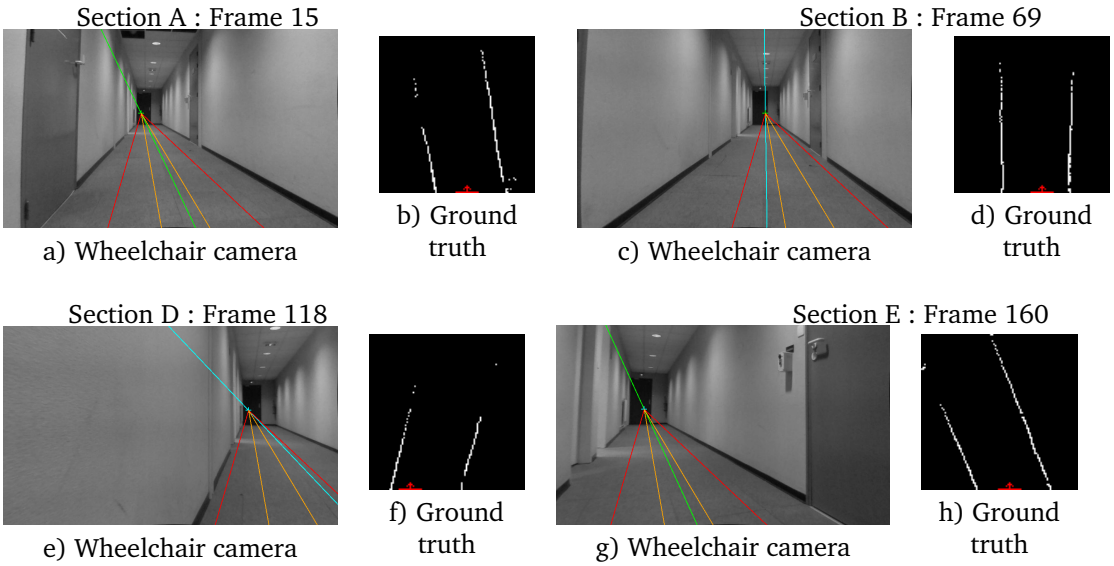

a) Wheelchair camera
b) Ground truth
c) Wheelchair camera
d) Ground truth
e) Wheelchair camera
f) Ground truth
g) Wheelchair camera
h) Ground truth

Figure 4.5: Wheelchair camera frames and ground truth during the experimentation

Each plot is divided into sections for easier analysis. Figure 4.5 presents outputs of the wheelchair camera together with visualization of the position of the wheelchair in the corridor from the laser range finder at different key points during the experimentation. On each camera output, the blue/green line represents the estimated middle line of the corridor and the cross represents the estimated position of the vanishing point (which is also the intersection of the

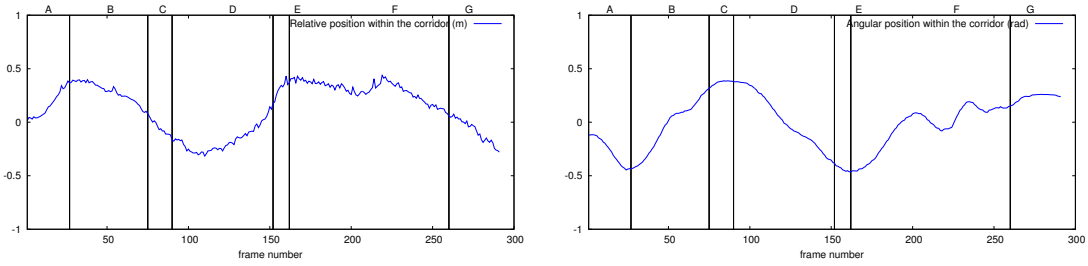

(a) (b)

Figure 4.6: (a). The relative position of the wheelchair with respect to the median of the corridor. (b). The heading of the wheelchair with respect to the median of the corridor. Plots are obtained by initially reconstructing the laser scan output (see Figure 4.5) using Hough transform in order to discriminate the longest lines in the image. The relative position and orientation can be then extracted be from the position and orientation of the two detected lines.

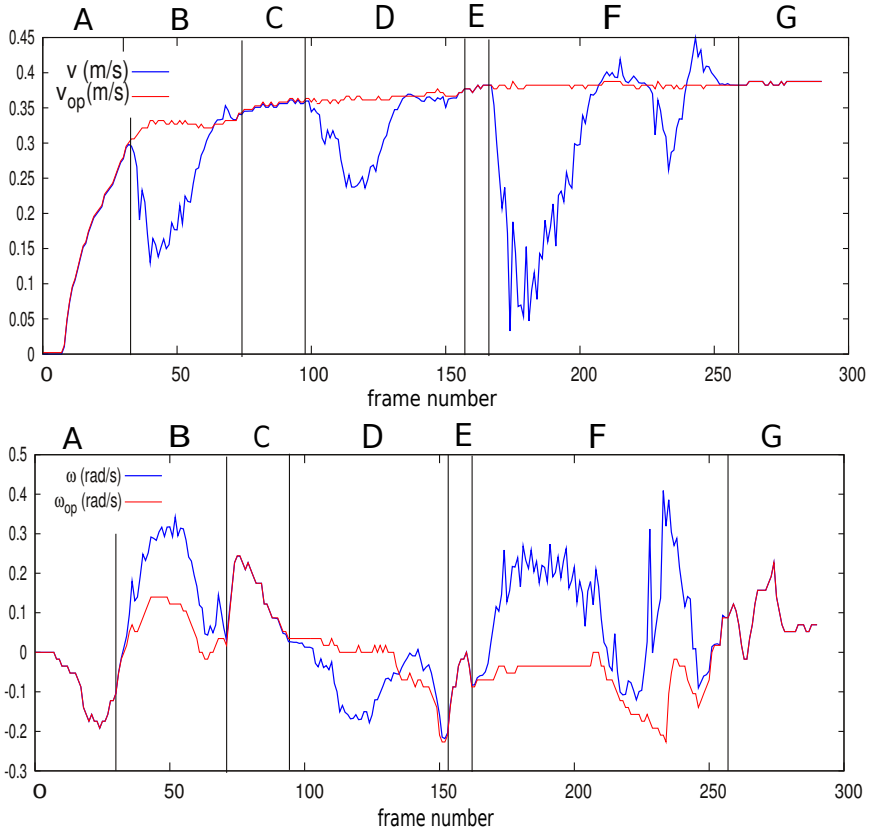

Figure 4.7: Evolution of v along with v_{op} and ω along with ω_{op}.

lines plotted in the images). The color of the line (cross) refers to the value of h_{θ_m} (h_{x_f}): it is green when $h_{\theta_m} = 0$ ($h_{x_f} = 0$) and blue when $h_{\theta_m} > 0$ ($h_{x_f} > 0$). The red and orange lines

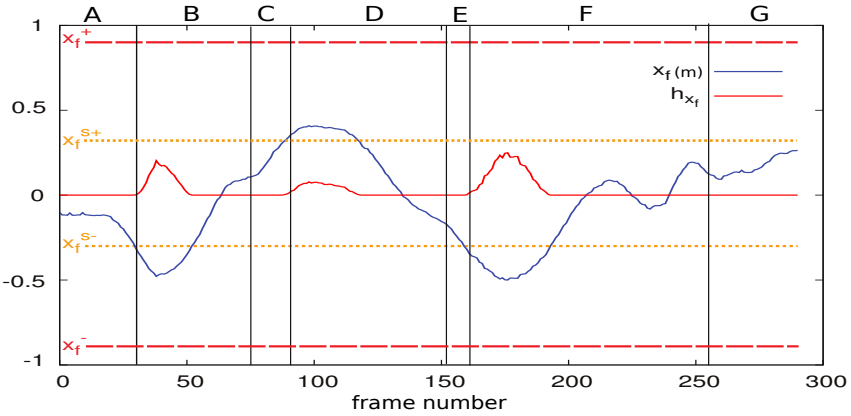

Figure 4.8: Evolution of x_f along with its activation factor h_{x_f}.

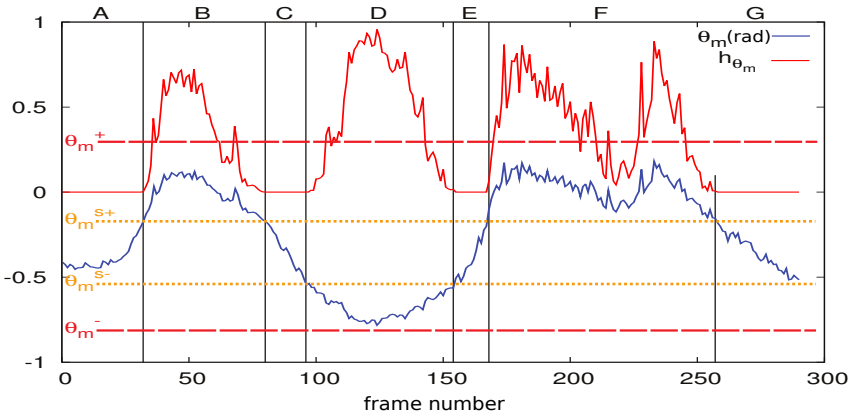

Figure 4.9: Evolution of θ_m along with its activation factor h_{θ_m}.

correspond to the boundary of θ_m according to (4.3). On each output of the laser range finder, the position of the wheelchair has been depicted in red with an arrow depicting the orientation. Finally for a better comprehension of the configuration of the wheelchair in the corridor, the relative position and heading of the wheelchair with respect to the median line of the corridor are shown in Figures 4.6a and 4.6b.

Note that for this experiment we obtained, from Eqns. (17) and (18), $\theta_m^+ = 0.3$ rad, $\theta_m^{s+} = -0.2$ rad, $\theta_m^- = -0.55$ rad and $\theta_m^{s-} = -0.8$ rad, since $W_{cor} = 1.8$m. Also the video stream from the camera corresponded to a resolution of 808x480 pixels with a frame rate of 15 frames per second.

In Figure 4.7, in parts A, C, E and G, we can then observe that $v = v_{op}$ and $\omega = \omega_{op}$ since $h_{x_f} = 0$ and $h_{\theta_m} = 0$. This is owing to the fact that x_f remains in the $[x_f^{s-}, x_f^{s+}]$ interval and θ_m remains in the $[\theta_m^{s-}, \theta_m^{s+}]$ interval (see Figures 4.8 and 4.9). The user has then full control of the

wheelchair in both translation and rotation. In Figure 4.5, frame 15 corresponds to part A and frame 160 corresponds to part E. On the laser range finder, we can observe that the wheelchair is in the middle of the corridor with a low orientation angle. In such a case, there is no risk of collision with the wall and the user has full control over the wheelchair motion.

Whereas in parts B,D and F, $h_{x_f} > 0$ and $h_{\theta_m} > 0$. We can then observe that $v \neq v_{op}$ and $\omega \neq \omega_{op}$. If we observe Figure 4.5c (Section B, frame 69), the wheelchair is close to the right wall with a low orientation angle. There is then a risk of collision if the user tries to turn right. Therefore, the control law is activated and augments v_{op} and ω_{op} to avoid wall collision. Moreover in part D (see Figure 4.5e, related to the frame 118), the wheelchair is close to the left wall and oriented toward the wall. There is an imminent risk of collision. The translation velocity v is reduced to avoid collision and the rotation velocity ω is forced to a negative value to get further from the wall.

We can observe that during the experimentation, x_f and θ_m were respectively forced by the visual servoing to remain in the interval $[x_f^{s-}, x_f^{s+}]$ and $[\theta_m^{s-}, \theta_m^{s+}]$ as expected. The behaviour of the system demonstrates that as the wheelchair gets closer to the corridor walls, the wall avoidance visual task is progressively activated thereby forcing the visual features into their safe intervals. This effectively steers the wheelchair away from the walls and into safety.

Semi-autonomous navigation with force feedback

A similar trial was carried out with force feedback added into the loop as explained in Section 4.1.4. In this case, we obtain $\theta_m^+ = 0.5$ rad, $\theta_m^{s+} = -0.1$ rad, $\theta_m^- = -0.6$ rad and $\theta_m^{s-} = -1$ rad and the video stream from the camera corresponded to a resolution of 640x480 pixels with a frame rate of 90 fps.

The evolution in the visual features x_f and θ_m along with their respective activation factors h_{x_f} and h_{θ_m} are plotted similarly in Figures 4.12 and 4.13. The variations in the forces f_x and f_y transmitted to the haptic joystick are given in Figure 4.14. Figure 4.15 represents the user teleoperation and final system velocity components namely v_{op} with v and ω_{op} with ω. Figure 4.16 shows the variation in the automatic correction applied by the system in order to avoid wall collisions that is $\mathbf{v_r} = [v_r, \omega_r]^T$ where $\mathbf{v_r} = -\lambda \mathbf{J}_s^{\oplus \mathbf{H}} \mathbf{e}$. Each plot is discretized into nine parts (A-I) for analysis. Finally, camera frames at specific points during the experiment are shown in Figures 4.26 and 4.11. The extracted features are overlayed onto each image as explained in the previous Section.

It can be seen that in parts A, E, G and I the visual features are within their safe intervals and no force is applied on the joystick. Also, the translational and rotational velocities v_{op} and ω_{op} transmitted by the user completely match the final system velocities v and ω. This means that the user has full control over the motion since there is no risk of collision with the walls. Figure 4.26 shows the camera frames at parts A, E and I. Again at this point it can be said that the wheelchair is nearly in the middle of the corridor and is executing a safe motion.

Whereas in parts B, C, D, F and H, either one or both visual features are outside their safe

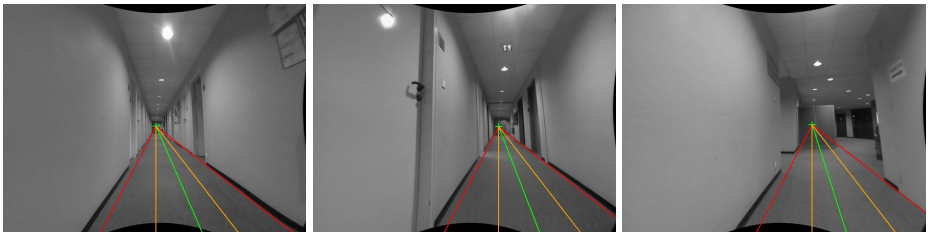

(a) Sec. A, Frame 213 (b) Sec. E, Frame 445 (c) Sec. I, Frame 1090

Figure 4.10: Camera frames at parts A, E and I where assistance and force feedback are not provided by the system.

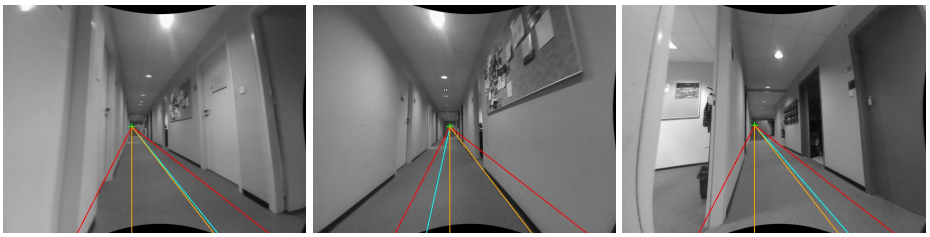

(a) Sec. B, Frame 256 (b) Sec. D, Frame 382 (c) Sec. F, Frame 643

Figure 4.11: Camera frames at parts B, D and F where assistance and force feedback are provided by the system.

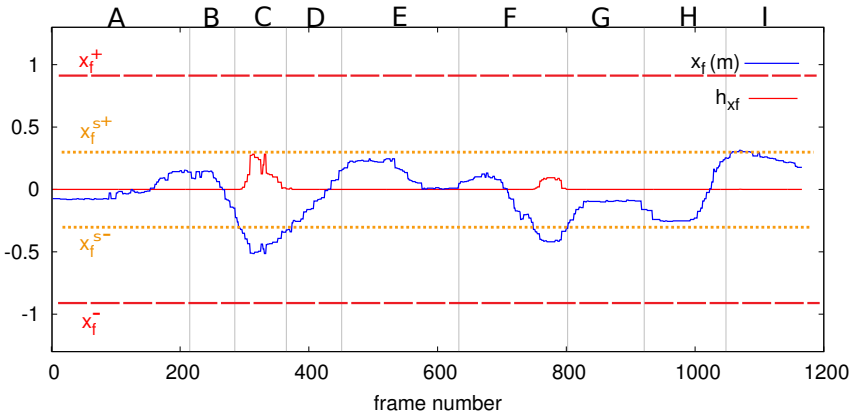

Figure 4.12: Visual feature x_f along with activation factor h_{x_f}.

intervals that leads to the activation of trajectory correction with force feedback. The camera frames at parts B, D and F are illustrated in Figure 4.11. Clearly the wheelchair is close to the walls: this can be observed from the orientation of the median line and the position of the vanishing point. As the activation factors h_{x_f} and h_{θ_m} moves from zero to non-zero, it can be seen that the feedback force applied on the joystick increases (and decreases) in a near smooth manner. When considering the velocities, it can be observed that the user and the system

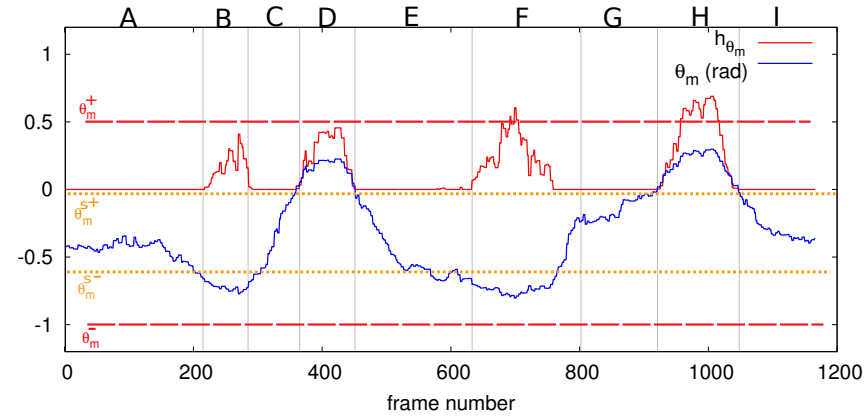

Figure 4.13: Visual feature θ_m along with activation factor h_{θ_m}.

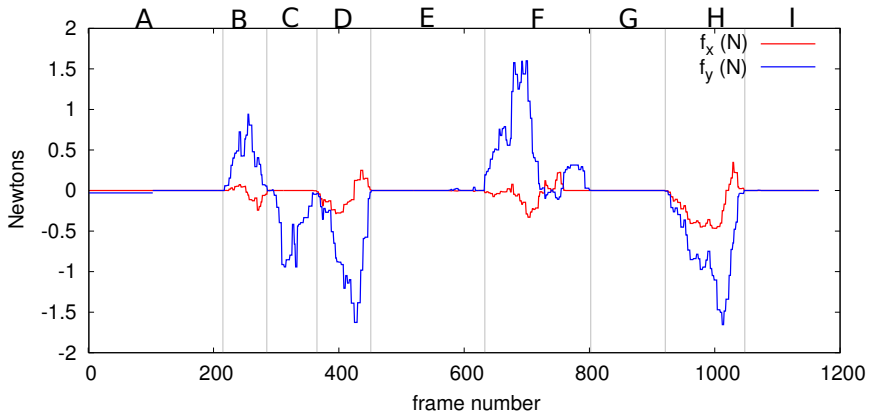

Figure 4.14: Evolution of the force applied on the haptic device in x and y directions of the haptic frame (see Figure 4.2).

velocities are not equal. But owing to the force feedback, the difference between the user and the system velocities is reduced. The corrective velocities in Figure 4.16 also show that the system does not have to automatically correct the trajectory even when there exists a risk of collision, especially during parts B,C and F. This is in contrast with the results presented in the above subsection where it can be seen that the difference between the user and the system velocities is proportional to the values of the activation factors h_{x_f} and h_{θ_m}. Moreover, the small difference in user and system (robot) velocities can be attributed to the force applied by the user against the feedback force provided by the system in order to execute his original *unsafe* maneouver.

Thus, the feedback force serves as a corrective mechanism by itself which modifies the user teleoperation progressively and thus automatically corrects the motion of the wheelchair. Also, this force can be related as a guidance tool which helps the user to identify the dangerousness (i.e. danger of wall collision) of the situation and act accordingly. Therefore, it can be said that the proposed haptic feedback system serves as a tool for intuitive trajectory correction.

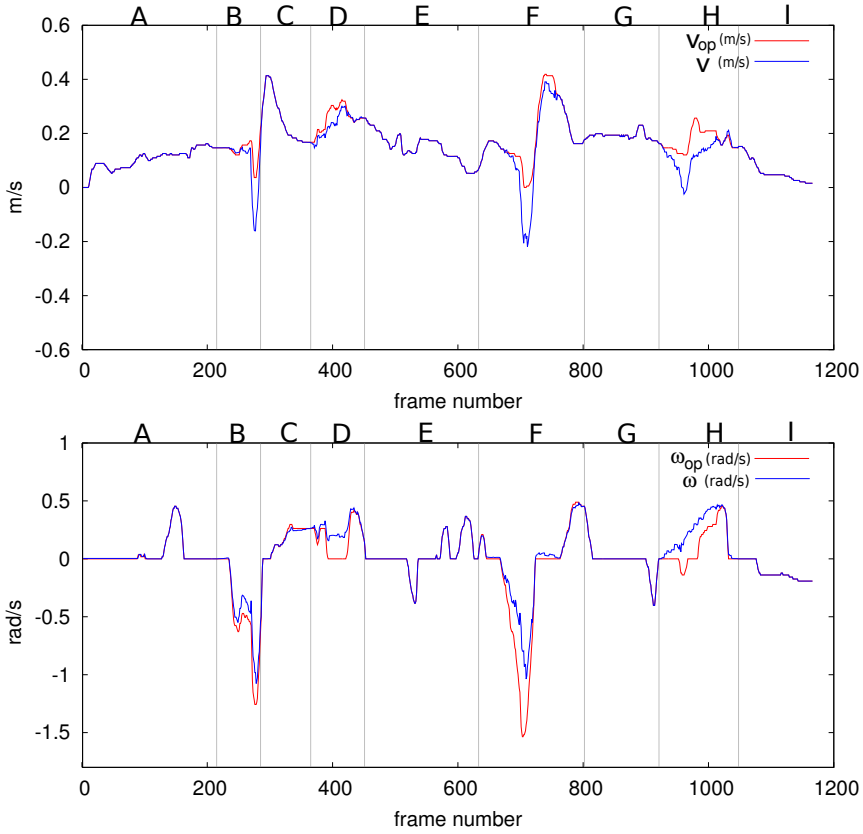

Figure 4.15: Evolution of v along with v_{op} and ω along with ω_{op}.

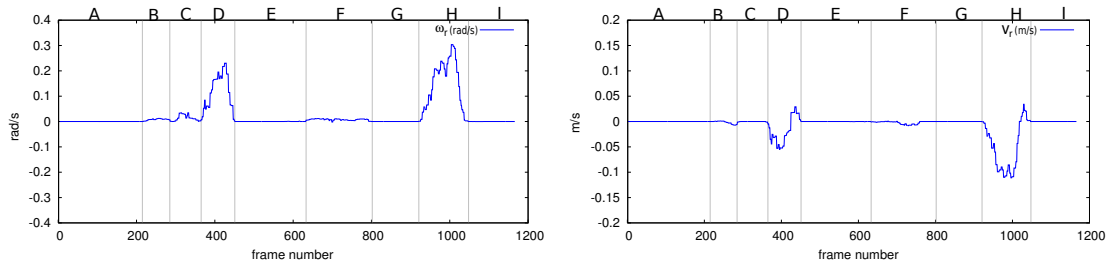

Figure 4.16: The corrective angular velocity (ω_r) and translational velocity (v_r) for wall collision avoidance

Robustness

In order to test the robustness of the solution, part of another run of the same experiment is presented where wheelchair is driven at a much higher velocity than normal in a lowly lit corridor. As we have already seen the robustness of feature extraction and tracking in the previous Chapter (see 3.2.2), we here aim to convey the robustness of the assistive controller with respect

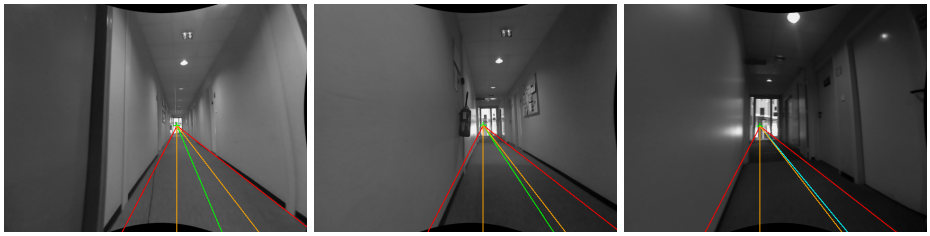

(a) (b) (c)

Figure 4.17: Camera frame snapshots pertaining to a corridor following experiment with force feedback where the user drove faster in a low illumination corridor.

to variations in speed and illumination. Figure 4.20 displays the translational and rotational components of the user and the final system velocities. It can be seen that the average speed is much higher when compared to the two previous experiments. Moreover, Figure 4.17 shows the camera frames at selected instants where it can be seen that the illumination is darker but the evolution of the visual features (Figures 4.18 and 4.19) remain consistent. This experiment verifies the robustness of the system particularly in cases where a wheelchair user may have erratic driving due to motor impairments.

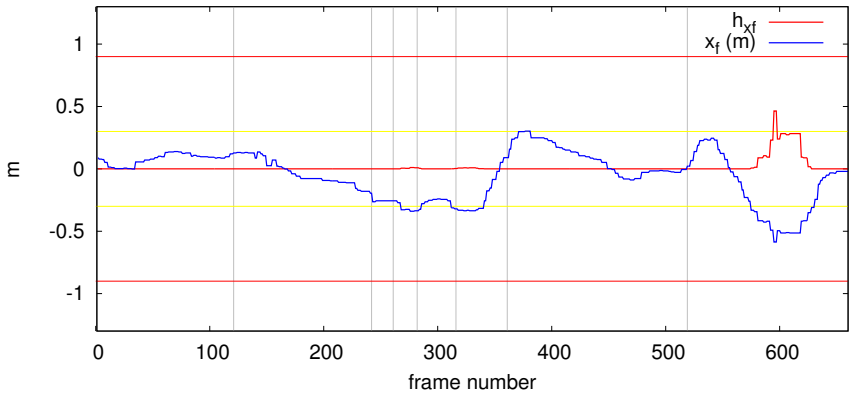

Figure 4.18: Visual feature x_f along with activation factor h_{x_f} (Faster Driving and Low Illumination).

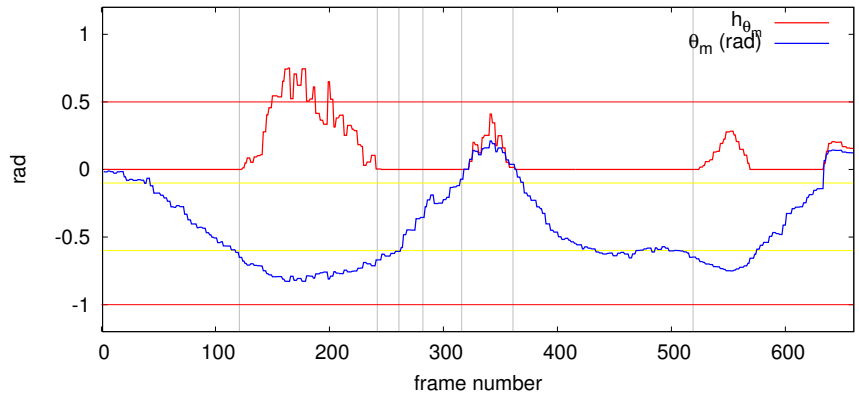

Figure 4.19: Visual feature θ_m along with activation factor h_{θ_m} (Faster Driving and Low Illumination).

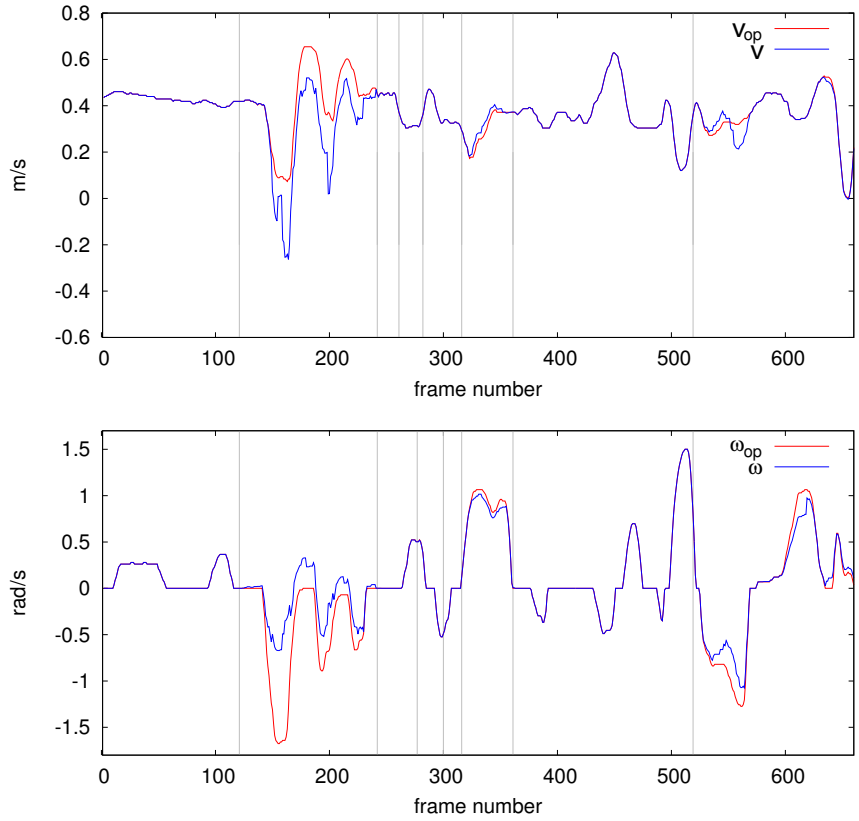

Figure 4.20: Evolution of v along with v_{op} and ω along with ω_{op} (Faster Driving and Low Illumination).

The results demonstrate the effectiveness of the proposed bottom-up vision-based solution as a robust assistive system for the fundamental indoor navigation task of corridor following.

A preliminary conclusion would be the inference of a linear control sharing formalism where we progressively tune a factor (**H**) that weights the velocities coming from the user and the vision-based controller for efficient assistance. We can thus move onto a top-down approach for designing an assistive controller for the task of doorway passing as in this case we need to incorporate the *intention of the user*.

4.2 Assisted Doorway Passing

As detailed in the previous section, we adhered to a bottom-up approach for designing assistance scheme in Section 4.1, by initially designing a wall collision avoidance task from the autonomous visual task of corridor following. The resulting control sharing formalism turned out to be a linear blending policy, where the major constraint in that the user must be the primary controller was satisfied. The system could progressively take control if there was perceived danger of collision with walls. Conversely, if the system identifies that the human has the potential to steer the wheelchair safely then it was preferable to assign full control to the user.

Meanwhile, the task of doorway passing is not trivial compared to the task of corridor following in that the *intention of the user* is an important factor to consider (i.e. whether the user want to pass through a specific doorway or not). Thus, inferring from the resulting assistive velocity controller from the previous section, we here propose a linear control sharing formalism for assisted doorway traversal, owing to the already established vision-based control scheme (Section 3.3) for autonomous doorway passing. But before moving onto the design, the following subsection summarizes the control law.

4.2.1 The control law

Recall that we used 2 cameras mounted on the wheelchair in order to propose vision-based controllers that allowed us to perform the task of corridor following as shown in Figure 3.9. In order to realize the task of doorway passing we formally defined a visual feature as the angle ϕ_d. The task was then realized by regulating this visual feature to a desired value of ϕ_d^* by the means of a visual control scheme. Owing to the desired behaviour of ϕ_d^*, a novel control scheme was designed which assures global asymptotic convergence of the visual feature ϕ_d to ϕ_d^* by assigning Lyapunov conditions to a function $V = \frac{1}{2}(\phi_d - \phi_d^*)^2$. Thus the angular velocity of the wheelchair can be expressed as a function of the estimable parameters ϕ_d and r, as follows

$$\omega = \frac{-k(\phi_d - \phi_d^*) - A(r, \phi_d)u^*}{1 + B(r, \phi_d)},$$

where when $r > m$

$$\begin{cases} A(r, \phi_d) = \dfrac{\sin(\phi_d - \phi_d^*)}{r\cos(\phi_d^* - \theta)} \\ B(r, \phi_d) = \dfrac{l\cos(\phi_d - \phi_d^*) - w\sin(\phi_d - \phi_d^*)}{r\cos(\phi_d^* - \theta)} \end{cases}$$

and when $r \leq m$

$$\begin{cases} A(r, \phi_d) = \dfrac{\sin(\phi_d - \theta)}{r} \\ B(r, \phi_d) = \dfrac{l\cos(\phi_d - \theta) - w\sin(\phi_d - \theta)}{r} \end{cases}.$$

This formulation ensured that the visual feature ϕ_d converges asymptotically to the desired value ϕ_d^* as can be seen from Section 3.3.

4.2.2 Fusion of User and Robot Control - Respecting user intention

If we have, at each time step, $\mathbf{v}_{op} = (v_{op}, \omega_{op})$ as the user teleoperation output and $\mathbf{v_r} = (v_r, \omega_r)$ as the calculated system velocity based on the above summarized control scheme (and detailed in Section 3.3), we propose to set the final velocity $\mathbf{v} = (v, \omega)$ to the motion control system as

$$v = \exp(-\alpha) v_{op}, \tag{4.13a}$$

$$\omega = (1 - \alpha)\omega_{op} + \alpha\omega_r. \tag{4.13b}$$

In order to arbitrate between the user and the robot velocities, we observe that the translational velocity component v is weighted by a factor $\exp(-\alpha)$ while the angular velocity component ω is shared using the linear control sharing formalism (as in Eqn. (4.7)). Indeed, we hypothesize here that, in tight or dangerous situations where the user may require assistance, the motion of the wheelchair can be adapted by correcting the angular velocity while *restricting* the user translational velocity. Note that ω_r is determined from the control law (3.30). An extensive stability analysis the shared control scheme for a non-holonomic mobile robot is detailed in [WL14]. The work uses convex analysis to prove that a linear assistive velocity controller of the form (4.13b) is stable unless the intersection of the set of possible user inputs and the set of possible robot commands is null. This condition can be avoided by tuning the gain k in (3.30).

This linear blending formalism is directly inferred from Equation (4.7). As we use only a single visual feature in the form of ϕ_d, the projection operator reduces to $(1 - \alpha)$. Therefore, the scalar assistance factor $\alpha \in [0, 1]$ encodes the level of control the robot (and thereby the user) has at a particular configuration. We then propose a perceptive and adaptive strategy for designing the assistance factor α by taking into account the intention of the user and the level of assistance required (based on safety considerations).

This strategy encodes a simple and intuitive concept that, the system should assist if and only if **the confidence in the predicted user intention is high** [DS12] and **if the user requires assistance in performing the task**. This differs from the design in previous Section 4.1 where we always assume that the user is following the corridor.

Thus the assistance factor α can be decomposed as

$$\alpha = \alpha_I \alpha_L \tag{4.14}$$

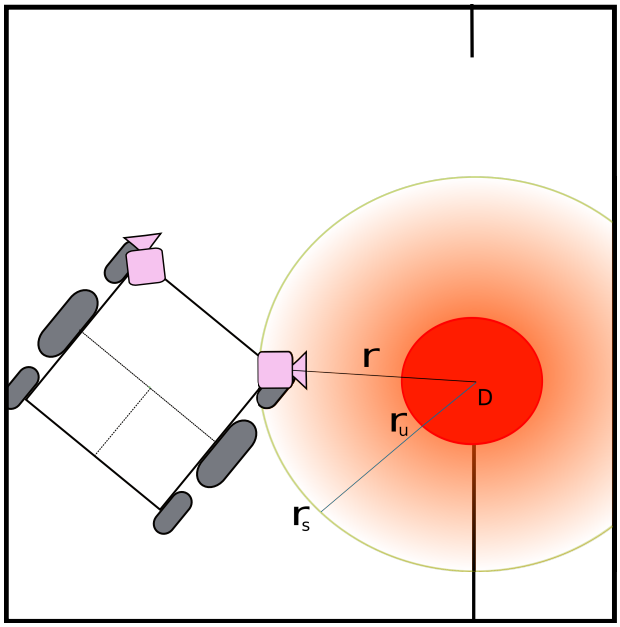

Figure 4.21: Representative system confidence in user intention with respect to a specific doorpost D. Redder zones indicate higher confidence

where α_I represents the confidence in user intention and α_L represents the level of assistance required by the user.

In the case of doorway passing, the user intention analysis provides us the specific doorway to pass through from a set of multiple detected doors. The confidence in the user intending to pass through a specific doorway can quite simply be a *progressive* normalization of the distance r to a specific doorpost. Accordingly, α_I is 0 when the value of r (for a specific detected doorpost) is outside a higher value r_s and gradually increases to 1 as r approaches the lower value r_u and remains 1 thereafter. This normalization can be defined as follows and can be visualised in Figure 4.21.

$$\alpha_I = \begin{cases} 0 & \text{if } r > r_s \\ (1 - \cos(\pi \frac{(r - r_s)}{(r_u - r_s)}))/2 & \text{if } r_u \geq r \geq r_s \\ 1 & \text{if } r < r_u \end{cases} . \tag{4.15}$$

Thus we can say that if the value of $\alpha_I \sim 1$ then the system is fully confident that the user wants to pass through the *specific* doorway.

But even if the controller is confident in the user intention, unnecessary assistance should not be provided if the user is not in danger (i.e. is executing a fairly safe motion). The level of assistance required by the user can be encoded in α_L which can be determined from the deviation of the user from normal behaviour (i.e desired trajectory). Therefore the feature error $(\phi_d - \phi_d^*)$ can be employed in order to design this factor. We then propose the following definition

$$\begin{cases} \alpha_L = 1 - e^{(-g|\phi_d - \phi_d^*|)} & \text{if} \quad r > m \\ \alpha_L = \alpha_L | r = m & \text{if} \quad r \leq m \end{cases} . \tag{4.16}$$

We observe that as the error increases, the value of α_L exponentially varies to 1 and it moves to zero as soon as the features error tends to zero. But as soon as the value of $r \leq m$, α_L takes up a constant value which it attains at the instant $r = m$. This is done to ensure that there is no discontinuity as the parameters of the control law (i.e $A(r, \phi_d)$ and $B(r, \phi_d)$) switches from one form to another at $r = m$ (See Eqns. (3.28) and (3.29)). In Equation (4.16), g is a normalizing factor that is adjusted empirically.

This means that the system takes control only when it is sure that the intention of the user is to pass through a specific doorway **and** when the user is not executing a fairly safe motion. Moreover, the definition of the assistance factor α could ensure a progressive variation in control sharing that is necessary for smooth assistance. Furthermore, the design of the shared control scheme also ensures a gradual trajectory correction process. It can be postulated that it may also serve as a doorpost collision avoidance mechanism. In practice the factor α is calculated for every detected doorpost and the highest value which invariably pertains to the *nearest doorpost* is used in the control process.

4.2.3 Simulations

In order to validate the developed fusion formulation, we have simulated two different cases. We aim to check the effectiveness of the proposed method as an assistive scheme for trajectory correction as well as a doorpost collision avoidance. A Cartesian frame centred at the doorpost is defined in order to visualise the trajectory of the wheelchair. The doorpost D_{sim} is located at the origin and the wheelchair starts at a position (x_{door}, y_{door}) with respect to D_{sim}. We simulate ideal cases where $w = 0$ and $l = 0$ in order to asses the performance.

- Case I, where the wheelchair is located at $(x_{door}, y_{door}) = (-1.5, -1)$m and is oriented so that it is facing the doorpost directly. This denotes that the user is en-route for a direct collision with the doorpost.

- Case II, where the initial position is set at $(x_{door}, y_{door}) = (-0.2, -1.0)$m and the initial heading is set at a low value of 0.05 rad with respect to x-axis. This case represents a situation where the user intends to move along the corridor but the initial heading and proximity to corridor wall may result in collision with the doorpost. $\mathbf{v}_{op}$ is set as constant $[0.2, 0]^T$ in both cases.

The interval $[r_s, r_u]$ was taken to be $[0.8, 0.1]$ m and the normalizing factor g was set at 2. The gain k of the control law (3.30) is set as 1.5. The trajectories taken by the wheelchair are shown in Figure 4.22. The evolution of α along with its components α_I and α_L for both the cases are shown in Figure 4.23.

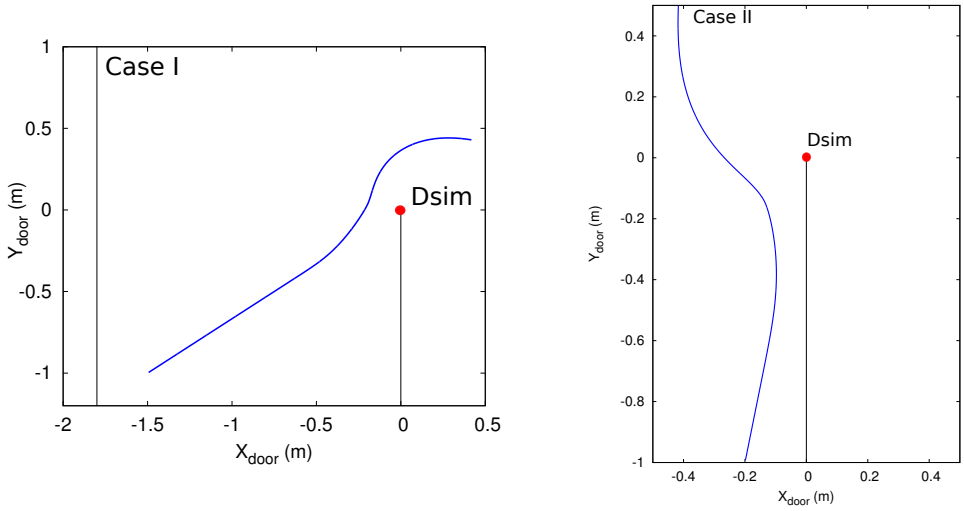

Figure 4.22: The trajectories taken by the robot for Cases I (left) and II (Right).

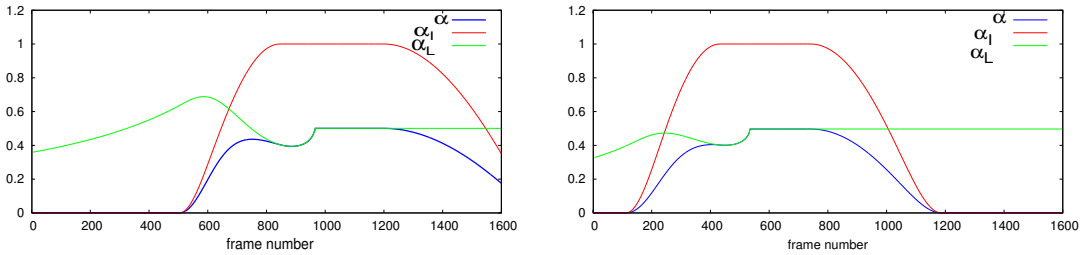

Figure 4.23: The evolution of the assistance factor α and its components α_I and α_L for Cases I (Left) and II (Right).

It is evident that the control scheme tries to avoid the doorpost located at $(0, 0)$ in both the cases. In Case I the control system manages to divert the wheelchair away from the doorpost while it assists the user to pass through the doorway safely. Whereas in Case II, as the user position is close to the doorpost, the control scheme again diverts the robot away. However, it can be seen that it just acts as a mechanism for collision avoidance. The user is effectively moving forward which is evident from the sharp decrease in α_I and thereby α. Therefore, we can validate the fusion formulation as an efficient tool for assistance in doorway passing as well as a mechanism for doorpost collision avoidance.

4.2.4 Initial Perspectives

We then identify two important points with respect to the proposed assistive velocity controller. Firstly, the control law just employs the position of the doorpost in the image as the input. Therefore, it can be postulated that the developed scheme may work with *corridor ends* as shown in the previous chapter. Secondly, the control scheme is not restricted to be used only with

an image sensor. Other sensors capable of estimating the parameters r and ϕ_d (including a monocular camera) may also be employed in conjunction with the shared control scheme.

As mentioned earlier, we designed the assistance scheme for corridor following through a bottom-up approach using a constrained control law. We projected the user teleoperation onto a wall collision avoidance task, which in turn resulted from constraining the visual features using a weight function $\mathbf{H}$.

This allowed us to explore a top-down approach for the task of doorway passing. From the linear control sharing formalism that resulted in Equation (4.7) for assisted corridor following, we were able to encode the constraints for assisted doorway passing within factor α. This in turn allowed us to set the assistance parameters within α based on user intention and also based on safety considerations.

4.2.5 Experimental Analysis

Test Setup

The system employed in this test was an off-the-shelf wheelchair manufactured by Sunrise adapted to robotic use with the Robot Operating System (ROS). As we have already assessed the assistance scheme (4.2.2) in simulation with respect to its performance, we aim to test the system with respect to its applicability in real world systems, particularly with different sensors.

A Microsoft Kinect with 56° field of view and which was aligned at an angle of $\theta = 40^\circ$ with respect to the frame $\mathcal{F}_r$ was equipped on the wheelchair in order to detect and track doorposts. The stream from the infrared camera corresponded to a frame width of 640 pixels and a frame height of 480 pixels. The sensor was calibrated with $h = 1.25$m, $l = -0.35$m and $w = 0.0$m.

To experimentally validate the proposed system as an effective assistance system for doorway passing, various trials were carried out. As we use an RGB-D sensor in the form of a Microsoft Kinect, before analysing the navigation results, we present an overview of the visual feature (ϕ_d) detection and tracking system used in the trials.

We employ a door detection and tracking framework specifically developed for such indoor navigation tasks [ZJX+14]. Using a naturally strong a-priori that the doorposts are nearly verticals in a processed depth image, it is possible to easily extract vertical lines that represent the doorpost. The processing of a depth image is done by initially filling the hole pixels with its closest effective depth value (or 0 if an effective value is not found) and then using a bilateral filter over it using both color and distance data. Further details on extracting vertical lines that corresponds to a doorpost can be obtained from [ZJX+14]. It is not delineated here as it is not the objective of this work. Once we have the vertical lines representing a specific doorpost, the distance r is estimated by using the Mean-Shift algorithm over an area of 5 pixels to the right and left of the line. Whereas ϕ_d can be easily estimated from the position of the line as explained in Equation (3.16).

But we observe that in the case of a normal doorway passing sequence, the doorpost at the

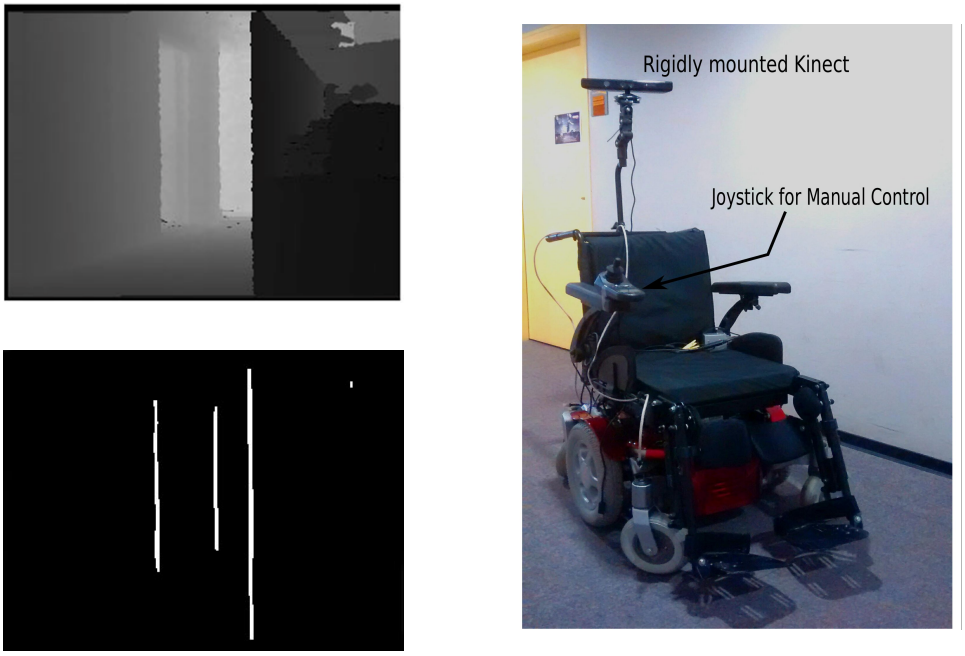

Figure 4.24: Vertical lines (Left-bottom) extracted from a processed depth image (Left-top). The robotized wheelchair setup for testing (Right).

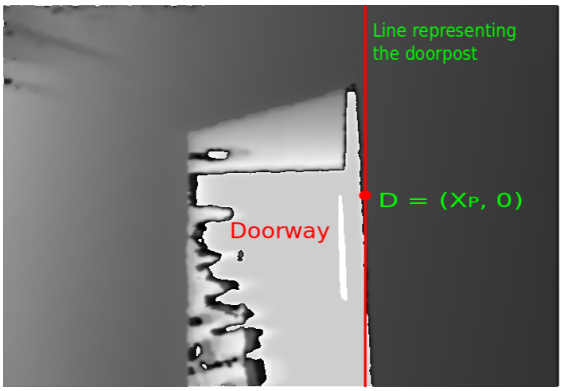

Figure 4.25: Geometrical top view of a wheelchair with respect to a doorway (a) along with a generic depth map representing the point D in the image (b).

far end of the door will not be present in the field of view of the camera as the wheelchair tries to position itself in front of the door. This is not an issue since the control law employs a solution which exploits only the position of the nearest doorpost in the image.

Analysis of the trial

To perform the experiments in order to test the fusion formulation, the interval of assistance $[r_s, r_u]$ has to be determined. Since r is the distance from the sensor to the doorpost and the

wheelchair ideally passes the doorway at $r = m = 0.4$m, we set safe value of $r_s = 1$m and the unsafe value of $r_u = 0.3$m. The gain k for the visual-control system was empirically tuned at 1.8 and the factor g was set at 2 (see Eqn. (4.16). A low-pass filter was added on the assistance factor α in order to further smooth the estimations.

The user initially starts close to the walls (see Fig. 4.26a) and was asked to move into a doorway at the end of the corridor. At this point the wheelchair is close to another doorpost. As the user starts moving forward, the wheelchair comes dangerously close to this doorpost which in turn activates the visual control task as the assistance factor α becomes non-zero which can be observed in Fig. 4.27 (Section B). This ensures that the wheelchair moves away from the doorpost. But as the intention of the user is not to pass through this doorway, the value of α_I reduces rapidly to zero which in turn facilitates the user to move along the corridor. Thus we effectively avoided a risk of collision with the doorpost.

As the user again moves forward towards the doorway of interest, he has full control as there is no threat of collision (Section C). But as the wheelchair comes closer to the doorpost of interest, the value of α again becomes non-zero and the system *progressively* takes part of the control of the motion (Section D). At this point, the user deliberately moves the joystick in order to collide with the doorpost, but the shared control scheme acts accordingly and diverts the wheelchair away from the doorpost and into the doorway. This can be seen by the evolution of α_L and α_I during Section D. The system is stopped as soon as the wheelchair is inside the doorway. The evolution of the user and final system velocities as shown in Figure 7.8 complement the desired behaviour and the analysis of the proposed system.

(a) Sec. A, Frame 20

(b) Sec. B, Frame 560

(c) Sec. Ca, Frame 1190

(d) Sec. Cb, Frame 2500

(e) Sec. D, Frame 2900

Figure 4.26: Depth and grayscale image frames at five points during the motion. Section B and D represent frames where assistance is provided

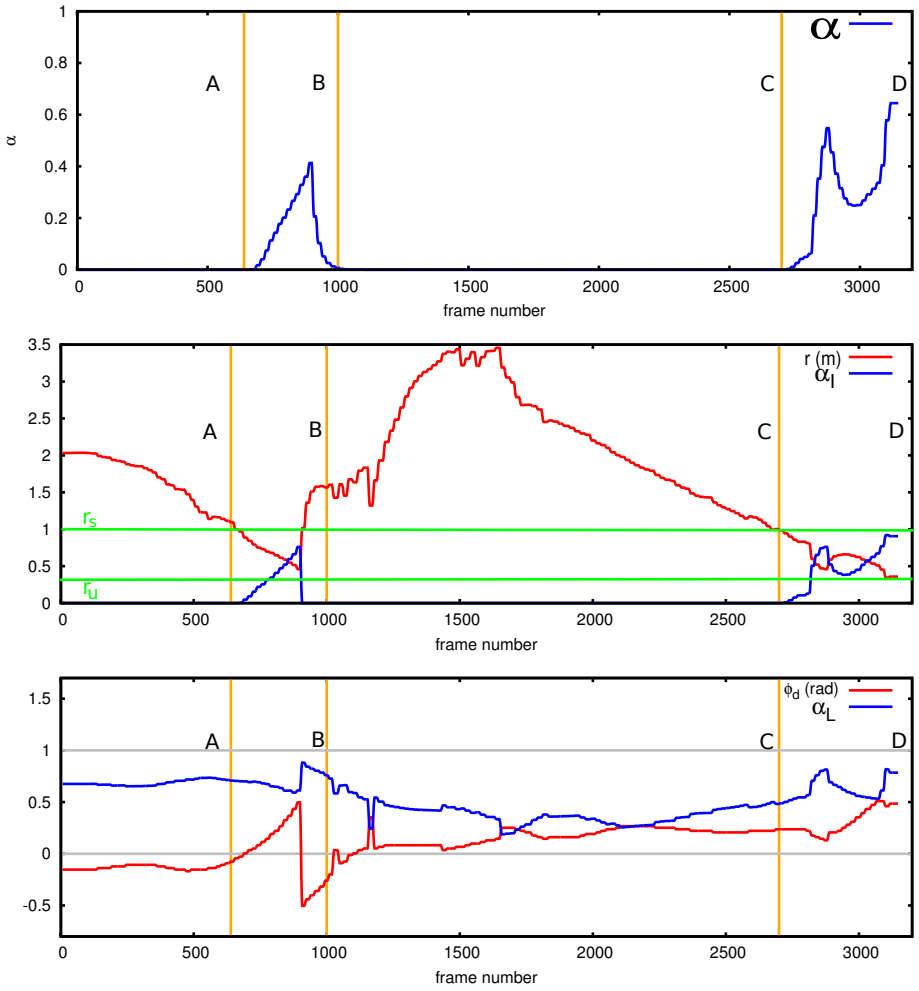

Figure 4.27: Evolution of the assistance factor α (top). Estimated value of r plotted along with α_I (middle) and the estimated value of ϕ_d plotted along with α_L (bottom).

4.3 Conclusion and Remarks

In the first section of this chapter, we proposed a vision-based semi-autonomous system for safe wheelchair navigation along corridors, designed from the bottom-up. The control system thus relied on a collaboration between two tasks: a wall collision avoidance task initially obtained by a dedicated visual servoing approach, and manual user teleoperation. The idea was then to correct the trajectory indicated by the user by servoing only the necessary degrees of freedom of the wheelchair. A smooth transition from manual driving to assisted navigation was obtained owing to an adapted weighting function, thus avoiding discontinuities that may lead to unpleasant experience. Experimental analyses also clearly showed the ability of the approach to provide an efficient solution for wall collision avoidance purposes. We inferred a linear control sharing

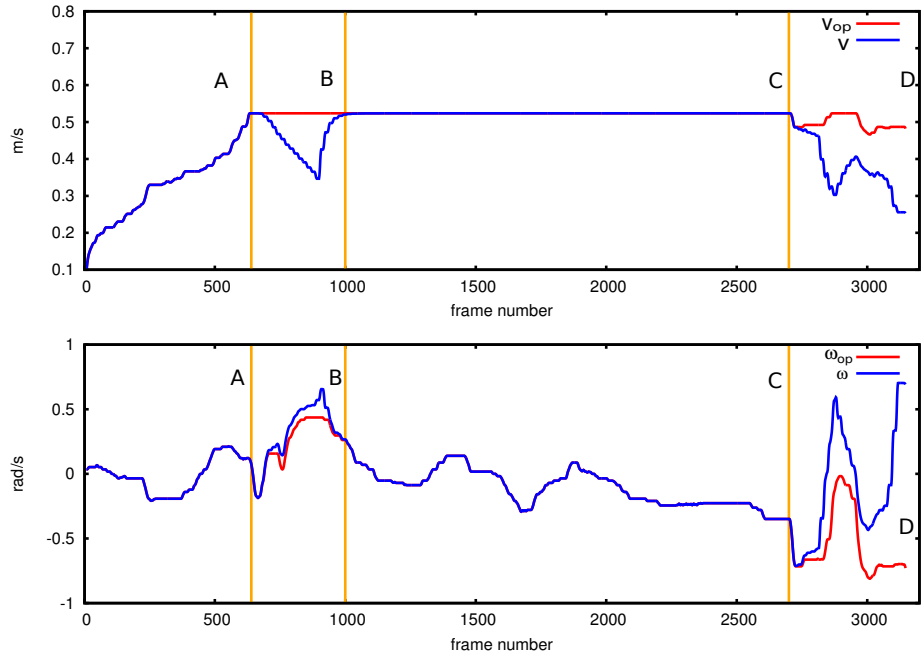

Figure 4.28: Evolution of the user ($\mathbf{v_{op}}$) and final system ($\mathbf{v}$) velocities. Translational component on top and angular component on the bottom.

formalism from the resulting assistive velocity controller.

Moreover haptic force feedback in conjunction with the assistance was provided in order to notify the user of danger and guide him/her over to a safer trajectory. We observed that the guidance force served as an automatic corrective mechanism which ensures minimal interference from the visual control process thus leading to a better quality of experience.

While in the second section of the chapter, we used the resulting linear control blending formalism in order to propose a similar assistive controller for the task of doorway passing. User teleoperation output was fused with a robust control task in order to devise an intuitive shared control scheme that was capable of assisting the user progressively when needed. The behaviour of the system in simulation as well as in practice demonstrated the effectiveness of the proposed control scheme as a low-level system for assisted doorway passing using a robotized wheelchair. We could also identify that the formulation of the underlying shared control framework (which can be characterized as a sensor-agnostic framework) was versatile in order to be deployed with different sensor configurations. Thus in this part of the thesis, we conclude that a linear control sharing policy is efficient for formalizing vision (sensor)-based assistance schemes for fundamental indoor navigation tasks like following a corridor and passing through doorways.

But in order to deploy such systems in the real world where there might be dynamic obstacles and other hindrances, we need to think about assistive navigation in a much broader sense. In the next part of this thesis we aim to take into account one such issue, i.e. human-awareness.

Humans are special objects for robots, and more so for assistive robots that operate among humans. Assistive shared control inadvertently relies on human-robot collaboration. Thus it is essential to incorporate human-awareness within social robots such as intelligent wheelchair for seamless human-robot collaboration and for deployment in a real world human environment.

Part II

Human-awareness in wheelchair navigation

Chapter 5

A primer on Human-aware Navigation

A KEY ISSUE that hinders the adoption of assistive robotic technologies such as the one described in part I of this thesis, in the real world, is that they need to operate in mostly human environments and among human crowds. Our motivation in tackling this issue comes partly from the realisation that social robots such as intelligent wheelchairs need to be deployed in a human environment thereby making it essential for such robots to incorporate a sense of *human-awareness*. Simply put, humans are special objects that have to be perceived and acted on in a special manner by robots that interact with us humans. Thus one can define *Human-aware Navigation* as an intersection between human-robot interaction and robotic motion planning [KPAK13].

Therefore, in this part of the thesis, we use a well developed theory of proxemics [Hal66] in order to quantify social space management by individuals and groups, and in order to understand its influence on robot navigation, particularly assistive wheelchair navigation. Part of the material in this introductory chapter is influenced from the doctoral work of Rios-Martinez [RMSL14].

5.1 Introduction

The core aim of human-aware robotic navigation is to autonomously/semi-autonomously navigate and interact in a dynamic human populated environment, where *social cues* are included in the navigation decisions [RMSL11]. A recent survey on human-aware navigation identified three key concepts within it, viz. *Comfort, Naturalness* and *Sociability* that drive research in this area [KPAK13]. Comfort differs from safety in that, even if the robot is moving safely according to the perception of the *system*, it may not *feel* safe from a human observer standpoint. Thus tackling comfort in robot navigation adds a new layer on top of safety constraints in navigation. The other two categories i.e. Naturalness and Sociability focus on modifying the robot behaviour to satisfy a given *ideal of behaviour*. Naturalness strives to imitate nature, such as human motion, as the target behaviour to recreate with a robot. Whereas Sociability uses known culture-dependent norms of civilized human behaviour, which is appropriate for high-level decisions, in order to formulate action sequences or distinct decision strategies. Focusing on both Naturalness and Sociability thus is also usually expected to contribute to Comfort.

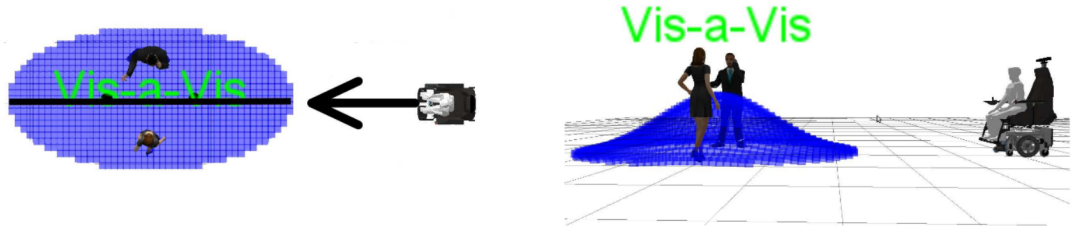

Figure 5.1: Schematic of a robotic moving alongside two people who are having a conversation. The blue points indicate the relative discomfort for the humans in interaction if the robotic wheelchair encroaches the space. This model of a *social space* is derived from a well defined proxemic theory [Hal66].

Human comfort is generally signalled through facial expressions, body posture, proximity, neuromuscular/physiological activities or specific social interactions [MS12, RMSL15]. Consequently, comfort in the above context is a subjective notion, and no sensor can measure it directly. Therefore, studies that tries to mathematically quantify the way distance, posture and visual behaviour affect comfort in humans can be used to implement human-awareness within real social robots such as intelligent wheelchairs. Specifically, the theory of Proxemics, a research theme in sociology, formalizes how humans manage physical spaces around them. Such a theory can be inadvertently utilized for designing human-aware navigation schemes. Before we briefly introduce the idea of social spaces, we provide an overview of some prior art in the field of human-aware or socially-aware robotic navigation.

5.2 Related work

As defined by [RMSL15], a socially-aware navigation (or human-aware navigation) is the strategy exhibited by a social robot (such as an intelligent wheelchair) which identifies and follows social conventions (for example, in terms of management of space) in order to preserve a comfortable cohabitation with humans. The resulting behaviour is predictable, adaptable comfortable, and easily understood by humans.

Among a plethora of works pertaining to human-aware and socially-aware navigation in the recent years [KUJ+14, AIK+04, RMSL11, ESL14, VSRM+13, KP15, RMSL11, VSRM+13, RMSL14, WDWK07, AIK+04, NMO+15, DWW+06, SLD+13, SKG+09, BWP07, SCAR08, WDWK07, CH10, SKD10, DA11], one can identify five main axes of motivation (application areas) for research, as follows:

- Minimizing probability of encounter [CH10, SKD10, DA11],
- Avoiding collisions [AIK+04, RMSL11, KP15, VSRM+13, ESL14],
- Passing people [KKSB12, KSF09],
- Approaching humans (and groups of humans) [DWW+06, SLD+13, SKG+09, BWP07, SCAR08, WDWK07, KUJ+14],
- Following humans [SSSL16, GFS07, ZJK07].

Moreover as mentioned earlier, surveys [KPAK13, RMSL15] of human-aware robot navigation identified three key objectives viz. Comfort, Naturalness and Sociability that drive research in this area. Importantly, we gather that, using traditional robotic objectives like the shortest path to a goal may not be optimal when emphasising human-awareness [VSRM+13, KP15]. Thus, in many previous and related works in this area, the path planner for human-aware navigation is designed to generate a *human-like* motion either using a specific performance criteria [WDWK07, KUJ+14, AIK+04, NMO+15, CH10] or by using machine learning [KP15, GFS07, ZJK07, KSF09].

Whereas another direction of research focuses on addressing the *virtual social spaces* that individuals maintain in various situations [RMSL11, ESL14, VSRM+13, RMSL14], where the goal is to reduce discomfort to humans and increase acceptability. In the present case, we aim to use such *general proxemic models of human physical space management* in order to better program the behaviour of social robots such as an intelligent wheelchair in human environments. Therefore, in this chapter, we illustrate a motion planner that explicitly takes into account proxemic issues in order to generate a socially-aware motion in human environments. We will employ this motion planner in Chapter 7 of this thesis in order to finally propose a general semi-autonomous framework for human-aware and user intention driven wheelchair mobility assistance.

Before we illustrate the motion planner, we present a brief overview of the proxemic idea of social spaces in physical human space management.

5.3 Proxemics: The idea of social spaces

Definition Proxemics is the study of spatial distances individuals maintain in various social and interpersonal situations. These distances vary depending on environmental or cultural factors. The term was first proposed by the social anthropologist P.E. Hall [Hal66] to describe the human management of space.

Hall [Hal66] studied the general conventions and rules followed by humans with respect to physical space management in public and private. He proposed a general theory describing the spatial distances that individuals maintain in social as well as interpersonal situations. Moreover, he added that physical spatial management by a single person (termed personal space) is different to physical spatial management by a group of persons (termed interaction space). The idea of social spaces is then crucial in tackling the problem of deploying a social robot such as

Figure 5.2: Humans tend to naturally arrange themselves as a consequence of respecting each other's personal space.

an assistive wheelchair in human environments, as it directly relates to the acceptability of the solution [WDWK07, BTK08].

5.3.1 Personal Spaces

A personal space is the region around humans that they actively maintain into which others cannot intrude without causing discomfort [Hay78]. A robot operating in human environments should take into account the personal space of humans in order to plan compliant paths to a certain goal. Figure 5.2 shows an intuitive idea of personal spaces around us humans.

A variety of shapes have been proposed for personal space as follows (see Figure 5.3):

- Concentric Circles: According to Hall who put forth the idea of personal spaces [Hal66], it is possible to classify the space around a person with respect to social interaction in four specific zones whose distances from human body.
  - the public zone > 3.6m.
  - the social zone > 1.2m
  - the personal zone > 0.45m.
  - the intimate zone ≤ 0.45m.
- Egg Shape: People are more demanding regarding the respect of their frontal space, therefore frontal invasions are more uncomfortable according to Hayuk et. al. [Hay78].
- Concentric Ellipses: Personal space refers to the private sphere in the Social Force Model proposed by Haebling et. al. [HM95]. The Social Force Model has been widely used

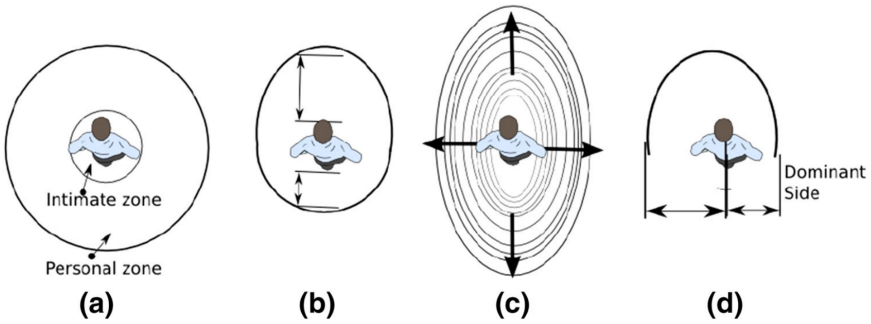

Figure 5.3: Different shapes for personal space as proposed by various social scientists: (a) Concentric circles, (b) Egg shape, (c) Ellipse shape and (d) Shape smaller in the dominant side.

to represent human behavior in agent simulation and has attracted the attention of the robotics community.

- Asymmetric Shape: More recent work [GLRFM08] claims that the size of the personal space does not vary according to the walking speed during circumvention of obstacles and that a personal space is asymmetrical, i.e., it is smaller in the pedestrian's dominant side.

It is evident that these measures are not strict and do vary with age, culture, and context. We can also say that cultural differences affect the behaviour related to spaces (i.e. some cultures avoid physical contact while others are more permissive). Moreover, personal spaces may be dynamic which means that they could change depending on the context for the same person or group of people. Nevertheless it is advantageous to have a generic mathematical model of the personal space around humans as a first step in designing human-aware robots.

5.3.2 Interaction Spaces

A social robot such as a humanoid or a robotic wheelchair should also respect the physical space that is created when two or more people join together to form a *focused interaction*. When a standing group of people agree to sustain a single focus of visual and cognitive attention, the resulting interaction is termed as a focused one [Erv66]. Conversations are then said to be focused interactions which can be translated into a common shared space in the environment. In order to represent a focused interaction in an environment where several individuals are present, the manner in which the individuals position and orient themselves with respect to others is the key factor. The ideas of O-spaces and F-formations are at the center of this solution.

As shown in Figure 5.4, people interacting in groups follow some spatial arrangement patterns. This spatial arrangement is termed as an *Interaction Space*. The O-space in a focused interaction is the shared area reserved for the activity that is established by the specific group. Only participants have access to it, they protect it and others tend to respect it [Ken10]. O-space varies depending on body size, posture, position and orientation of each participant during the

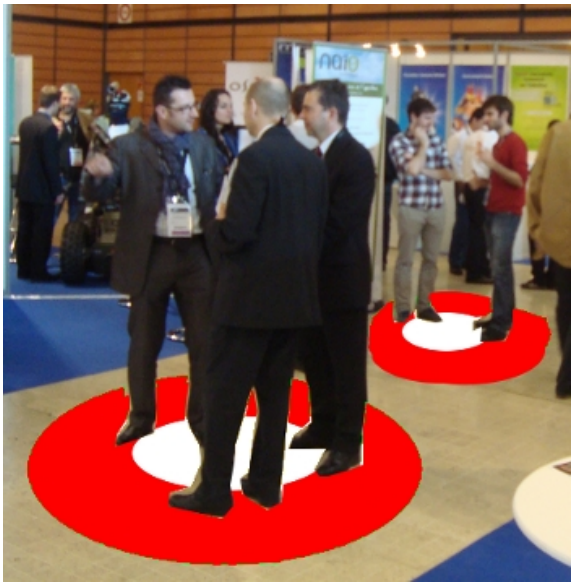

Figure 5.4: People in conversation follow specific patterns of spatial arrangement. The situation of O-Space is marked with a white circle for the two groups in the scene and it is surrounded by the p-Space in which is marked with red.

activity. The p-space is the space surrounding the O-space which is used for the placement of the participant bodies and also personal belongings.

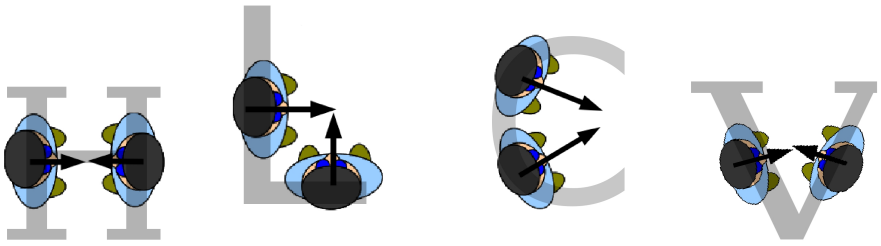

(a) Vis-a-Vis (b) L-shape (c) C-shape (d) V-shape

Figure 5.5: Frequent F-formations for 2 people groups

Now according to [CK80], the term F-formation is used to designate the system of spatial-orientation arrangement and postural behaviours that people create and maintain in order to sustain their O-space. The shape of the F-formation strongly depends on the number of people involved, the relationship among them, the group attentional focus and on relevant environmental constraints. For example when we consider two people in conversation, six formations are the most frequent: N-shape, Vis-a-vis, V-shape, L-shape, C-shape and side-by-side [Ken10, CK80]. Illustrations for four formations namely Vis-a-vis, L-Shape, C-Shape and V-Shape are given in Figure 5.5 for reference.

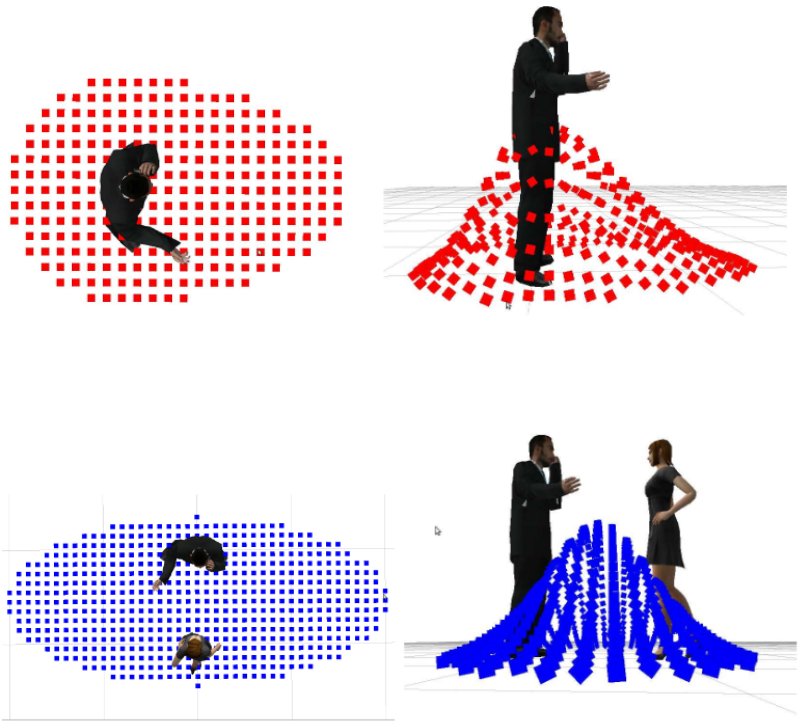

Figure 5.6: The Personal Space (top) of an individual and the Interaction Space (bottom) of a group can be modelled within a 2D configuration space as shown above. The height of the points in the figures represents the relative risk of disturbance to the humans at that position. For a single human, maximum disturbance is located at human position. For a group, maximum disturbance is located at the group center. A full mathematical modelling is given in [RMSL11].

5.3.3 RiskRRT - A human-aware motion planner

Since intelligent wheelchairs need to operate in populated environments, it is essential to encode compliant social behaviours within the control algorithms. For example, people tend to become uncomfortable if they are approached at a distance that is deemed too close. The level of discomfort generally depends on the *personal space* of an individual or on the *interaction space* of a group of humans as described earlier [Hal66]. The notion of personal and interaction spaces can be explicitly characterized using general models.

RiskRRT [FSLT10] is a local path planner that explores the environment using a Rapidly Exploring Random Tree (RRT) that is constantly updated with perceived data as well as obstacle motion predictions. It is an extension of the popular RRT algorithm where the *likelihood of an obstacle's future trajectory* and the risk of collision are taken into account. Thus the probable trajectory of dynamic obstacles (including humans) are predicted at each instant. Meanwhile, the tree (comprising of branches corresponding, for example, to a set of topological robot poses in the 2D configuration space) is grown in a random fashion but is heavily biased towards a goal,

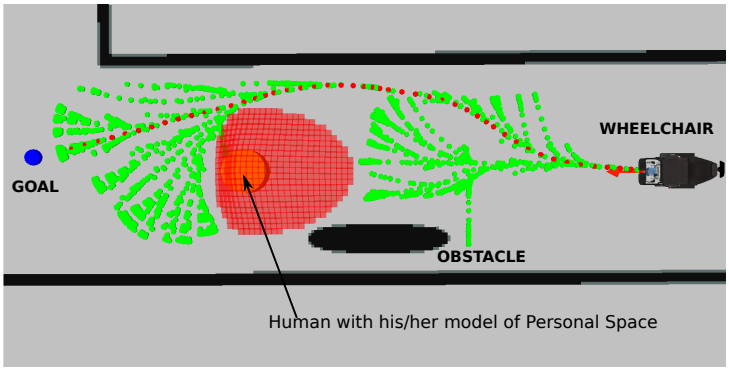

Figure 5.7: The risk-based RRT planner grows trees heavily biased toward a pre-set goal taking into account the perceived information. The best trajectory (branch) of the tree (in red) among the possible trajectories (in green) is the one which is closest to the goal and which carries the lowest risk of collision and the lowest risk of disturbance to other humans.

that is checked for at each iteration. The best trajectory or path in the tree is the one with the least farthest from the goal (in terms of Euclidean distance) and which carries the lowest risk of collision with the probable trajectory of dynamic objects. Thus the best trajectory (path in the tree) is chosen using a heuristic the *probability of success* and distance to the goal of its nodes.

An extension of this motion planner includes the knowledge of personal space of pedestrians and the possible interactions between them [RMSL11]. The interactions that are incorporated are conversations between pedestrians (focused interactions as described in the previous subsection). It is possible to penalize paths that passes through the personal space of pedestrians and through the o-space of interactions taking place in the environment.

Assuming that a robot is operating in a 2D configuration space, the models of personal and interaction spaces are given in Fig. 5.6. The height of the points represent the relative risk of disturbance to the person(s) (in terms of comfort). The personal space can be modelled as a blending of two Gaussian functions, one for the front of the human and one for the rear (see Fig. 5.6 top). Evidently, the Gaussian for the front is wider than the one for the rear. On the other hand, the interaction space is represented by a two dimensional Gaussian (see Fig. 5.6 bottom). The Gaussian is centered at the group *focus of attention* which is the group point of visual and cognitive attention. This point in turn can be extracted from the orientation of the humans within the group. These models of social spaces can be directly transformed to cost functions that allows a path planner to plan optimal trajectories in order to reduce the risk of disturbance [RMSL11].

Within the Risk-RRT algorithm, the risk of disturbance is then integrated for each person and each interaction as the *probability of collision with virtual dynamic objects*. In such a case the models of the social spaces serve as cost functions for the probability of occupancy. Once the trajectory is generated, in order to traverse the path, kinematically permissible velocities (for a non-holonomic unicycle type robot) are generated using a well defined stable tracking algorithm proposed by Kanayama et.al. [KKMN91]. We here do not go into the technical details

of the algorithm as it is not relevant within the topic of this thesis but provide a algorithmic overview of the motion planner in Algorithm 1. Finally Figure 5.7 shows the execution of the path planner within a specific scenario. Further details regarding the algorithm design as well as a primer on how to detect and represent social spaces are provided in [RMSL11].

Data: Information from extroperceptive sensors
Result: A human-aware motion to a specific goal
initialization;
trajectory = empty;
Tree = empty;
Goal = read();
t = clock();
N_t = max prediction time;
while *Goal not reached* **do**
  if *trajectory is empty* **then**
    brake;
  else
    move along the trajectory one step;
  observe(Data);
  delete unreachable trajectories;
  t = clock();
  predict moving obstacles and humans at time t .....$t + N_t$;
  assign costs to obstacles and varying costs to social spaces;
  if *environment different (eg: motion of obstacles)* **then**
    update trajectories(Data);
  while *clock()* $< t + N_t$ **do**
    grow trajectories with depth $\leq N$ in Tree;
  trajectory = Choose best trajectory in Tree;
  t = clock();
brake;

Algorithm 1: Risk-RRT: The algorithm

5.3.4 Equitably approaching and joining human interactions

The core aim of human-aware navigation is to autonomously navigate and interact in a dynamic human populated environment, where social awareness is included in the navigation decisions [RMSL11]. As described earlier, most of the literature available in this area focuses on how a robot can safely navigate *around* the social spaces of humans, in order to avoid disturbance [RMSL11, SCM+06, SAS+05] or in order to make room for human passing [PCJ06]. Evidently, as described above, the Risk-RRT motion planner can be used to plan human-aware trajectories towards a *specific goal* in the environment.

But encoding human-aware behaviours does not exclusively pertain to avoiding the social spaces of humans. Complementary works [DWW+06, SLD+13, SKG+09, BWP07, SCAR08, WDWK07, KUJ+14] also describe how a robot should *initiate a conversation with a human being*, where approach distances, gaze directions, the greeting process etc., are analysed in order to obtain solutions. Consequently, the key issue of *how to approach* humans with the intention of initiating conversation was initially tackled by Satake et. al. [SKG+09]. They designed a probabilistic path planning approach in order to frontally approach a single human target by taking into account the predicted trajectory of human target motion.

As a further step, we here aim to investigate the issue of *how to approach a group of humans in interaction, with the aim of becoming a part of the group*. This behaviour is essential for social robots that interact with humans, especially intelligent wheelchair users who desire to *equitably* approach and join an interaction. Equitably here refers to the robot being held with the same social standard as humans.

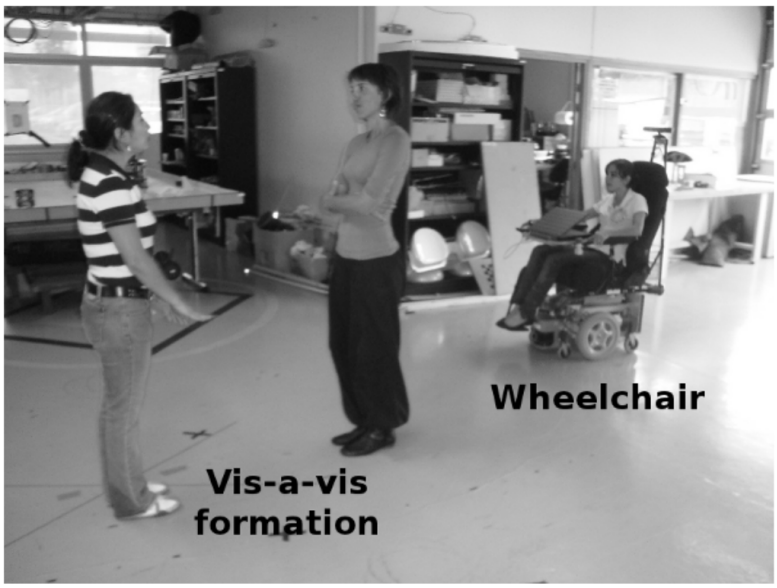

Figure 5.8: In this Figure, we observe a snapshot of a scenario where an intelligent wheelchair should autonomously/semi-autonomously plan a trajectory towards a two-person interaction. Performing this action in a socially-aware manner is not trivial [SKG+09].

In this context, preliminary studies conducted by Butler [BA01] indicated that an indirect pattern of approach by the robot is typically considered as the favourite, as it decreases the threat of contact. In contrast recent studies have shown that a frontal approach is more desirable for humans and even more so in the case of groups [SKG+09, DWW+06, KUJ+14]. But the problem of designing algorithms that can be utilized by a social robot in order to perform a frontal approach while respecting spatial social constraints is highly non-trivial. Works by Escobedo et. al.[ESL13, ESL14] have defined an algorithm which is able to calculate meeting points for *detected* interacting groups. The said meeting point was reached by planning a trajectory using an A^* algorithm and Dynamic Window path planner. But, as mentioned earlier, using traditional robotic objectives such as the shortest path to a goal may not be socially conventional.

Thus we design a robust sensor-based (and sensor-agnostic) velocity controller that is capable of reaching the optimal meeting point in a way that is socially conventional. Evidently, we also define what motion criteria can be termed as socially conventional alongside the proposed velocity controller. We also argue and prove that the system could be stacked onto a higher level controller for enhancing its capabilities (like obstacle avoidance). The following chapter illustrates the proposed velocity controller and presents analyses that validate the system for real world application.

Chapter 6

Equitably Approaching and Joining Human Interactions

THIS CHAPTER introduces a low-level velocity controller (similar to the one deigned in Section 3.2) that could be employed by a social robot like a robotic wheelchair or a humanoid, for approaching a group of interacting humans, in order to become a part of the interaction. Taking into account an *interaction space* that is created when at least two humans interact, a meeting point can be calculated where the robot should reach in order to equitably share space among the interacting group. We propose a sensor-based control task which uses the position and orientation of the humans with respect to the sensor as inputs, to reach the said meeting point *while respecting spatial social constraints*.

The work in this chapter has been presented at the IEEE/RSJ International Conference on Robots and Systems (IROS)[**C.3**] in 2015 and the IEEE International Symposium on Robot and Human Interactive Communication (RO-MAN)[**C.2**] in 2016.

6.1 Motivation and Objective

As described earlier, social robots, particularly in the form of service robots, expose a wide range of opportunities for research in mobile robot navigation [SCM+06, SAS+05, BWP07, SCAR08, WDWK07]. Since it is evident that such robots need to navigate, operate and share physical space between humans, it is essential to assign navigation behaviours in accordance with social expectations.

A fundamental navigation task for social and service robots is to *detect, approach and join an interacting group of humans*. Especially in the case of an intelligent wheelchair that assists a human user, there exists a perceptual dichotomy for the group in the fact that the group could perceive it either as a human or a robot. It is expected that a manual wheelchair will approach the group in a socially conventional manner, while the same can be *generally* expected for intelligent wheelchairs (as they can be considered social robots) [BTK08].

Thus, considering physical social space management, humans naturally tend to hold social robots with similar spatial social conventions as themselves [BTK08]. Therefore much emphasis should also be given to the idea of performing this action in an *equitable* and socially conventional manner. Equitably refers to the idea of robots being held to the same social standards as humans.

In the previous chapter, we saw that anthropologist P.E. Hall [Hal66] studied the general conventions and rules followed by humans with respect to physical space management in public and private. He proposed a general proxemic theory describing the spatial distances that individuals maintain in social as well as interpersonal situations. Moreover, he added that physical spatial management by a single person (termed personal space) is different to physical spatial management by a group of persons (termed interaction space). The idea of interaction spaces is then crucial in tackling the problem of a social robot approaching and joining a group of humans as it directly relates to the acceptability of the solution [WDWK07][BTK08].

In this chapter, we introduce a feature-based motion strategy that utilizes easily extractable features from a detected human group, in order to generate a socially acceptable motion to approach and join the group in an equitable manner and to maintain formation. The applicability of the strategy is wide, from humanoid robots to service robots to intelligent wheelchairs. We also present a detailed analysis focused on the stability, convergence and robustness with a variety of simulated cases. Furthermore, we couple the motion strategy with reactive obstacle avoidance in order to demonstrate its adaptability. Experimental evidence is also demonstrated using a mobile robot and the applicability of the approach is discussed with respect to its deployment in real world cases.

6.2 Comparison to state of the art

Initial studies using Hall's proxemic theory [Hal66] in social robotics focused on how a robot could safely navigate *around* social spaces, in some cases to reduce disturbance [RMSL11, SCM+06, SAS+05] or in order to make room for human passing [PCJ06].

Complementary works began to emerge that investigated how a robot should approach a single human target [DWW+06, SLD+13, SKG+09, BWP07, SCAR08, WDWK07, KUJ+14] especially for performing a task such as object handovers [DWW+06, BWP07] or for fetch and carry [WDWK07]. These works analysed approach distances, gaze directions, the greeting process etc., for planning socially compliant paths. Within the context of approaching a human/group with the intention of initiating conversation, a fundamental work by Satake et.al. [SKG+09], provided a solution in the form of a probabilistic path planning approach that also took into account the predicted trajectory of human motion. In the specific case of approaching a group of people, Althaus et.al. [AIK+04] introduced a control scheme that uses the relative distance and orientation of the humans in order to approach and then maintain a formation. Both the works were based on a highly *context specific* velocity controllers. Thus there exists a need for an adaptive system capable of being deployed without a strong a-priori.

With respect to approaching a group, Karreman et.al [KUJ+14] conducted a preliminary user study that concluded that executing a frontal approach is more desirable for a group of people in interaction. In this context recent works by Escobedo et. al.[ESL13, ESL14] have defined an algorithm which is able to calculate meeting points for *detected* interacting groups. The meeting point was reached by planning a trajectory using an A^* algorithm and a Dynamic Window path planner. But as prefaced, traditional robotic objectives such as taking the shortest path to a goal is not always socially conventional and developing planning heuristics based on the proxemic theory state of the art may be tedious [Mar12]. Moreover, in order to integrate other behaviours (possibly high-level) such as local obstacle avoidance, a sensor-based control law offers an easy approach. Therefore, we propose a robust feature-based (while sensor-agnostic) control system that is capable of reaching the optimal meeting point in a *socially conventional manner*. Also, since the control law is feature-based, it is reactive (adaptive) to feature variations in a way planning algorithms may not be. The next section defines how to approach the group in a socially conventional manner.

6.3 Approaching an Interaction

As briefed in the previous chapter, a social robot must respect the physical *space* created when two or more people join to form a focused interaction. We also saw that the interaction space is comprised of an O-space and a p-space. Then it is possible to ask two important questions on how to approach a group in interaction:

- Where should the robot arrive within the Interaction Space?
- How should the robot arrive at this *meeting point*?

The meeting point

A geometric representation of the interaction space (i.e the O-space and p-space) for two people formations can be extracted from the position and orientation of the humans (say with respect

to a global map or with respect to a sensor frame). For two humans H_1 and H_2, the geometry of the O-spaces and the p-spaces with respect to the ground/floor plane is given in Figure 6.1 for various F-formations. H_{12} is the center of the line that joins the two humans, ϕ_1 and ϕ_2 the orientation angles with respect to an arbitrary frame, C is the center of the O-space and V_i is the focus point of the interaction. The distance between the two humans is denoted by D_H. Judging the meeting point (i.e the point where a robot should place itself in order to become a part of this group) is fairly simple. We can see that ideally, the robot should position itself on a specific point, within the p-space where the line that joins H_{12} and V_i passes through. The robot should also be facing the focus point of the interaction which is V_i.

In the case of formations with more than 2 people, the O-space is represented as a circle with the focus of attention located at the center of the circle. This phenomenon is more obvious as number of humans in the groups increases. With regards to calculating the meeting point, there can be a variety of solutions depending on the number, positions and orientations of the participating humans. For example, one solution would be to calculate the meeting point by considering the group as a 2 people formation with the 2 people who are farthest in terms of Euclidean distance.

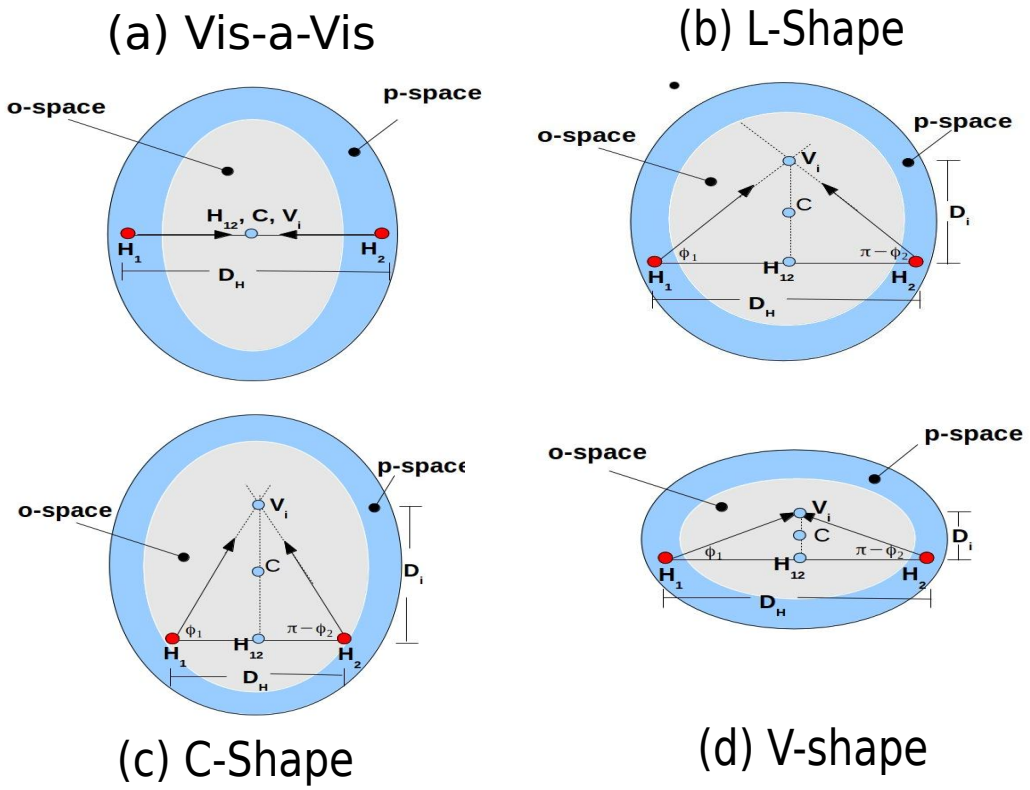

Figure 6.1: The shape of the O-space and p-space with respect to the ground/floor plane for the 4 frequent F-formations in 2 people interactions. We employ the geometrical relation between the participants in order to design *socially-aware* velocity controller to approach and join the group.

Approaching an interaction

Since the aim of the robot is to approach and join a focused interaction, we here assert three simple but key points in the way it should approach a group.

- The robot should approach in a frontal manner (i.e., the robot should be *facing* the interaction as it reaches the meeting point) [SKG+09].
- The robot should approach without invading the O-space of the interaction.
- A robot should reveal its *intention* of imminent approach to the group members. This can be achieved by ensuring the fact that the robot initially faces the group and at no point during the motion faces away from the group (i.e. the sensor always gazes at the group).

6.4 Control System

6.4.1 Modelling

Similar to the system modelling in Section 3.1, considering a sensor frame $\mathcal{F}_s(P_S, x_s, y_s, z_s)$, we assume that the position and orientation of the detected humans and all geometric information regarding the interactions are available in this frame. We model the (social) robot as a non-holonomic unicycle-type robot, which holds for systems such as robotic wheelchairs, while unicycle-type dynamics can be converted to walking motions for humanoids easily as demonstrated in [FOPV13b]. Therefore we control two velocities namely the translational velocity v and the angular velocity ω. The robot frame is denoted by $\mathcal{F}_r(P_O, x_r, y_r, z_r)$. If the sensor is rigidly fixed so that we have a translation vector ${}^s\mathbf{t}_r = (w, 0, -l)$ between $\mathcal{F}_s$ and $\mathcal{F}_r$, we have the relationship between the velocity expressed in the robot frame $\mathbf{v} = [v, 0, 0, 0, 0, \omega]^T$ and the velocity expressed in sensor frame $\mathbf{v_s}$ as

$$\mathbf{v_s} = {}^s\mathbf{W}_r\mathbf{v}, \tag{6.1}$$

with ${}^s\mathbf{W}_r$ representing the velocity transformation matrix given by

$${}^s\mathbf{W}_r = \begin{bmatrix} {}^s\mathbf{R}_r & [{}^s\mathbf{t}_r]_\times \, {}^s\mathbf{R}_r \\ 0_{3\times 3} & {}^s\mathbf{R}_r \end{bmatrix}. \tag{6.2}$$

Note that $[{}^s\mathbf{t}_r]_\times$ represents the skew-symmetric matrix of ${}^s\mathbf{t}_r$, and ${}^s\mathbf{R}_r$ represents the rotation matrix that models the fixed orientation of the sensor frame relatively to the robot frame and which is given by

$${}^s\mathbf{R}_r = \begin{bmatrix} 0 & -1 & 0 \\ 0 & 0 & -1 \\ 1 & 0 & 0 \end{bmatrix}. \tag{6.3}$$

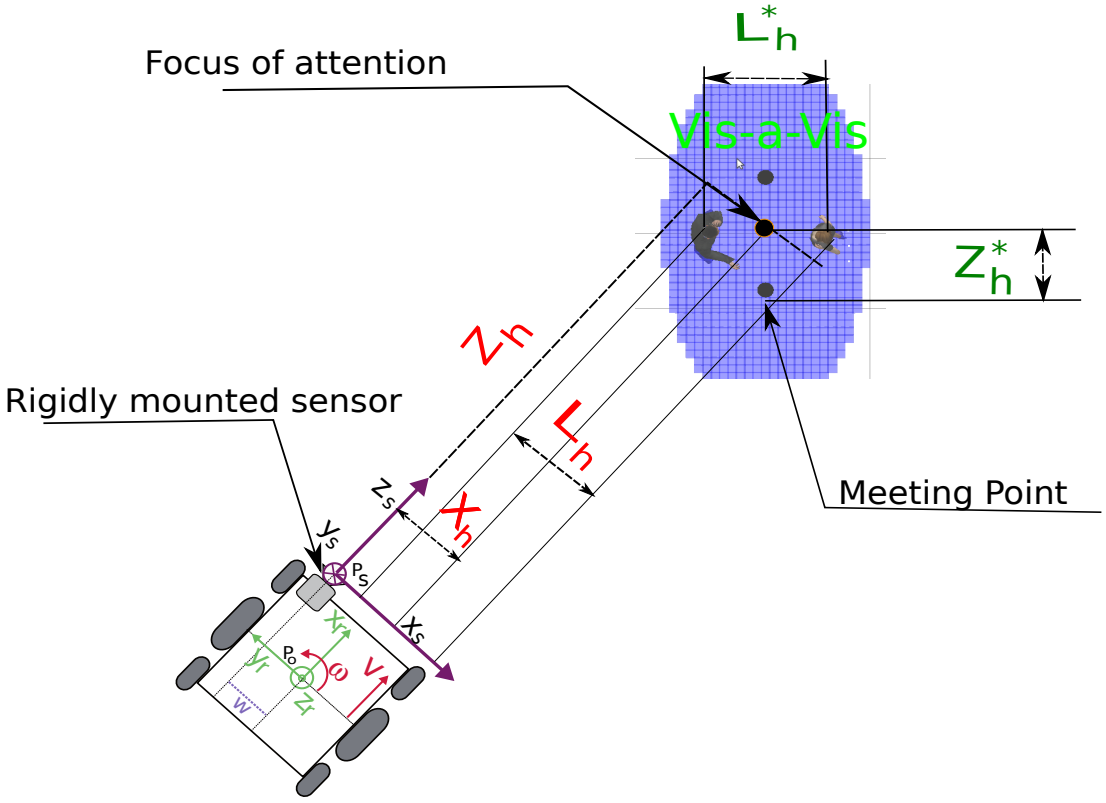

Figure 6.2: A unicycle-type robot with respect to an interacting group. Robot and sensor frames along with the geometric representation of the task features are shown.

6.4.2 Task Features

In order to approach a specific interaction in an equitable way, we design a control task which allows the robot to reach an optimal meeting point by planning a socially acceptable spatial trajectory. Here we need to identify some features related to the group that can be exploited to design a control law that ensures that the robot reaches the said meeting point. We select the x_s coordinate X_h and the z_s coordinate Z_h, with respect to the sensor frame, of the point representing the focus of attention, as the two initial task features. If the robot reaches the meeting point we observe that Z_h should reach a desired value Z_h^* that depends on the type of F-formation of the group (see Fig. 6.1). As for X_h, it should attain a desired value of $X_h^* = 0$ which ensures that the sensor is aligned towards the group focus point V_i.

But we observe that regulating the errors $Z_h - Z_h^*$ and $X_h - X_h^*$ to zero does not ensure that the robot reaches the optimal meeting point. If we observe Figure 6.2, if the robot reaches at any point on a circle around the center of the group with a radius of Z_h^* while *looking forward*, the errors $Z_h - Z_h^*$ and $X_h - X_h^*$ are zero.

Therefore we introduce a new feature L_h which is termed as the group length. In two-

people formations, L_h is the projection, on x_s, of the line segment connecting the two humans H_1 and H_2. In groups with more that two people L_h is the projection, on x_s, of the line segment connecting the two farthest humans (in terms of Euclidean distance). The feature L_h should reach a value of $L_h^* = D_H$ in two-people formations and D_O (the diameter of the O-space) in groups with more that two people.

Therefore, in order to design the control law, we create a task $\mathbf{e}$ defined as

$$\mathbf{e} = [Z_h - Z_h^*, X_h - X_h^*, L_h - L_h^*]^T. \tag{6.4}$$

We can see that realizing the above task (i.e. regulating the errors $Z_h - Z_h^*$, $X_h - X_h^*$ and $L_h - L_h^*$ to zero) ensures that the robot reaches the said meeting point. In order to exponentially decrease the feature errors for the task $\mathbf{e}$, we can design a velocity controller as

$$\mathbf{v} = -\lambda \mathbf{J}_e^+ \mathbf{e}, \tag{6.5}$$

where $\mathbf{J}_e^+$ represents the Moore-Penrose pseudo inverse of the task Jacobian $\mathbf{J}_e$ and λ denotes the control gain.

Let $\mathbf{L} = [\mathbf{L}_{Z_h}, \mathbf{L}_{X_h}, \mathbf{L}_{L_h}]^T$ represent the interaction matrix that relates the dynamics of the task features Z_h, X_h and L_h with respect to the sensor velocity screw $\mathbf{v_s}$ such that $\mathbf{L}\mathbf{v_s} = \dot{\mathbf{e}}$. The first two rows of the matrix $\mathbf{L}$ (i.e $\mathbf{L}_{Z_h}$ and $\mathbf{L}_{X_h}$, representing the features Z_h and X_h) were determined specifically for the case of visual servoing by [ECR92] and [CH06] for controlling a robot end-effector with respect to a 3-D image point, while the third row ($\mathbf{L}_{L_h}$, representing the feature L_h) was determined by [CH06] for visual servoing with respect to a line segment in the image. For the present case, the interaction matrix $\mathbf{L}$ takes up a form as follows

$$\mathbf{L} = [\mathbf{L}_{Z_h}, \mathbf{L}_{X_h}, \mathbf{L}_{L_h}]^T = \begin{bmatrix} 0 & 0 & -1 & 0 & X_h & 0 \\ -1 & 0 & 0 & 0 & -Z_h & 0 \\ A_Z & 0 & B_Z & 0 & -L_h X_h & 0 \end{bmatrix} \tag{6.6}$$

,

where $A_Z = \frac{Z_1 - Z_2}{Z_1 Z_2}$ and $B_Z = \left(\frac{Z_1 + Z_2}{2 Z_1 Z_2} L_h - \frac{Z_1 - Z_2}{Z_1 Z_2} X_h \right)$.

Here Z_1 and Z_2 represent the z_s coordinates of the positions of the two humans in a two-people formation. In a formation with more than three people, Z_1 and Z_2 represent the z_s coordinates of the positions of the two farthest humans in terms of Euclidean distance.

As the robot Jacobian ${}^r\mathbf{J}_r$ expressed in the robot frame is equal to

$${}^r\mathbf{J}_r = \begin{bmatrix} 1 & 0 & 0 & 0 & 0 & 0 \\ 0 & 0 & 0 & 0 & 0 & 1 \end{bmatrix}^T, \tag{6.7}$$

we can finally define the task Jacobian $\mathbf{J}_e = \mathbf{L}\, {}^s\mathbf{W}_r\, {}^r\mathbf{J}_r$.

6.4.3 Task Division and Stacking using Redundancy Formalism

A simple look into the controller design given in Eqn. (6.5) would tell us that the the controller would be at most locally stable and would not perform well for the majority of cases as we regulate three features using two control variables. In order to ensure that the system is able to converge to a near global minima, and in addition, generates a motion that respects social constraints, we divide the above problem into 2 separate tasks: task 1 denoted by $\mathbf{e_1} = [Z_h - Z_h^*, X_h - X_h^*]^T$ and task 2 denoted by $\mathbf{e_2} = [L_h - L_h^*]$.

Task 1 can be intuitively seen as the robot moving forward in order to minimize the distance with respect to the group while simultaneously ensuring that the sensor gazes at the group. Whereas task 2 can be seen as a motion which ensures that the robot reaches the exact meeting point and is well aligned in order to face the group.

Here we observe that both the tasks are of full rank (i.e. they constrain both the DOFs of the robot). Thus it is essential to devise a method that facilitates the regulation of both the tasks simultaneously. Therefore we propose to activate (and/or partially activate) task 1 at specific intervals using an activation matrix. Consequently we can then project task 2 onto the null space of this new task 1 which means that task 2 can be activated (or partially activated) when task 1 is not activated (or partially activated). The activation matrix can be designed in such a way that the task priority is switched between task 1 and task 2 at optimum intervals so that the system converges to a near global minima. Moreover we can address the following issues while designing the said activation matrix:

1 The system should not fall into a local minima, particularly when the robot starts at a position as shown in Figure 6.3,

2 The robot should move in such a manner that respects the known social conventions described above,

3 The robot should not encroach the O-space if the meeting point is behind the humans in interaction.

Thus, in order to modify the control law in Eqn. (6.5), the Jacobian $\mathbf{J}_e$ can be decomposed as

$$\mathbf{J}_e = [\mathbf{J}_{Z_h}, \mathbf{J}_{X_h}, \mathbf{J}_{L_h}]^T = \begin{bmatrix} \mathbf{L}_{X_h}\, {}^s\mathbf{W}_r\, {}^r\mathbf{J}_r \\ \mathbf{L}_{Z_h}\, {}^s\mathbf{W}_r\, {}^r\mathbf{J}_r \\ \mathbf{L}_{L_h}\, {}^s\mathbf{W}_r\, {}^r\mathbf{J}_r \end{bmatrix} \tag{6.8}$$

.

Consequently the Jacobians for tasks 1 and 2 can be defined as

$$\begin{aligned} \mathbf{J}_1 &= \begin{bmatrix} \mathbf{J}_{Z_h} \\ \mathbf{J}_{X_h} \end{bmatrix} \\ \mathbf{J}_2 &= \mathbf{J}_{L_h}. \end{aligned} \tag{6.9}$$

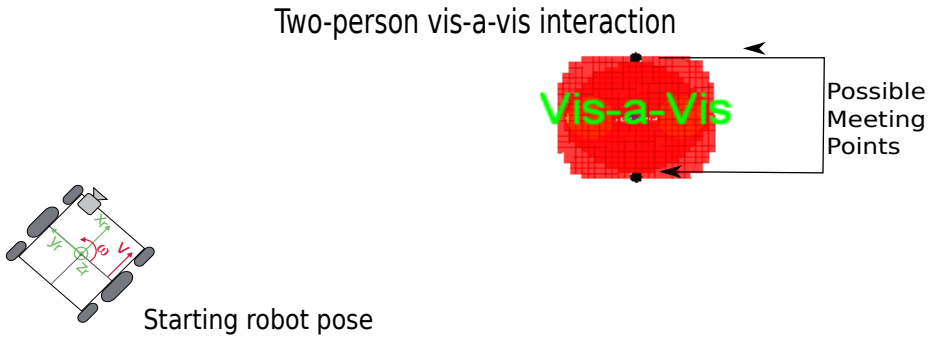

Figure 6.3: A robot starting position where there is a high possibility that the robot may encroach the O-space if it moves in order to join the group.

If the activation function is denoted by $\mathbf{H}$, the velocity controller for the new task 1, which is activated at specific intervals, can be written as

$$\mathbf{v} = -\lambda(\mathbf{H}\mathbf{J}_1)^{+}\mathbf{H}\mathbf{e_1}, \tag{6.10}$$

where $\mathbf{H} = \text{Diag}(h_{Z_h}, h_{X_h})$ is a diagonal matrix that weights the error $\mathbf{e_1}$ where $h_{Z_h} \in [0;1]$ and $h_{X_h} \in [0;1]$ are the varying weights respectively associated to the features Z_h and X_h. Note that we have already proposed a similar design in order to formulate the vision-based wall collision avoidance task in Section 4.1.

As seen earlier, we can note that the matrix $(\mathbf{H}\mathbf{J}_1)^{+}\mathbf{H}$ does not remain continuous, as the rank of the matrix $\mathbf{H}\mathbf{J}_1$ may change from zero to 2 depending on the values of h_{Z_h} and h_{X_h}. Therefore, in order to ensure a continuous control law, the pseudo-inverse operator $^{+}$ is replaced by the continuous pseudo-inverse operator $\oplus^{\mathbf{H}}$ which was introduced in the framework of varying-feature-set [MRC09]. The continuous inversion of the Jacobian $\mathbf{J}_1$ activated by the weight matrix $\mathbf{H}$ is given by

$$\begin{aligned}\mathbf{J}_1^{\oplus^{\mathbf{H}}} = \quad & h_{Z_h}(1-h_{X_h})\begin{bmatrix}\mathbf{J}_{Z_h}\\ \mathbf{0}_{1\times 2}\end{bmatrix}^{+} \\ & +(1-h_{Z_h})h_{X_h}\begin{bmatrix}\mathbf{0}_{1\times 2}\\ \mathbf{J}_{X_h}\end{bmatrix}^{+} \\ & +h_{Z_h}h_{X_h}\mathbf{J}_1^{+}.\end{aligned} \tag{6.11}$$

All the theoretical bases including the proof of continuity of this operator are detailed in [MRC09].

Now, task 2 can be stacked on top of this varying rank task 1 so that task 2 is projected onto the null space of the new task 1 (i.e task 2 is activated when task 1 is not activated and vice versa). It can be achieved using the projection operator $\mathbf{P}_H = \mathbb{I}_2 - \mathbf{J}_1^{\oplus^{\mathbf{H}}}\mathbf{J}_1$ as illustrated in [MC07]. According to [MC07], the controller will thus take up a form as follows:

$$\mathbf{v} = -\lambda[\mathbf{J}_1^{\oplus^{\mathbf{H}}}\mathbf{e_1} - \mathbf{P}_H(\mathbf{J}_2\mathbf{P}_H)^{+}(\mathbf{e_2} - \mathbf{J}_2\mathbf{J}_1^{\oplus^{\mathbf{H}}}\mathbf{e_1})]. \tag{6.12}$$

But, we also observe that the expression $\mathbf{P}_H(\mathbf{J}_2\mathbf{P}_H)^+$ in Eqn. (6.12) is discontinuous over the whole task space. Therefore, this expression can be replaced by its continuous inversion $\mathbf{J}_2^{\mathbf{P}_H\oplus}$ where $\mathbf{J}_2^{\mathbf{P}_H\oplus} = ((\mathbf{J}_2^T)^{\oplus\mathbf{P}_H})^T$. The inversion $(\mathbf{J}_2^T)^{\oplus\mathbf{P}_H}$ is computed in the same fashion as described in Eqn. (6.11).

Consequently we can finally re-write the velocity controller (6.12) as

$$\mathbf{v} = -\lambda[\mathbf{J}_1^{\oplus\mathbf{H}}\mathbf{e_1} - \mathbf{J}_2^{\mathbf{P}_H\oplus}(\mathbf{e_2} - \mathbf{J}_2\mathbf{J}_1^{\oplus\mathbf{H}}\mathbf{e_1})]. \tag{6.13}$$

Lastly, in order to eliminate the initially perceived failure cases we design the weight matrix $\mathbf{H} = \text{Diag}(h_{Z_h}, h_{X_h})$ and perform the task of joining a group using the following definitions:

$$h_{Z_h} = \begin{cases} 0.5 + \cos\left(\frac{\pi}{2}\frac{Z_h - \frac{2}{3}Z_{min}}{Z_{max} - \frac{2}{3}Z_{min}}\right) & \text{if } \frac{2}{3}Z_{min} \leq Z_h \leq Z_{max} \\ 1 & \text{if } \frac{1}{3}Z_{min} < Z_h < \frac{2}{3}Z_{min} \\ 0.5 - \cos\left(\frac{\pi}{2}\frac{Z_h - Z_h^*}{\frac{1}{3}Z_{min} - Z_h^*}\right) & \text{if } Z_h^* \leq Z_h \leq \frac{1}{3}Z_{min} \\ 0 & \text{otherwise} \end{cases} \tag{6.14}$$

$$h_{X_h} = \begin{cases} 0.5 - \cos\left(\frac{\pi}{2}\frac{X_h - X_{min}}{X_{max} - X_{min}}\right) & \text{if } X_{min} \leq X_h \leq X_{max} \\ 0 & \text{if } -X_{min} < X_h < X_{min} \\ 0.5 - \cos\left(\frac{\pi}{2}\frac{X_h - X_{min}}{X_{max} - X_{min}}\right) & \text{if } -X_{max} \leq X_h \leq -X_{min} \\ 1 & \text{otherwise.} \end{cases} \tag{6.15}$$

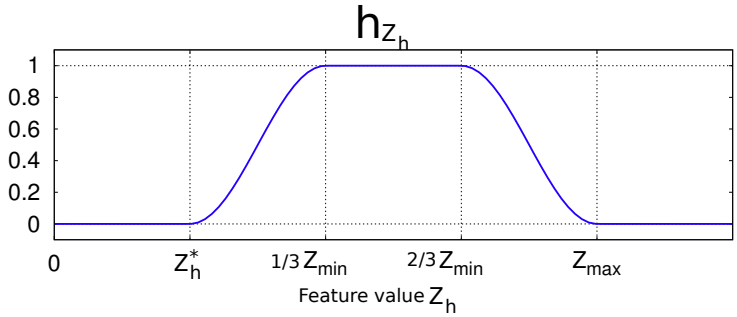

Figure 6.4: The evolution of h_{Z_h} with respect to the feature Z_h

Figure 6.4 visually represents the evolution of the activation factor h_{Z_h} with respect to the parameters Z_{min} and Z_{max}. Z_{max} is defined as the maximum possible positive value Z_h could obtain at a particular configuration. It can be obtained from the estimations of X_h (X_{init}) and Z_h (Z_{init}) at the first instant when $Z_h > 0$. Therefore $Z_{max} = \sqrt{X_{init}^2 + Z_{init}^2}$. Whereas $Z_{min} = Z_{max} - Z_h^*$. The above definition of h_{Z_h} ensures that the activation of the feature Z_h is 0 as long as Z_h becomes positive. Z_h is positive only if the interacting group is within the field of view of the sensor.

This definition ensures that the robot performs a motion that regulates the errors on X_h and L_h which is essentially aligning the sensor towards the group (gazing at the group). It can serve as a notification of approach for the group members. As soon as $Z_h > 0$, the control over this feature is returned in a smooth fashion as the robot moves forward and towards the meeting point (see Figure 6.4 interval $[\frac{1}{3}Z_{min}, Z_{max}]$). Also, as the feature error $Z_h - Z_h^* \to 0$, the activation gradually decreases to zero which essentially allows the other two features to converge to their desired values (see Figure 6.4 interval $[Z_h^*, \frac{1}{3}Z_{min}]$).

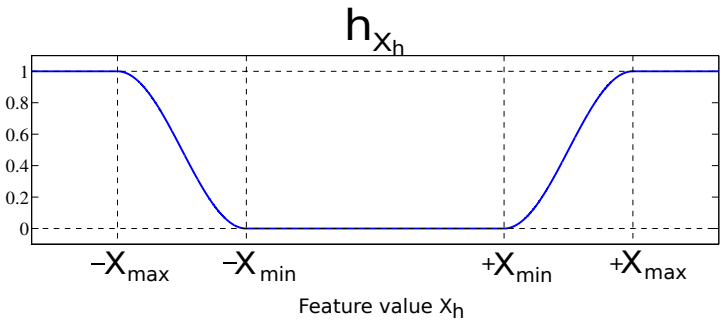

Figure 6.5: The evolution of h_{X_h} with respect to the feature X_h

Figure 6.5 represents the evolution of h_{X_h} with respect to the intervals $[X_{min}, X_{max}]$ and $[-X_{min}, -X_{max}]$. This interval is designed as a dynamic interval which varies proportionally with the absolute value of the error of task 2 namely $|\mathbf{e_2}|$.

If we have two positive scalars k_1 and k_2, we can define $X_{min} = k_1|\mathbf{e_2}|$ and $X_{max} = k_2 X_{min}$. This variation ensures that the task priority can be switched from task 1 (when $|\mathbf{e_2}|$ is low) to task 2 (when $|\mathbf{e_2}|$ is high) at optimum intervals. If $|\mathbf{e_2}|$ is low, then the interval $[-X_{min}, X_{min}]$ is small which facilitates more regulation over the feature X_h and when $|\mathbf{e_2}|$ is high, then the interval $[-X_{min}, X_{min}]$ is large which facilitates more regulation over the feature L_h. This also ensures that a local minima is avoided and the system reaches a near global minima. The value of the factors k_1 and k_2 can be tuned empirically so that the sensor is always gazing at the group during the motion[1].

The above definition of the matrix $\mathbf{H} = \text{Diag}(h_{Z_h}, h_{X_h})$ solves the first two of the three issue mentioned in Section 6.4.3. With respect to the third limiting issue (described in the beginning of this section), if the meeting point is behind the humans which means that the humans are facing away from the robot, the only way to solve this case is to move the robot in open loop till the meeting point is in front of the humans with respect to the robot (nevertheless this is not an issue in an two person vis-a-vis formation).

It is also evident to note that the control law is capable of self adapting to the dynamic motions of the humans within an interaction as long as the interaction does not break.

[1] k_1 and k_2 were empirically set according to the formula $k_1 = fov/120$ and $k_2 = 1\frac{1}{3}k_1$. Where fov is the field of view of the sensor in degrees. It can be postulated that this assignment is valid for any sensor up to $180°$ field of view.

Table 6.1: Absolute error values at the final position - 12 random initial positions

Error	Mean (m)	Low (m)	High (m)	Std. Dev (m)
$\lvert Z_h - Z_h^* \rvert$	0.091	0.012	0.233	0.081
$\lvert X_h - X_h^* \rvert$	0.066	0.012	0.230	0.065
$\lvert L_h - L_h^* \rvert$	0.089	0.002	0.251	0.092

6.5 Analysis in Simulation

We analyse the control strategy presented in the previous section with respect to its stability, convergence and robustness. The scenario is designed as a robotic wheelchair approaching a two-person interaction for a variety of configurations. All the presented simulations are modelled within the ROS middleware.

6.5.1 Stability

From [MRC09], stability of the control law (6.13) can be asserted for two conditions viz: **asymptotic stability in the sense of Lyapunov** at binary activation (i.e $\forall i = X_h, Z_h$, $h_i = 0$ or $h_i = 1$.) and **local asymptotic stability around the desired position (i.e. at the meeting point)**. These assertions are true if the tasks $\dot{\mathbf{e_1}} = \mathbf{J}_1\mathbf{v}$ and $\dot{\mathbf{e_2}} = \mathbf{J}_2\mathbf{v}$ are locally asymptotically stable.

Let $V = \frac{1}{2}\mathbf{e_i}^T\mathbf{e_i}$, $\forall i = 1, 2$, be a positive continuous Lyapunov candidate, then the task $\mathbf{e_i}$ is said to be asymptotically stable if $\dot{V} < 0$. Now, $\dot{V} = -\mathbf{e_i}^T\mathbf{J}_i\mathbf{J}_i^+\mathbf{e_i}$. Therefore if $\mathbf{J}_i\mathbf{J}_i^+$ is positive definite, then $\dot{V} < 0$. This condition is true (since the product is Identity) as per the definition of the Jacobians $\mathbf{J}_1$ and $\mathbf{J}_2$ in the previous section, and as the interaction matrix $\mathbf{L}$ is well defined. The only singularity occurs when the robot starts at a position in the same hyperplane as, and directly facing, the interacting humans (i.e. $L_h = 0$). This case can be resolved by moving the robot in open loop till a non-singular position is reached.

6.5.2 Convergence

In order to analyse the convergence, the simulated wheelchair robot is tasked with joining the group from a variety of random initial positions. The control gain λ was set at 0.1 unless otherwise specified. Table 7.1 provides the statistics for the feature errors (i.e $Z_h - Z_h^*$, $X_h - X_h^*$ and $L_h - L_h^*$) at the final robot pose (i.e at the meeting point) for 12 different robot starting poses. It can be seen that the mean feature error at the final pose is sufficiently low, thus proving that the control law is able to converge to the desired pose satisfactorily. The maximum feature error was around 24cm, in some cases due to the robot starting at an almost singular position as represented in Fig. 6.6c.

Furthermore, Fig. 6.6 shows two cases of the simulation where, in case I, the robot started in a straightforward position and in case II, the robot started in an almost singular position. We

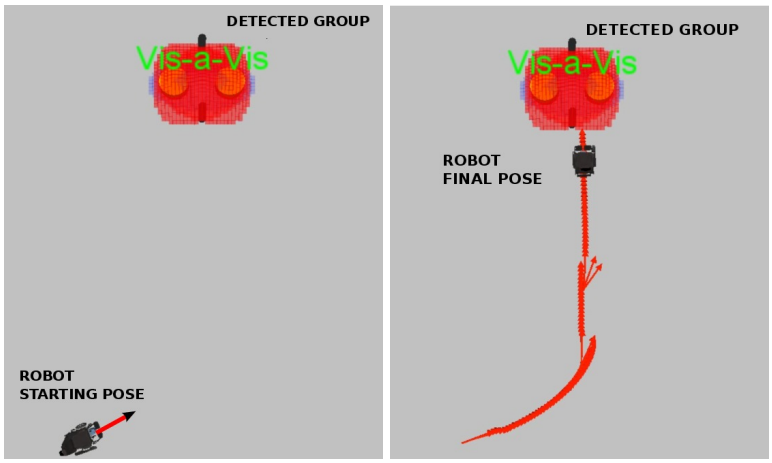

(a) Case I - Start (b) Case I - End

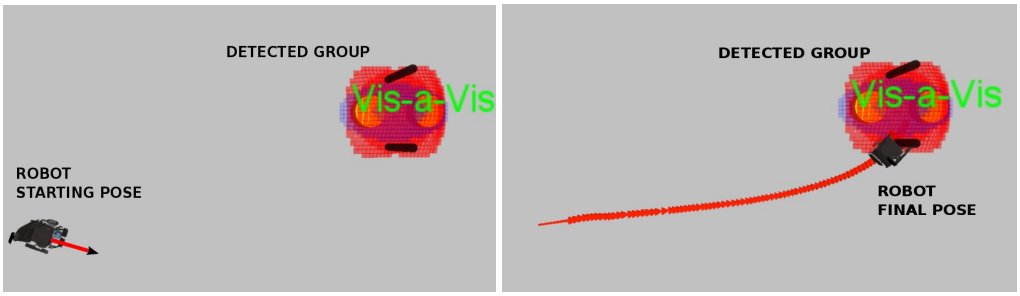

(c) Case II - Start (d) Case II - End

Figure 6.6: The starting and final robot poses with respect to a detected group for two simulation cases.

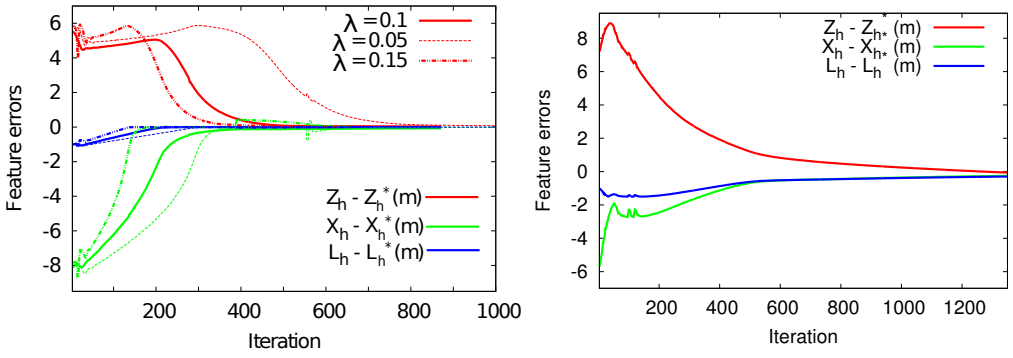

(a) Case I (b) Case II

Figure 6.7: The evolution of the feature errors. (a) 3 runs of Case I with different gains and, (b) Case II with gain $\lambda = 0.1$.

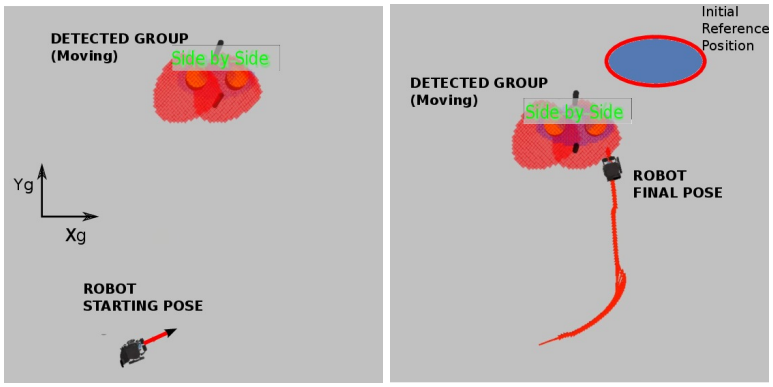

(a) Start (b) End

Figure 6.8: The starting and final robot poses with respect to a continuously moving detected group.

can see that the meeting point is reached in both the cases. In both the cases, the robot initially turns towards the group, essentially facing the sensor towards the group, and then performs the motion for approaching the group. This is consistent with the design of the control law.

The evolution of the errors in Fig. 6.7 also corroborate this fact. Moreover, case I is is also simulated in Fig. 6.7 with three different control gains where a three degrees of magnitude change in λ does not affect the convergence. Thus we can say that the control law is robust to large variations in the gain.

6.5.3 Robustness

In order to assess the robustness of the control strategy, two scenarios are presented. In both the scenarios the robot is tasked with joining a two person side-by-side group from a starting configuration as presented in case I (Figure 6.6a). The first scenario involves the robot approaching and joining a group which is moving at a constant speed of 0.1m/s at an angle of -135° with respect to a 2-D reference global frame (see Figure 6.8). In such a case, even though the group is in continuous motion, the robot is able to reach a satisfactory position (Figure 6.8b) in order to become an equitable part of the interaction. It has to be noted that the group remains in motion even as the robot closes in to the meeting point. This is necessarily not the case in the real world as a moving group of people do not form meeting points. But with respect to the control law adapting to the motion of the group, this scenario provides a clear evidence of the robustness of the proposed solution albeit in simulation.

The second scenario involves the robot tasked with joining a group in the presence of dynamic humans. An ultrasound-based reactive collision avoidance mechanism [BPG+15] was employed in conjunction with the proposed motion strategy. The collision avoidance mechanism essentially constrained the velocities (using a standard redundancy formalism) coming from the proposed velocity controller (6.13) using information coming from the sensors. The technical de-

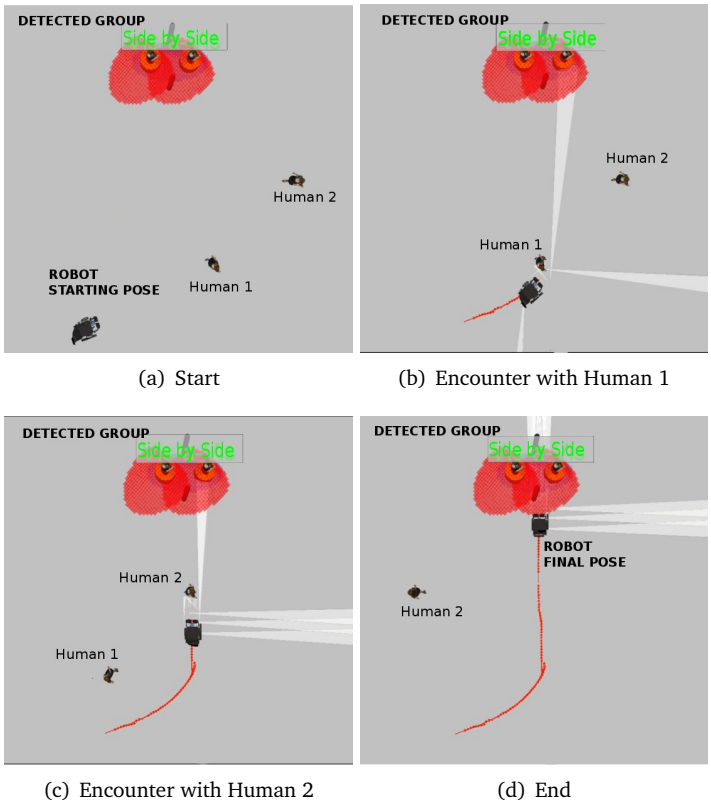

(a) Start (b) Encounter with Human 1

(c) Encounter with Human 2 (d) End

Figure 6.9: The robot trying to approach and join a group in the presence of other moving humans.

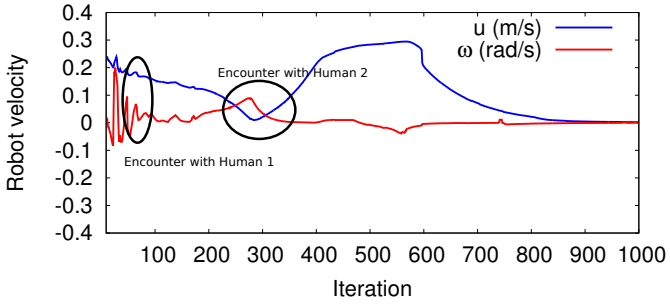

Figure 6.10: The evolution of the robot translational (u) and angular (ω) velocities during the simulation for the above Case.

tails of the final controller is not delineated here as it does not contribute towards the objective of this work. Figure 6.9 demonstrates that the robot is able to avoid collision with the moving humans while attempting to join the group. This is corroborated from the velocity plots (Figure 6.10) that show variation during human encounters. During the first encounter, the angular velocity is erratic due to the robot simultaneously turning towards the group while attempting

to avoid collision with the human. This is caused by the reactive obstacle controller generating opposite velocity commands to the control strategy. It can be essentially be resolved by using a higher level decision making algorithm which could provide importance to the specific task to be performed using some well defined heuristic. But in the second encounter, which is more straightforward, it can be seen that the robot slows down (see Figure 6.10) to accommodate the human passing.

6.6 Experiments

We carried out trials using a non-holonomic mobile robot in order to validate the control law in a noisy real world situation. A mobile robot equipped with a single laser scanner capable of detecting and classifying humans based on a leg detection algorithm was used for the trials.

The robot was localised using the said laser and odometry, within a map generated on-line using a widely implemented Simultaneous Localization and Mapping (SLAM) algorithm [GSB07]. Again the framework was designed within a ROS architecture while the computations were performed using the ViSP software.

The robot was tasked with autonomously approaching and joining the two person human interaction from three random initial positions. We can see from Figures 6.11 that the robot was able to reach the optimal meeting point based on the spatial constraints described in Section 6.3 by taking an appropriate trajectory towards the interaction. As designed, the robot is always gazing at the group during the motion. Particularly in the third run, where the robot is gazing away from the group at its initial position. The specific definition of the weight matrix $\mathbf{H}$ allows the robot to turn towards the group initially and approach in a frontal manner order to join the group. Also, the robot does not encroach the O-space of the interaction thus matching all the constraints presented in Section 6.3. An exponential decrease of the feature errors as shown in Figure 6.12 for the three trials also corroborate the analysis.

6.7 Further Discussion

6.7.1 Adaptability

It can be asserted that the motion strategy analysed here is adaptable and modular in the sense that such a feature based design allows adaptation of the system into a variety of general cases owing to the fact that it is sensor-agnostic. It is due to the fact that the features presented here are easily extractable once the robot is able to detect people. As such a non-holonomic constraint on the robot applies to the majority of social and service robots. Moreover, the framework developed within a ROS system facilitates redistribution and widespread usage.

(a) Trial 1

(b) Trial 2

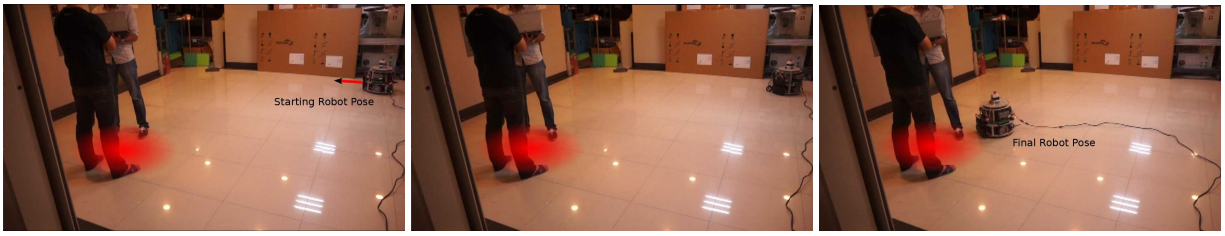

(c) Trial 3

Figure 6.11: Snapshots of the starting robot pose, a moment during the motion and the final robot pose for 3 experimental trials (each row). We can observe that the robot initially aligns itself towards the group and is able to reach the desired meeting point without encroaching the O-space of the interaction.

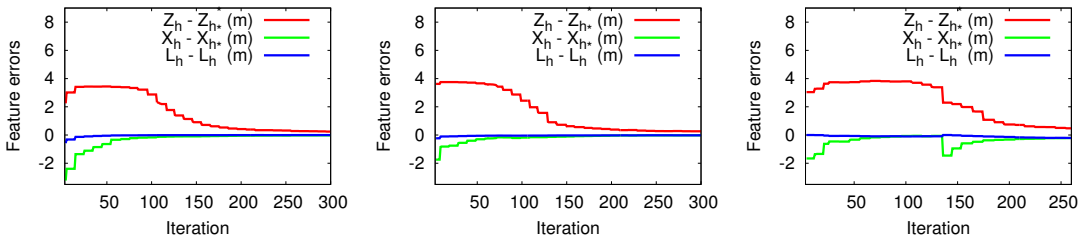

Figure 6.12: The variation on feature errors for Trials 1 (left), 2 (middle) and 3 (right) respectively.

6.7.2 Context Dependency

With respect to applying the control law within a variety of contexts, for example esoteric cases like a group waiting in line, the theory that is derived from proxemics along with the features presented here can be modified in order to accommodate such contexts. The control strategy (i.e. the features) does not depend on the type of group nor does it take into account the perception of the humans with the group. Thus context specific behaviours can be easily integrated onto the system.

6.7.3 Group Perception

Perception of the group is a vital issue to be tackled when designing such algorithms for social robots and thus a motivation for future work. It would be very interesting to assess the human perception of the path chosen by the robot and perform a subjective analysis. This can also help in adapting the algorithm for a variety of context specific behaviours.

6.8 Conclusion

In this chapter, we demonstrated a feature-based velocity control law targeted at social roots such as intelligent wheelchairs, which can serve as a low-level controller for equitably joining interacting groups, while confirming to social conventions. The system uses the position and orientation of the participating humans with respect to a rigid sensor (for example, a laser scanner) frame in order to control the translational and rotational velocity of a non-holonomic robot so that the robot positions itself aptly and *equitably* at the meeting point. A novel algorithm was designed which ensures that the motion adhered to spatial social standards while ensuring that the controller does not fall into a local minima. The analyses in simulation demonstrate modularity, convergence and robustness with respect to a variety of cases. Experiments performed on a non-holonomic mobile robot equipped with a single laser scanner also verify the efficacy of the system in real and dynamic world. We also want to reinforce the idea that the solution also fits with robotic wheelchairs having on-board or distributed human sensing capabilities, as the modelling is general enough to be adapted to any non-holonomic mobile robot.

Finally, to summarize the second part of the thesis, we initially presented a formal understanding of the concepts on social spaces essential for designing human-aware navigation systems while including a brief look into a risk-based RRT motion planner for socially aware navigation. Further, in this chapter, we designed a sensor-agnostic velocity control law for equitably approaching and joining human groups in interaction.

In the next part of the thesis, we use the concepts learned from the work until now in order to propose a semi-autonomous framework for human-aware wheelchair navigation assistance. Finally, as the concluding contribution, we use ideas derived from this semi-autonomous framework in order to propose a general solution for assistive shared control.

Part III

Towards Assistive Shared Control

Chapter 7

Semi-autonomous Framework for Human-aware Wheelchair Navigation

THIS CHAPTER proposes a general semi-autonomous framework for human-aware and *user intention driven* wheelchair navigation assistance.

From Part I of this thesis, we inferred a linear control sharing formalism for efficiently providing assistance for wheelchair corridor navigation. Meanwhile, from Part II, we modelled spatial social constraints that should be integrated onto any social robot such as an intelligent wheelchair. Moreover we also briefed a risk-based motion planner (RiskRRT) that encoded these spatial constraints for human-aware navigation.

Whereas, another important component in the design of robotic assistance solutions is *the estimation of user intention*. In Part I, we saw that the task of doorway passing is not trivial compared to the task of corridor following, as in a *low-level estimation of user intention* provides us the specific doorway the user wishes to pass through. Consequently, while designing more general solutions, as the one proposed in this chapter, we need to define and provide a method to efficiently estimate user intention. This allows us to finally formalize the semi-autonomous framework as a system, that *probabilistically* estimates the user destination (intention) and then assists the user in order to safely reach the desired destination, owing to a linear control sharing policy, that blends the user teleoperation coming from a joystick and the velocities coming from a *human-aware* motion planner.

The work in this chapter will be presented at the IEEE/RSJ International Conference on Robots and Systems (IROS)[**C.1**] this year.

7.1 Introduction

7.1.1 Objective

Keeping in line with the crux of this thesis we aim to introduce a semi-autonomous framework for wheelchair mobility assistance that is adaptable in order to be deployed in real world systems. Therefore, the aim is to blend user teleoperation coming from a traditional joystick that is equipped on the wheelchair, with the velocity coming from the previously briefed human-aware motion planner RiskRRT.

Thus, the objective is then to initially estimate the user intended goal at regular intervals, which in turn may serve as the goal for RiskRRT. In addition, we need to propose an *efficient and optimal* control sharing policy in order to produce a final motion that mitigates not only the risk of collision with dynamic obstacles, but also the risk of disturbance to other humans.

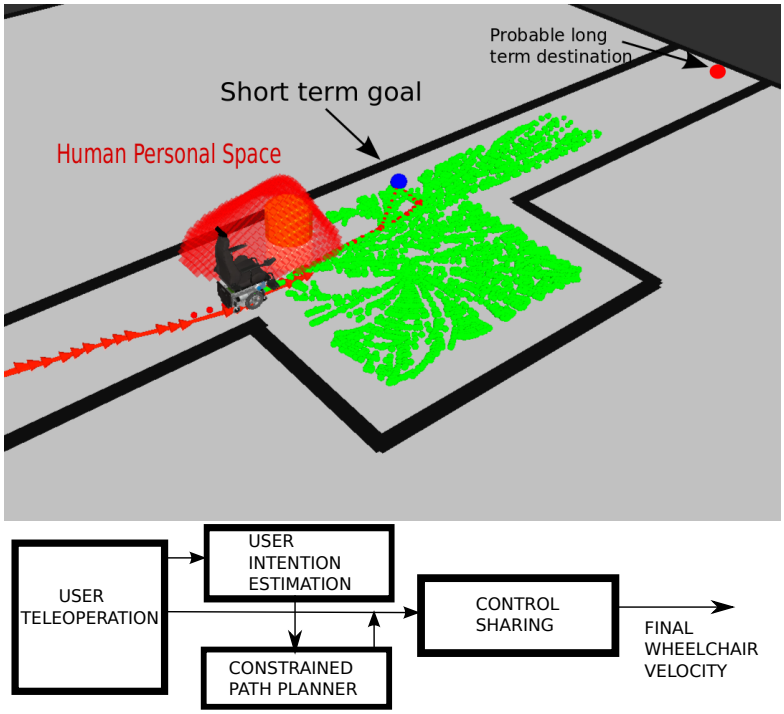

Figure 7.1: Robots in human environments need to respect the virtual social spaces that is created when humans are present. This Figure shows a robotic wheelchair following a corridor by planning a trajectory (in red) toward a *short term* goal (in blue) while taking into account these spatial social constraints, within a 2D configuration space. We augment the user teleoperation with velocities coming from the motion planner while regularly predicting these short term goals that drive the said motion planner.

7.1.2 Components of the assistance framework

We can see that the two components which constitute the semi-autonomous (or any robotic) assistance framework are, viz. a user intention estimation module, and a control sharing module. In the present case, user intention estimation yields us the specific pose in the world (map), the user wishes to navigate to. This pose can serve as a goal for the motion planner RiskRRT, which in turn can be used to augment user teleoperation by assigning an *assistance* function that shares control between the user and the robot motion planner.

Predicting User Intention

As described in Chapter 2, initial designs for wheelchair navigation assistance provided higher level control to the user where the final goal was given by the user and the wheelchair performed as an autonomous robot [Tak98, LBJ+99, ESL14]. Following this, untraditional interfaces such as Brain-Controlled Interfaces (BCIs) [CDRM13] and RGB-D sensors able to track faces [ESL14] were utilized to infer user intention in the form of topological poses in the wheelchair configuration space. Approaches that relied on plan/action recognition [CD12] (eg. providing assistance for a specific task) also were introduced. Finally learning techniques such as using Partially Observable Markov Decision Processes [TMD08], or Leaning from Demonstration [GDA13] were investigated for long term intention prediction. All intention prediction mechanisms described above are highly deterministic and do not have the capability of estimating user intention uncertainty which may cause much discomfort to the user if the wheelchair does not behave as intended. A Bayesian based approach was presented in [DHV+06] where the uncertainty in user intention was explicitly modelled. This allowed for a more user centric design.

In Part I, for the task of corridor following, user intention was not integrated, as the goal was to design a low-cost and low-level vision-based scheme for providing assistance. In fact, for the task of corridor following, we always assumed that the user is planning to drive along the corridor. Meanwhile, for the task of doorway passing, this assumption is not true even in the lower level, as the user may select from a different number of doorways present in a corridor to navigate through. Thus we encoded user intention in the assistance factor α (see Eqn. (4.13)) as a progressively increasing factor that varies as the wheelchair distance to a specific doorway decreases.

But if the distance to a specific doorpost was higher than a specific value, this factor reduced to zero. From this concept, we arrive at an idea of predicting *short term goals*. We here argue that the user intention uncertainty can be avoided by only predicting *short term goals* that are sub-optimal and agnostic to the user's probable long term intention (refer to Figure 7.1 for an intuitive understanding of the concept of short term goals). We can then use Bayesian reasoning to infer such short term goals (as topological poses within a well defined map) where they only depend on the *current wheelchair state* and the *current direction of the user's intended motion*. The proposed formulation can be used to predict goals at regular intervals and also be used to learn the user's frequent goals, which in turn may further improve performance.

Sharing Control

As stated earlier, intelligent wheelchairs initially were designed as autonomous robots where the user was given the freedom to choose his final destination [Tak98, LBJ+99, ESL14]. Consequently, lower level control in the form of augmenting the user teleoperation, was introduced [CDRM13, GDA13, CD12, DEVPHDS12, Arg16]. The final wheelchair velocity was calculated using a linear control sharing formalism of the general form $(1-\alpha)\mathbf{v}_{op} + \alpha\mathbf{v}_r$ with $\mathbf{v}_{op}$ and $\mathbf{v}_r$ representing the user teleoperation and the corrective velocity respectively (eg. velocity coming from a motion planner). Evidently, for vision-based corridor following assistance, the usage of the continuous inverse (see Eqn. (4.7)) led to the inference of such a linear control sharing formalism. We successfully employed this formalism for the task of doorway passing assistance. Here α henceforth termed the assistance factor represents the *amount* of control the autonomous controller has at a particular instant as it translates to an allocation weight for each contributing velocity.

In fact, this formalism has been studied thoroughly in the field and in majority of the studies [GDA13, CD12, DEVPHDS12, Arg16], the assistance factor is set as a scalar (i.e all the Degrees of Freedom (DOFs) of the wheelchair respond to the same assistance factor) and is determined according to the specific needs of the control system. We aim to extend this formalism towards a more general, stable and user centric design based on the designs presented in Part I. Moreover, as argued before, a progressive increase (or decrease) in control sharing is also a key factor for better quality of driving.

Thus, based the introduced considerations, the following section presents the design of the semi-autonomous framework based on a probabilistic paradigm for predicting short term goals, and on an efficient and stable fusion of the user and robot generated control.

7.2 Semi-autonomous Framework

The semi-autonomous framework thus comprises of two components: the user intention estimation process that generates short term goals which drives the motion planner briefed in Chapter 5 and the shared control system that fuses the velocities generated from the motion planner in order to augment the user teleoperation.

7.2.1 Modelling

Consequently, we model the wheelchair as a non-holonomic unicycle-type robot moving on a horizontal or inclined plane, while assuming that the user teleoperates it via an adapted interface such as a traditional 2D joystick. We thus have the following definitions:

- $\mathbf{v} = [v, \omega]^T$: The wheelchair control velocity with its translational (v) and angular (ω) components.
- $\mathbf{v}_{op} = [v_{op}, \omega_{op}]^T$: The user teleoperation velocity coming from the adapted interface.

- $\mathbf{v}_r = [v_r, \omega_r]^T$: The velocity from the constrained local motion planner.

If the wheelchair navigates within a 2D configuration space ($\mathbf{SE}(2)$ represented by (x, y, ϕ)) we have,

- $\mathbf{X}_t = (x_t, y_t, \phi_t)$: The wheelchair configuration at a particular instant t.
- $\mathbf{X}_g = (x_g, y_g, \phi_g)$: The estimated short term goal towards which the user intends to navigate.

We assert that at any instant t of goal prediction, $\mathbf{X}_g$ is a function of $\mathbf{X}_t$ and ϕ_t^* where ϕ_t^* is the angle between the 2D joystick direction at t with respect to the x axis of the space (we can think about it as the desired direction attempted by the user, see Fig 7.2). Our goal is then to fuse $\mathbf{v}_{op}$ and $\mathbf{v}_r$ in order to derive a progressive assistive system for semi-autonomous navigation among human crowds while estimating $\mathbf{X}_g$ at regular intervals.

7.2.2 User Intention Estimation

We estimate the user intention as topological poses within the configuration space which serve as short-term goals for the motion planner that is in turn used to augment the user teleoperation. We here propose a formulation for predicting goals that nullifies user intention uncertainty i.e. short term goals that are agnostic but compatible with the user's long term intention. In order to generalize, we can consider two scenarios:

1. The wheelchair operates in a constrained and mapped environment with a list of frequent user destinations previously learned or determined.
2. The wheelchair operates in an unconstrained and unmapped environment.

Assuming $\mathbf{X}_r = function(\mathbf{X}_t, \phi_t^*)$ a random goal estimated at each instance of goal prediction (see Fig 7.2) and $\{\mathbf{X}_1, \mathbf{X}_2 ..... \mathbf{X}_n\}$ be the set of n determined/learned goals, then we can define a set $\mathbf{X_G} = \{\mathbf{X}_r, \mathbf{X}_1, \mathbf{X}_2 ..... \mathbf{X}_n\}$ of $n+1$ goals. The short term goal $\mathbf{X}_g$ can then be formulated using a Bayesian approach as,

$$\mathbf{X}_g = \underset{\mathbf{X}_i \in \mathbf{X_G}}{\arg\max}\, P(\mathbf{X}_i | \mathbf{X}_t, \phi_t^*). \tag{7.1}$$

Thus, $\mathbf{X}_g$ is the goal that maximises the posterior probability P of selecting a goal $\mathbf{X}_i$ given the current wheelchair configuration $\mathbf{X}_t$ and the user joystick directional angle ϕ_t^* at the prediction instant t. In order to determine $P(\mathbf{X}_i | \mathbf{X}_t, \phi_t^*)\ \forall i$, we can use Bayes' theorem:

$$P(\mathbf{X}_i | \mathbf{X}_t, \phi_t^*) = \frac{P(\phi_t^* | \mathbf{X}_t, \mathbf{X}_i) P(\mathbf{X}_i | \mathbf{X}_t)}{P(\phi_t^* | \mathbf{X}_t)}. \tag{7.2}$$

The above relation can be normalized using a constant η as

$$P(\mathbf{X}_i | \mathbf{X}_t, \phi_t^*) = \eta P(\phi_t^* | \mathbf{X}_t, \mathbf{X}_i) P(\mathbf{X}_i | \mathbf{X}_t). \tag{7.3}$$

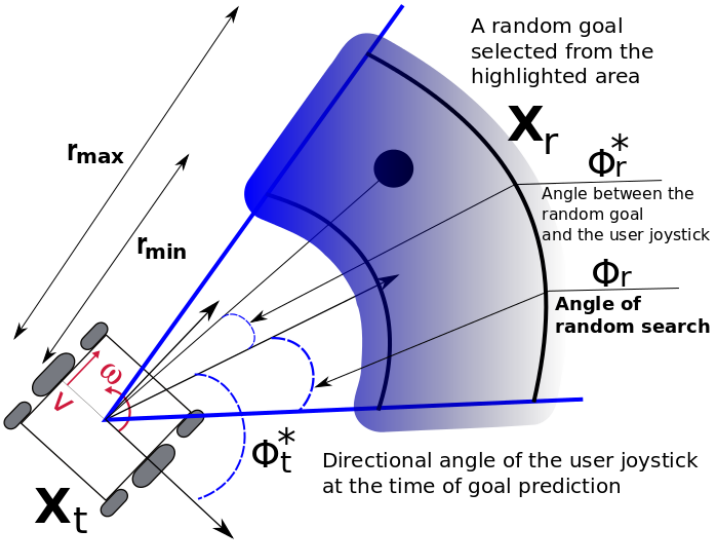

Figure 7.2: Random short term goals: A random 2D point (x_r, y_r) is searched from within the circular segment as shown in the figure and the random goal $\mathbf{X}_r$ is set as $\mathbf{X}_r = (x_r, y_r, \phi_t^*)$. The distances r_{min} and r_{max} as well as the search angle ϕ_r determine the size of the search area. The angle between the random goal and the user joystick direction ϕ_r^* is also shown here (see Eqn. (7.4)).

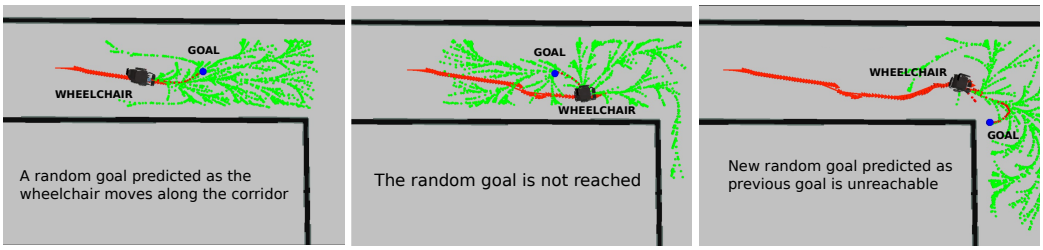

Figure 7.3: Random short term goal predictions: A sequence depicting a wheelchair moving within a corridor and into a doorway

$P(\phi_t^*|\mathbf{X}_t, \mathbf{X}_i)$ represents the probability of the user assigning a joystick directional angle ϕ_t^* given the current configuration $\mathbf{X}_t$ and the intended goal $\mathbf{X}_i$. Since the prediction window is short term, we design this probability as,

$$P(\phi_t^*|\mathbf{X}_t, \mathbf{X}_i) = \frac{\frac{1-|\phi_i^*|}{\pi}}{\sum_i \frac{1-|\phi_i^*|}{\pi}}, \tag{7.4}$$

where ϕ_i^* is the angle between the user joystick direction and the goal $\mathbf{X}_i$ (see Fig. 7.2 for a representation of ϕ_r^* where $i = r$). Thus at each instant we predict the short term goal $\mathbf{X}_g$ as,

$$\mathbf{X}_g = \underset{\mathbf{X}_i \in \mathbf{X_G}}{\arg\max} \frac{\frac{1-|\phi_i^*|}{\pi}}{\sum_i \frac{1-|\phi_i^*|}{\pi}} P(\mathbf{X}_i|\mathbf{X}_t). \tag{7.5}$$

Discussion: In a constrained and mapped environment where a set of goals are previously learnt or determined, we can postulate that the probability $P(\mathbf{X}_i|\mathbf{X}_t)$ be assigned using specific criteria with the Euclidean distance norm (d) being the most straightforward where

$$P(\mathbf{X}_i|\mathbf{X}_t) \propto \frac{1}{d(\mathbf{X}_t, \mathbf{X}_i)}. \tag{7.6}$$

For any random goal $\mathbf{X}_r$, $P(\mathbf{X}_r|\mathbf{X}_t)$ can then be set as a minimum positive threshold δ in order to give priority to the learnt or determined goals.

Whereas in unconstrained and unmapped environments, it is evident that the random goals will take priority as there are no pre-set goals to reason over. But estimation of intentions over a long time could provide data that captures user sequential decisions, which can be used to learn user habits. In such a case and since we have a low dimensional state space, frequent goals and the prior $P(\mathbf{X}_i|\mathbf{X}_t)\ \forall i$ can be learnt using algorithms for Bayesian Inverse Reinforcement Learning, as we can effectively argue that the user performs an optimal sequence of actions in order to reach his/her short term goals [ZMBD08]. Further explanation of this concept is provided in the following chapter.

In terms of prediction interval, we propose that a new goal be determined if the present goal is reached (i.e. $d(\mathbf{X}_t, \mathbf{X}_g) < d_{min}$) or if the distance to the present goal is high enough to be unreachable (i.e $d(\mathbf{X}_t, \mathbf{X}_g) \geq d_{max}$). Here d_{min} and d_{max} represent the distances within which the short term estimated goal is to be considered.

Fig. 7.3 shows some instances of random short term goal predictions for a wheelchair moving within a corridor and into a doorway. Since the random goal is dependent on ϕ_t^*, the short term user intention is always respected albeit sub-optimal. In addition, since the user is deemed to have primary control of the wheelchair, in many cases the estimated goals (especially if they are random) will not be reached. This is not an issue as a new goal will be predicted as soon as $d(\mathbf{X}_t, \mathbf{X}_g) = d_{max}$.

Therefore user intention uncertainty can effectively be ignored. Moreover, a random goal may also lie within the social space of a human nearby or on an obstacle (see Fig. 7.4). This again is not an issue since the motion planner plans safe paths toward the goal and the shared control formalism would ensure that the wheelchair avoids the danger as can be seen from the next subsection.

7.2.3 Control Sharing

The shared control system should take part of the control from the user only in order to reduce the risk of collision or the risk of disturbance to other humans. Also, control sharing should be progressive and smooth in order to ensure that the user is able to perceive the danger and is not frustrated by sudden changes in motion.

Let $\mathbf{A} = \text{diag}(\alpha_v, \alpha_\omega)$ be a positive definite diagonal assistance function such that $\alpha_v \in [0, 1]$ and $\alpha_\omega \in [0, 1]$, we can design the wheelchair velocity controller as

$$\mathbf{v} = (\mathbb{I}_2 - \mathbf{A})\mathbf{v}_{op} + \mathbf{A}\mathbf{v}_r, \tag{7.7}$$

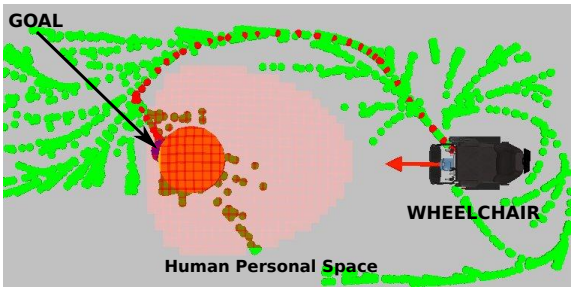

Figure 7.4: Here we see a goal being estimated that is in collision with a human. But the motion planner RiskRRT plans a safe and socially compliant path towards the goal. The design of the shared control formalism (see Section 7.2.3) also ensures that the user teleoperation is augmented in order to evade this danger.

where $\mathbb{I}_2$ is a size 2x2 Identity matrix.

We assert that the only criterion for providing assistance would be the distance to danger. Assume that the **closest** topological pose where either an obstacle is detected or is part of the human personal or interaction space, is located at a Euclidean distance $d_{\mathbf{A}}$ from the wheelchair (see Fig 7.5). Then if $[d_{\mathbf{A_{max}}}, d_{\mathbf{A_{min}}}]$ with $d_{\mathbf{A_{max}}} > d_{\mathbf{A_{min}}}$ is a pre-defined interval with $d_{\mathbf{A_{max}}}$ representing the maximum distance from the danger beyond which no assistance should be provided and $d_{\mathbf{A_{min}}}$ representing the minimum distance from the danger below which the motion controller should essentially take full control, we can assign

$$\alpha_\omega = \begin{cases} 0 & \text{if } d_{\mathbf{A}} > d_{\mathbf{A_{max}}} \\ 1 + \cos(\frac{\pi}{2} \frac{d_{\mathbf{A}} - d_{\mathbf{A_{min}}}}{d_{\mathbf{A_{max}}} - d_{\mathbf{A_{min}}}}) & \text{if } d_{\mathbf{A_{min}}} \leq d_{\mathbf{A}} \leq d_{\mathbf{A_{max}}} \\ 1 & \text{otherwise} \end{cases} \tag{7.8}$$

$$\alpha_v = \frac{1 - \exp(-\alpha_\omega)}{2}. \tag{7.9}$$

Such a definition allows us to progressively and smoothly activate (and deactivate) assistance within the interval $[d_{\mathbf{A_{max}}}, d_{\mathbf{A_{min}}}]$ (see Fig. 7.5).

Compatibility with user intention estimation

We see that the motion planner will take control only if the wheelchair is at risk of collision with an obstacle or at risk of disturbance to others. Control is soon returned as danger is evaded. Moreover, we hypothesize that since the goal prediction window is short term and dependent on $\mathbf{X}_t$ and ϕ_t^*, the specific case of $\mathbf{A} \neq \mathbf{0}_{2,2}$ at the goal prediction instant will not lead to erratic motions.

Stability

An analysis of stability of the formulation is essential in order to keep the system user centric and acceptable to wheelchair users. It was proved by Wang et.al. [WL14] that given that the set of feasible inputs from the user (i.e. $\mathbf{V}_{op} = \{\mathbf{v}_{op}\}, \forall \mathbf{v}_{op}$) and the set of feasible robot motion

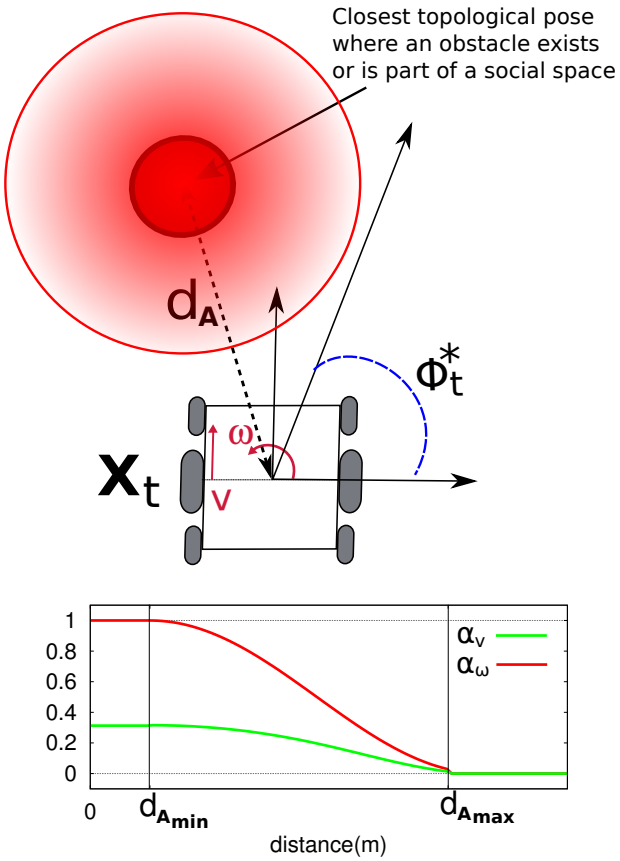

Figure 7.5: The illustration on top provides an intuitive idea of the evolution of the factor α_ω with respect to a detected obstacle (or social space). The graph at the bottom shows the related functions α_v and α_ω with respect to the distance to the closest topological pose where an objects exists or which is part of a social space.

commands (i.e. $\mathbf{V}_r = \{\mathbf{v}_r\}, \forall \mathbf{v}_r$) is convex, the controller $\mathbf{v} = (\mathbb{I}_2 - \mathbf{A})\mathbf{v}_{op} + \mathbf{A}\mathbf{v}_r$ is stable in the sense of Lyapunov unless $\mathbf{V}_{op} \cap \mathbf{V}_r = \emptyset$. If the motion planner generates motion commands ($\mathbf{v}_r$) bounded by the maximum permissible velocities of the wheelchair, the instability condition is never encountered.

A simple approach taken by Dragan et al. [DS12] (within the context of manipulation) considering the same control sharing formulation, proved that an inescapable local minima does not occur unless $\forall \mathbf{v}_{op}$, $\mathbf{v}_r = -k\mathbf{v}_{op}$ for any $k \geq 0$ and $\alpha_v = \frac{1}{k+1}$ as well as $\alpha_\omega = \frac{1}{k+1}$. Within the proposed formulation, this case does not occur at all since at no point where $\alpha_v > 0$ and $\alpha_\omega > 0$ is $\alpha_v = \alpha_\omega$.

Full robot control is never taken

It can be seen from Eqn (7.9) that α_v never goes to its maximum value of 1. We here hypothesize that altering the angular velocity (ω) of the wheelchair is sufficient for efficiently eliminating the

risks of collision and disturbance. This also allows for a trajectory correction in the direction of the user intended motion wherein, it respects the desired forward velocity owing to the fact that it is the best solution to respect the user intention. This also means that the user will be able to collide with an obstacle or move into the social spaces if he/she tries hard enough. This property is required firstly in order to keep the primary control with the user, secondly to learn the user habits and finally to teach the user how to efficiently operate a wheelchair [MMAM06].

Gateway to learning and teaching

An essential case to consider while designing mobility assistance systems is to facilitate the learning of user habits. For example, since the formulation (7.7) is directly dependent on the distance to the closest *dangerous* pose, the interval $[d_{\mathbf{A_{max}}}, d_{\mathbf{A_{min}}}]$ can be optimised online by reasoning within user teleoperation data and the assistance function $\mathbf{A}$. This could allow the motion controller to assist depending on the handicap and needs of the user. On the other hand, it is also advantageous to teach the users how to optimally use the system for better quality of experience [MMAM06]. As theorized by Dragan et. al. [DS12], we can provide the assistance $\mathbf{A}$ depending on the *confidence* in whether the user is intending to navigate to a specific goal $\mathbf{X}_g$. This confidence is of course obtained from the argument of Eqn. (7.5) where $\mathbf{X}_i = \mathbf{X}_g$. If P_g represents this confidence, we can alter controller (7.7) as $\mathbf{v} = (\mathbb{I}_2 - P_g\mathbf{A})\mathbf{v}_{op} + P_g\mathbf{A}\mathbf{v}_r$. In such a scenario, the system does not provide assistance unless it is confident of the user's intention thus inadvertently rewarding the user for good driving with smooth assistance.

7.3 Analysis

7.3.1 Simulations

Our goal is to quantitatively analyse the proposed framework and also to try and verify the hypotheses put forward. An able bodied user rendered with a *right weak signal* teleoperates a robot in simulation using a 2D joystick (Logitech Gamepad F310). A right weak signal commonly occurs in people who have suffered stroke on their right side. In such case, the users are not able to give a strong signal on the right side and the user teleoperation is distorted as follows: $\omega_{op} = \omega_{th}$ if $\omega_{op} < \omega_{th}$ and $v_{op} = v_{op}\ \forall\ \mathbf{v}_{op} = [v_{op}, \omega_{op}]^T$. $\omega_{th} = -0.1$ rad/s is a threshold value.

The user is tasked with following a corridor and then joining a human group in a hallway (see. Fig. 7.6). This task is particularly difficult for a person with a right weak signal as he has to turn towards the hallway while avoiding collision with the human as well as the wall.

The simulation was carried out within a ROS framework and the calculations were performed using the ViSP software [MSC05]. In order to provide assistance based on the proposed framework, the parameters for searching the random goal were set as $r_{min} = 1.5$m, $r_{max} = 3.5$m and $\phi_r = 0.18$rad. The interval for considering a goal was set as $d_{min} = 0.5$m and $d_{max} = 3$m. η was set as 0.5 (see Eqn. (7.3)). Only a single goal pose ($\mathbf{X}_1$) was pre-set for the simulation: the meeting point for the group where the robot should reach in order to

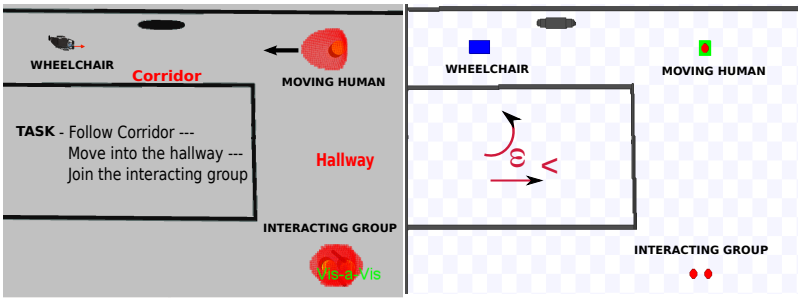

Figure 7.6: The simulation scenario (Left) and the view of the user (Right). The user is not explicitly aware of the personal and interaction spaces around the humans.

Table 7.1: Comparison of Quantitative factors (Lower the better)

Framework	AvgC	AvgS	AvgEx
No Assistance	0.2	1.6	20.98
Uniform control sharing	0	0	16.56
Proposed control sharing	**0**	**0**	**14.51**

equitably share space among the group (see Chapter 6). The probability $P(\mathbf{X}_1|\mathbf{X}_t)$ was designed as $\max(0, 1 - \frac{d(\mathbf{X}_t,\mathbf{X}_1)}{3})$. Therefore the pre-set goal is not considered unless $d(\mathbf{X}_t, \mathbf{X}_1) \leq 3$m. Finally we set $d_{\mathbf{A}_{\max}} = 3$m and $d_{\mathbf{A}_{\min}} = 0.5$m

Fig. 7.7 shows specific important frames for a single trial of the task. We see from Fig. 7.7(a), a random short term goal being predicted as the user follows the corridor, which is consistent with the user intended motion. Fig. 7.7(b) shows a frame where the user avoids the personal space of the human owing to the control sharing policy. In Fig. 7.7(c), we see a change in goal while assistance is still being provided (i.e $\mathbf{A} \neq \mathbf{0}_{2,2}$). But we observe from Figs. 7.8(c) and 7.8(d) that there is no erratic velocity changes due to the fact that the goals predicted are short term and compliant with the user intended direction. This is consistent with our hypothesis stated in Sec. VB, Part 1. Finally Fig. 7.7(d) shows the pre-set goal being predicted as the user moves onto join the group.

We also test three control (sharing) frameworks: No assistance, Uniform assistance (i.e. $\alpha_v = \alpha_\omega$), and the proposed framework (Eqn. (7.7)). The user performs 5 trials for each framework. Three factors are selected for analysis: *average number of collisions with obstacles* (**AvgC**), *average number of encroachment of personal/interaction space* (**AvgS**) and the *average user exertion* (**AvgEx**). The user exertion for each trial was calculated as $\sum_t |\omega_{op} - \omega_{th}|$, $\forall \omega_{op} < \omega_{th}$ [1]. The results are tabulated in Table 7.1.

We can see that the shared control approaches are successful in avoiding collisions as well as avoiding social space encroachment. Moreover, our proposed approach performs equally as the uniform control sharing framework in terms of avoiding collision and encroachment thus

[1] It can be intuitively seen as the stress of the user trying to signal an angular velocity of $\omega_{op} < \omega_{th}$.

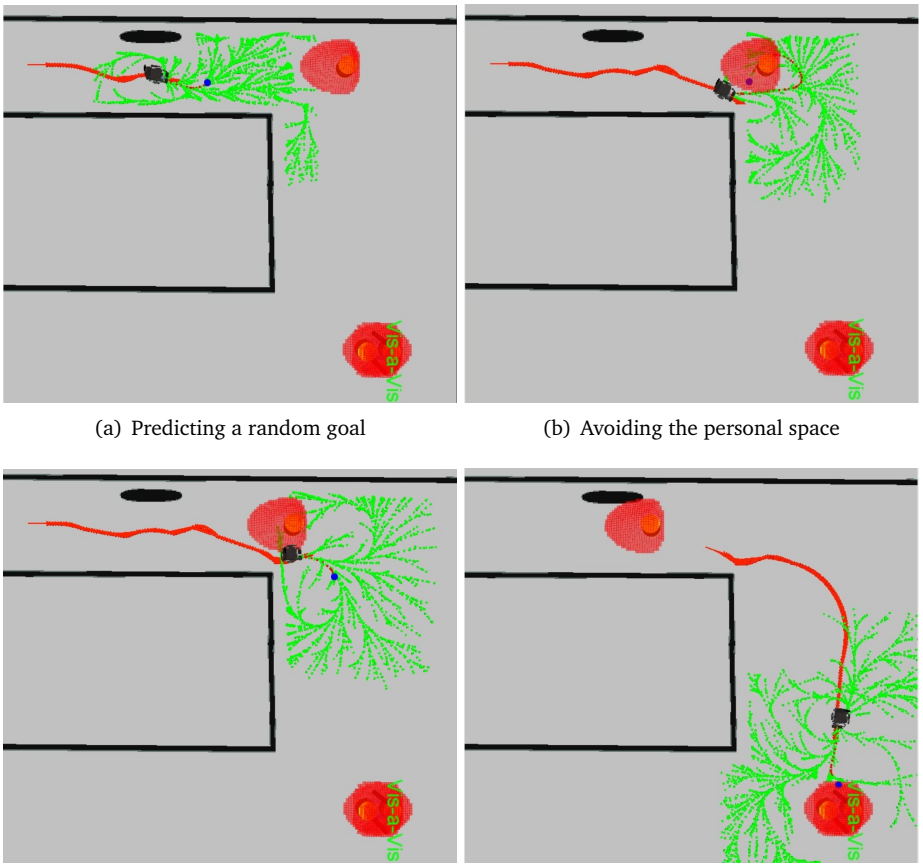

(a) Predicting a random goal

(b) Avoiding the personal space

(c) Change in goal while $\mathbf{A} \neq \mathbf{0}_{2,2}$

(d) Prediction of pre-set goal

Figure 7.7: Important frames captured during the task execution using the semi-autonomous framework.

verifying our hypothesis that a correction in angular velocity is enough in order to avoid danger. But user exertion is reduced while using the proposed control sharing framework. This is in part due to the fact that the correction is in the direction of the user intention motion (see Figs. 7.8(c) and 7.8(d)). From the angular velocity plots (Figs. 7.8(b) and 7.8(d)), we can also asses the level of exertion in terms of the user trying to signal $\omega_{op} < \omega_{th}$. Importantly, the evolution of the factors α_v and α_ω (Figs. 7.8(c) and 7.8(d)) shows a progressive increase (and decrease) which is essential for better quality of experience.

7.3.2 Experiments

The framework was tested on an off-the-shelf powered wheelchair (You-Q Luca) which could be teleoperated using a standard joystick coming from Penny & Giles. A Hokuyo URG-04LX Laser Scanner was equipped as shown Fig. 7.9. As the only exteroceptive sensor, the laser scanner was used to localize the wheelchair and also to detect people. Initially a coarse map of the operating

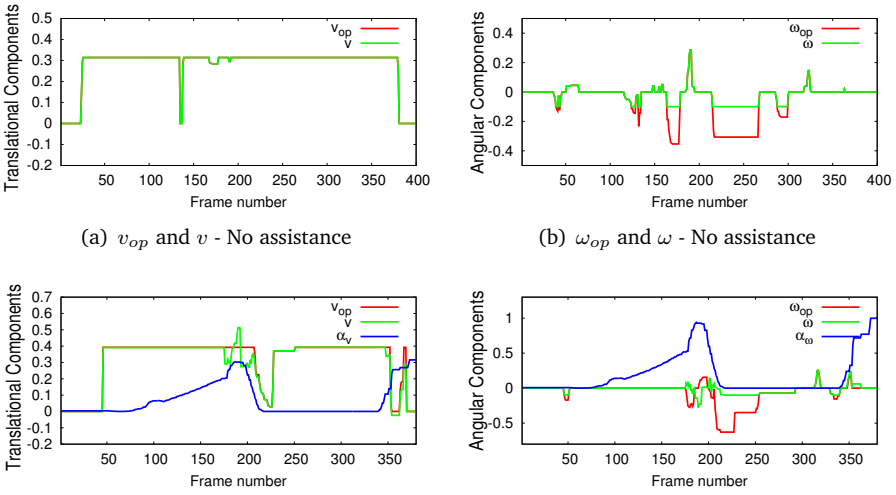

(a) v_{op} and v - No assistance

(b) ω_{op} and ω - No assistance

(c) v_{op}, v and α_v - Proposed control sharing

(d) ω_{op}, ω and α_ω - Proposed control sharing

Figure 7.8: The evolution of the velocity components during the task execution.

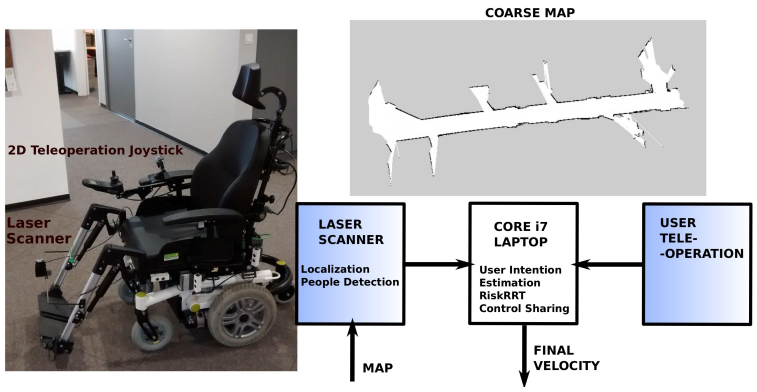

Figure 7.9: Experimental setup along with the coarse map of the corridor created using the laser.

environment (a long corridor) was created (Fig. 7.9). Since we don't use odometry, a scan matching technique [Cen08] was used to localize within the map. Such a map is not required if odometry can be leveraged alongside a Simultaneous Localization and Mapping (SLAM) scheme (the obvious constraint to be added in such a case is that the short term goals that can be leveraged for the framework should be within the already explored area). Finally, a laser-based leg tracking algorithm was used to classify and track people. The objective of conducting such an experiment is to try and prove the efficacy of the proposed framework in an off-the-shelf real world system.

Again the framework was designed within ROS and the calculations were performed on an off-board core i7 laptop (connected via ethernet) using ViSP. Such a setup amounted to a 15ms latency from user teleoperation to the motion controller which is undetectable to the users.

(a) Human 1 (b) Human 2 (c) Human 3 - Moving away from his own path

Figure 7.10: Frames captured during one of the tests that depict encounters of the wheelchair with humans while following a corridor.

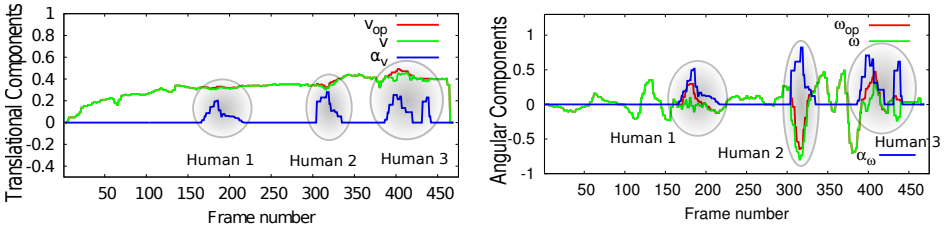

Figure 7.11: The evolution of the velocity components during the experiment execution. We can observe the progressive increase of the factors α_v and α_ω.

The random goal and the goal consideration window parameters were kept the same as in the simulations. But no goal was pre-set in the map. Therefore all estimated goals were random short term goals.

An able bodied user with a simulated right weak signal (with $\omega_{th} = -0.7$rad/s) was tasked with following along the corridor in the presence of some moving humans. Fig. 7.10 shows instances from one execution of the task when the wheelchair is in operating close to humans. These instances are highlighted in the velocity plots (Fig. 7.11) where we can see that the user teleoperation is augmented as expected in order to avoid the personal space of the moving humans in order to reduce the risk of disturbance to the walking humans.

Furthermore, we observed that while testing with human volunteers, in most cases, they were polite enough to move out of the way of the wheelchair (see Fig 7.10(c)). Since human perception of the wheelchair behaviour is not considered within the framework, it would be also advantageous to subjectively analyse this in order to create a more optimal solution. Preliminary experiments on the perception of walking humans, and walking group of humans on wheelchairs have corroborated this observation. Further analyses are necessary to model the walking pattern of humans alongside devices such as powered wheelchairs.

7.4 Conclusion

This chapter presented an adaptive semi-autonomous framework for wheelchair navigation assistance in human environments. A socially compliant motion planner in the form of RiskRRT was leveraged to augment the user teleoperation so that progressive assistance could be provided for safe navigation. Generalized formulations for estimating short term user intentions and for sharing control were also provided as the two components of the framework. This shows that the framework is not restricted to be employed alongside the RiskRRT motion planner.

The system was quantitatively analysed in simulation wherein the effectiveness of the framework was proved. Experimental results corroborated the analyses and also showed the adaptability of the system in a real-world deployment. Subjective measures regarding human perception and reaction to the behaviour of the wheelchair are important perspectives that have to be analysed further.

In the next chapter, we conclude by using the idea of estimating *short term user intention* in order to propose a more general formulation for assistive shared control that is not restricted to the wheelchair domain, but can be adapted to a wide array of robotic assistance tasks.

Chapter 8

A formalism for Assistive Shared Control

THIS CHAPTER formalizes a general framework for assistive shared control that allows a robotic system that is being operated/teleoperated by a user (for example, an intelligent wheelchair, a robotic exoskeleton, or a teleoperated manipulator), to *efficiently* assist the user in order to perform a task or a sequence of tasks.

Based on the concept of predicting short term user goals demonstrated in the previous chapter, we propose a formulation for sharing control that also aims to resolve the idea of *adaptivity* within assistive shared control. Adaptivity, in this case, can be defined as the idea wherein the robot adapts to the user's ability/disability.

8.1 Motivation

A major motivation for proposing a general framework for assistive shared control comes from the fact that, among the research on robotic assistance, most of the work is highly *contextual* and targeted at the specific application domain. Shared control solutions utilize a diversity of algorithms, operations modes, and most importantly, different levels of sharing the user's autonomy [DS12, DS13, GG04, CG02, KBS+06, Tra15]. For example, the vision-based assistive controllers that we presented in Part I, are targeted at the specific problem of wheelchair corridor navigation. But from the controller design, we inferred a linear control sharing formalism that was successfully adapted to the task of doorway passing as well as, to a more general system for human-aware wheelchair navigation assistance.

Another interesting factor is that, when we observe user teleoperation, we can adjudge that it will be rarely optimal (at least intuitively). The user can (and should be able to) provide a sub-optimal operation/teleoperation command that may be fine in reality but not permissible according to some specific shared control algorithms. In fact, there are very few works in literature that address this issue. A notable exception being a work from Trautman [Tra15], where the uncertainty in user intention was solved by proposing a probabilistic framework for shared control.

In the last chapter, we proposed and demonstrated the idea of estimating short term user goals, that aims to eliminate user intention uncertainty, in order to provide efficient assistance for assisted wheelchair navigation. Thus, in this chapter, we aim to answer the question on whether is it possible to propose a general framework for assistive shared control *using short term goals*, that is applicable for a variety of robotic assistance tasks.

8.2 Objective

Therefore the objective is to design an algorithm that allows a robot to assist a user in performing a task or a sequence of tasks based on the following set of constraints:

- the formalism should be general enough to be applicable to a variety of robotics assistance tasks,
- the user should be able to provide a sub-optimal control (i.e the assumption that the user teleoperation is not always optimal),
- the robot should be able to adapt to the user's ability/disability.

8.3 Related Research

Related work in shared control for robotic assistance can be characterized based on how the specified work approaches the following two components: prediction of user intent, and arbitration of user and robot control.

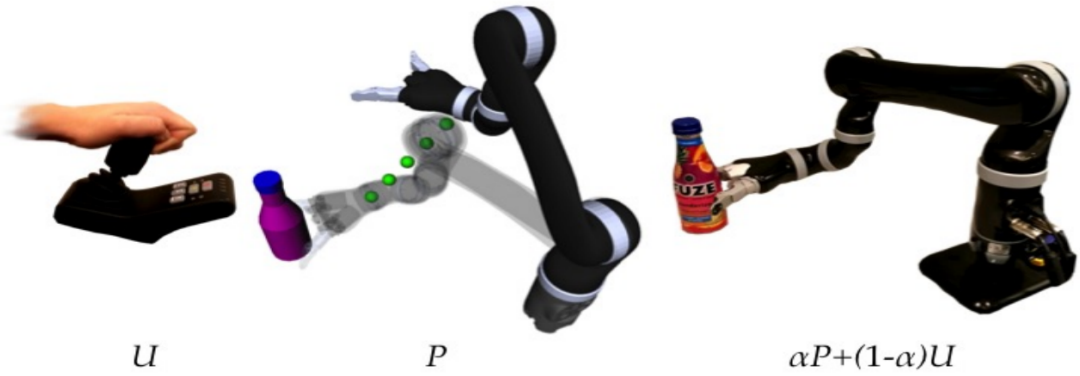

Figure 8.1: Sharing control with a human in order to perform a collaborative task or in order to provide assistance to the user is a key component, and an open problem in human robot interaction. (Image courtesy Anca Dragan)

8.3.1 On User Intent Estimation

A majority of the work on shared control assume that the user intention is either known [GG04, CG02, KBS+06, DH02, DSHD01, CG02, AM97, CDRM13, CDRM13, GDA13, CD12] or the user is following a pre-defined set of commands in order to perform a task [TMD08, LBJ+99, Tak98, Arg16, YADP05]. This is the simplest form of shared control where a well defined algorithm can be targeted for efficiently assisting the user for performing a task. An example from this thesis would be the vision-based assistance controller for corridor following proposed in Part I where we assumed that the user is always intending to follow a corridor.

Machine learning, particularly inverse reinforcement learning [KP15, ZMBD08, DS12, RBZ06] was heavily used in many recent works to model user teleoperation. Using machine learning, it is possible to learn the user teleoperation model by assuming that the user minimizes a cost function in order to reach his/her goal (intention). But this assumption predicates that the user generally *optimizes* his behaviour while teleoperating.

In order to negate the assumption that the user behaviour is optimal, Trautman [Tra15] proposed a complete probabilistic framework for representing not just the user intention, but also shared control. In our case, we aim to use a linear control sharing framework. Therefore, the idea of predicting the short term user intention as described in the last chapter may open some solution avenues for better formalising assistive shared control.

8.3.2 On Control Sharing

Since the start of the research on shared human/robot control, a range of methods have been proposed for sharing control between the user and the robot. Some of the most frequently proposed methods include, giving full control to the robot on some specific aspects of the task [GG04, CG02, KBS+06, DH02, KHKCG+12, YH12, DSHD01], to giving control based on some

trigger by the user [TMD08, LBJ+99, Tak98, KWLV05, LO03], to continuously fusing user and robot controls using specific performance criteria [CG02, AM97, CDRM13, GDA13, CD12, DEVPHDS12, Arg16, DS12, Tra15].

Especially for robotic assistance, continuous shared control at the servo-level using a linear control sharing formalism has received much attention, as described in the last chapter [CDRM13, GDA13, CD12, DEVPHDS12, Arg16]. But the major issue in generalizing such a system is that there should be a definite consensus on *how and when the robot should take control*. In fact, perspectives on this issue have been at most contradictory, with some works [YH12] concluding that the users preferred more autonomy for complex planning tasks, while other works [KHKCG+12] concluding that the users preferred less autonomy for tasks like manipulation.

Thus we can conclude that the issue of designing the level of autonomy, is highly contextual, and must be adapted to the specific task as well as adapted to the user's ability/disability. In order to generalize, we can propose a set of guidelines that allows us to fully formalize assistive shared control such that it is adaptable to most of the robotic assistance tasks. In fact, a recent attempt from Dragan et. al. [DS12] put forth an idea that the robot should assist based on notions that depend on *the robot's confidence in itself and in the user, as well as on the particulars of the user*. Therefore, a minimal set of guidelines, that in part are influenced from the thesis, could serve as a general criteria for efficient control sharing within a linear control sharing framework.

8.4 Approach

Therefore, our approach for proposing a solution for assistive shared control follows a two step thread.

1 **Predict short term user intention at short term intervals, such that,**
   - they are agnostic to the long term user intention (i.e. the desired goal),
   - they are necessarily sub-optimal and compatible with long term user intention,
   - the prediction is *adapted* to the user teleoperation model.

2 **Share control between user and robot, based on,**
   - a linear control sharing formalism,
   - a realization that the control sharing is contextual,
   - a minimal set of guidelines for assistance

8.5 Assistive Shared Control using Short term Goals

8.5.1 Assumptions

We model the robot as a deterministic dynamical system operating in an n dimensional smooth sub-manifold $\mathcal{X}$ of $SE(3)^{n+1}$, locally diffeomorphic to $\mathbb{R}^n$. We can then parametrize the config-

uration (or state) of the robot using an n dimensional vector $\mathbf{X} \in \mathcal{X}$ (eg. position, velocity). Assuming that the robot can be *autonomously* controlled using an m dimensional vector $\mathbf{v}_r \in \mathcal{R}$ (eg. velocity, torque) where $\mathcal{R}$ is the set of continuous controls. We also thus assume access to a goal-driven asymptotically optimal motion planner that plans *safe* trajectories between configurations (for example, a motion planner, a visual servoing scheme, etc.).

The user teleoperates the robot using an interface (such as a joystick) and an input $\mathbf{v}_{op} \in \mathcal{U}$ where we have the knowledge of a deterministic function $\mathcal{D}$ which maps the set of continuous user inputs $\mathcal{U}$ to the set of controls $\mathcal{R}$. We also assume that the user is teleoperating the robot in order to achieve a known *long term* goal or more importantly, a sequence of known *long term* goals (eg. reach a particular configuration, perform a certain task such as grasping).

The core concept we introduce in this work is that the user traverses a set of k short term goals $\{\mathbf{X_{g_1}}, \mathbf{X_{g_2}}, ...\mathbf{X_{g_k}}\}$ in order to achieve a specific *long term* goal. Thus the goal of the system is to predict the short term goals at regular pre-set intervals while *efficiently* assisting the user in order to reach the said short term goal.

Thus, along with short term goal prediction, the issue of control sharing is to be formalised in order to gracefully assist the user. It is clearly evident that this is a highly contextual issue. But we here aim to design a framework that is globally implementable. If the final control sent to the robot's motor controller is denoted by $\mathbf{v}$, then naturally a linear control sharing formalism of the form $\mathbf{v} = \mathbf{A_U}\mathbf{v}_{op} + \mathbf{A}\mathbf{v}_r$ would suffice to efficiently share control. Without loss of generality we can assert that $\mathbf{A_U} = (\mathbb{I}_m - \mathbf{A})$ with $\mathbf{A}$ being the *assistance* function that controls the level of autonomy given to the user and $\mathbb{I}_m$ is the m dimensional Identity matrix. Note that the formalism has the exact same form as the one proposed in Chapter 7, thus we use the same notation i.e. $\mathbf{A}$ for the assistance function.

8.5.2 Predicting Short term Goals

Let

- $\mathbf{X_t}$: The robot state at any goal prediction instant t.
- $\{\mathbf{X_1}, \mathbf{X_2}, ...\mathbf{X_k}\}$: A set of k known goals (For example, a set of desired poses, a grasping pose, etc. This set can also be null).
- d : A distance metric over the manifold $\mathcal{X}$.
- $(0, D]$: The short term interval (where D is a per-defined distance on the manifold).
- $\mathbf{X_g}$: The predicted *short term goal*.

Using the same principles as in the last chapter, we propose a Bayesian approach in order to predict short term goals. We select a set of (say x) *random goals* $\{\mathbf{X_{r_1}}, \mathbf{X_{r_2}}, ...\mathbf{X_{r_x}}\}$, within the short term interval $(0, D]$. Then we can create a set that is the union of the known goal set

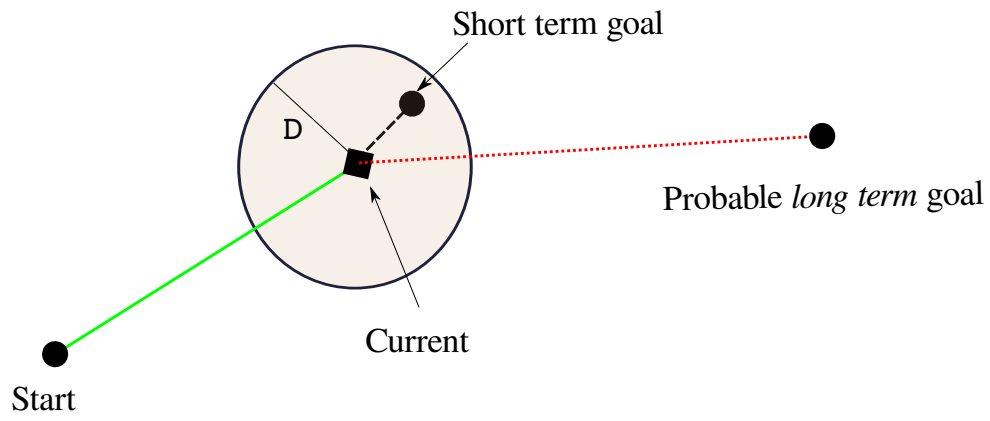

Figure 8.2: A goal is predicted that is consistent with the current robot state $\mathbf{X_t}$ and the current user teleoepration output $\mathbf{v}_{op}$, and that is within a short term interval defined by D. An illustrative schematic is shown here.

and the random goal set as $\mathbf{X_G} = \{\mathbf{X_1}, \mathbf{X_2}, ...\mathbf{X_k}, \mathbf{X_{r_1}}, \mathbf{X_{r_2}}, ...\mathbf{X_{r_x}}\}$. Owing to this definition, we assert that the short term goal at any goal prediction instant is given by:

$$\mathbf{X_g} = \arg \max_{\mathbf{X_i} \in \mathbf{X_G}} P(\mathbf{X_i}|\mathbf{X_t}, \mathbf{v}_{op}) \tag{8.1}$$

Thus the short term goal is any goal $\mathbf{X_i} \in \mathbf{X_G}$ that maximises the posterior probability given the current robot state $\mathbf{X_t}$ and the current user teleoperation output $\mathbf{v}_{op}$.

Using Bayes' rule on Eqn. (8.1),

$$P(\mathbf{X_i}|\mathbf{X_t}, \mathbf{v}_{op}) = \frac{P(\mathbf{v}_{op}|\mathbf{X_t}, \mathbf{X_i})P(\mathbf{X_i}|\mathbf{X_t})}{P(\mathbf{v}_{op}|\mathbf{X_t})} \tag{8.2}$$

and this can be normalized as

$$P(\mathbf{X_i}|\mathbf{X_t}, \mathbf{v}_{op}) = \eta P(\mathbf{v}_{op}|\mathbf{X_t}, \mathbf{X_i})P(\mathbf{X_i}|\mathbf{X_t}), \tag{8.3}$$

where η is a constant.

Since we predict short term goals, for known goals, the Prior probability $P(\mathbf{X_i}|\mathbf{X_t})$ i.e. the probability of the user selecting any goal $\mathbf{X_i}$ given the current robot state $\mathbf{X_t}$, is inversely proportional to the distance to the goal $P(\mathbf{X_i}|\mathbf{X_t}) \propto \frac{1}{d(\mathbf{X_i}, \mathbf{X_t})}$. Therefore,

$$P(\mathbf{X_i}|\mathbf{X_t}) = \max(0, 1 - \frac{d(\mathbf{X_i}, \mathbf{X_i})}{D}) \quad \text{if} \quad \mathbf{X_i} \in \{\mathbf{X_1}, \mathbf{X_2}, ...\mathbf{X_k}\}. \tag{8.4}$$

This means that any goals that are located at a distance of more that D from the current robot state are discarded. Meanwhile for random goals, this probability can be designed as a minimum positive threshold value δ in order to give advantage to the known goals (within the short term interval). Therefore,

$$P(\mathbf{X_i}|\mathbf{X_t}) = \delta \quad \text{if} \quad \mathbf{X_i} \in \{\mathbf{X_{r_1}}, \mathbf{X_{r_2}}, ...\mathbf{X_{r_x}}\}. \tag{8.5}$$

Thus from Eqn. (8.3) we can see that the known goals will be advantaged over random goals within the short term interval $(0, D)$.

But another term i.e. the likelihood $P(\mathbf{v}_{op}|\mathbf{X_t}, \mathbf{X_i})$ in Eqn. (8.3) also affects the goal prediction (thus nullifying the effect of $P(\mathbf{X_i}|\mathbf{X_t})$, if we are reasoning among random goals). We assert that the user tries to exponentially minimize a cost function C_U in order to reach his short term goal from the current robot state $\mathbf{X_t}$. This is known as the principle of maximum entropy [ZMBD08, DS12], and this assertion differs from the assumption that the user teleoperation is (globally) optimal, in the sense that we hypothesise that the user teleoperation is optimal *only* to reach his short term goal. This property is also essential in order to keep the prediction of user intention at most sub-optimal to the user's long term goal. Evidently,

$$P(\mathbf{v}_{op}|\mathbf{X_t}, \mathbf{X_i}) \propto \exp(-C_U(\mathbf{X_i})). \tag{8.6}$$

Therefore, the final expression for predicting the short term goal at any instant t can be written as

$$\mathbf{X_g} = \arg \max_{\mathbf{X_i} \in \mathbf{X_G}} \exp(-C_U(\mathbf{X_i}))P(\mathbf{X_i}|\mathbf{X_t}). \tag{8.7}$$

Part of the applicability of the proposed user intention estimation scheme for assistive shared control can be attributed to how one should select (or design or learn) the cost funtion C_U. In fact, we can rename it as *short term goal driven user teleoperation model*. We here propose a two step process to characterize this function:

- Start with a simple estimation based on the application
- Then learn/optimize owing to the sequence of state and user teleoperation data $\mathcal{D}_\mathcal{U}$ up to a discrete time y where $\mathcal{D}_\mathcal{U} = \{(\mathbf{X_1}, \mathbf{v}_{op_1}), (\mathbf{X_2}, \mathbf{v}_{op_2}).....(\mathbf{X_y}, \mathbf{v}_{op_y})\}$.

Among a plethora of methods for Bayesian model learning [Bar12], we can use inverse reinforcement learning or inverse optimal control [NR00] in order to learn this cost function online. But this is an ill-posed problem. There can be many solutions, and zero is always a solution, for C_U. But in the machine learning literature, many algorithms exist that provide graceful approximations to efficiently solve the inverse problem [ZMBD08, RBZ06].

One straightforward solution would be to parametrize the cost function C_U as a linear combination of a set of features that depend on the goal and the user teleoperation (maybe equal to the initial estimation for C_U) such that $C_U = \theta^T \mathbf{f}(\mathbf{X_t}, \mathbf{v}_{op})$. Here θ represents the set of scalar weights while $\mathbf{f}$ represents a set of features. Then the goal would be to learn the weights θ owing to the user teleoperation sequence $\mathcal{D}_\mathcal{U}$ using algorithms for inverse reinforcement learning as specified in [NR00, ZMBD08, RBZ06].

Finally, another issue to consider is *when* to predict new short term goals. The simple solution for this issue is to predict a new short term goal as soon as $d(\mathbf{X_t}, \mathbf{X_g}) > D$. Thus if the current predict short term goal is father than the short term interval, then predict an new short term goal. As seen in the last chapter, many of the short term goals will not be reached. But this is not an issue as a new goal will be predicted as soon the condition $d(\mathbf{X_t}, \mathbf{X_g}) > D$ is reached.

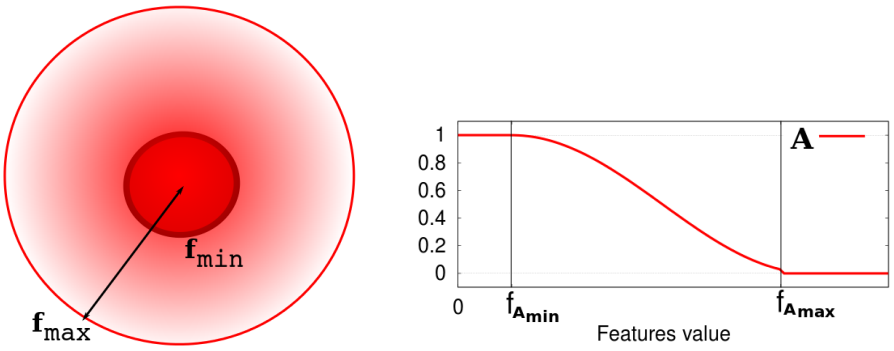

Figure 8.3: A schematic of the *progressive* evolution of the assistance function $\mathbf{A}$ based on some well defined feature interval that is derived from the minimal set of guidelines.

8.5.3 Sharing Control

Owing to a control sharing formalism given by $\mathbf{v} = (\mathbb{I}_m - \mathbf{A})\mathbf{v}_{op} + \mathbf{A}\mathbf{v}_r$, where $\mathbf{v}_r$ is the output from an asymptotically optimal autonomous controller needed to reach the predicted short term goal $\mathbf{X_g}$ from the current robot state $\mathbf{X_t}$, one can see that the function $\mathbf{A}$ is the sole governor of this policy.

Section 7.2.3 from the last chapter commented on the stability (in the sense of Lyapunov) of the proposed linear control sharing formalism while also noting that an inescapable local minima does not occur unless unless $\forall \mathbf{v}_{op}$, $\mathbf{v}_r = -\mathbf{k}\mathbf{v}_{op}$ for any positive definite $\mathbf{k}$ and $\mathbf{A} = \frac{1}{\mathbf{k}+1}$.

But the major question is, *how does one design the assistance function* $\mathbf{A}$*?*

As stated earlier, the design of the assistance function is highly contextual and does depend on the application. But it is possible to provide a minimal set of guidelines that allow us to generalize control sharing under the same umbrella. The minimal set of guidelines *in the order of importance* are as follows:

1. Assist the user in order to avoid joint limits.
2. Assist the user in order to avoid obstacles.
3. Assist the user in order to perform the task.
4. *Progressively* take or relinquish control (see Figure 8.3).
5. Assist the user if the *confidence* in the short term goal (i.e. $P(\mathbf{X_g}|\mathbf{X_t}, \mathbf{v}_{op})$) is high [DS12].

Finally, it is also possible to characterize how to provide user feedback that communicates the assistance provided by the robot using haptics. We specify that in order to haptically guide the user, provide a feedback that is *proportional* to the assistance provided by the robot as demonstrated in Chapter 3 for assisted corridor following. Therefore the evolution of the assistance function $\mathbf{A}$ can directly be used in the scheme for proportional feedback design.

8.6 Conclusion

In the final Chapter of this thesis, we laid the preliminary foundations for a general framework for assistive shared control. The core idea is to use the short term user intention, in order to nullify the sub-optimality in user teleoperation, and provide assistance in order to attain this short term goal based on a linear control sharing framework. A minimal set of guidelines can be provided in order to efficiently assist the user and generalise the framework. Moreover, it is possible to adapt to how a specific user utilises the robot in order to reach his/her short term goal by learning the cost function C_U owing to the sequence of user teleoperation data.

The previous chapter can be seen as a derived solution of the scheme proposed in this chapter where we used short term goals in order to design a semi-autonomous framework for human-aware wheelchair navigation. But, further user oriented tests on a variety of assistive robotic systems are necessary to fully analyse and finally understand the potential of the proposed preliminary system.

In Closing

AS THE CLOSING STATEMENTS for this thesis, we summarize the theoretical and experimental contributions of this work, while addressing relevant unresolved open issues by proposing directions for future research in order to solve these issues.

Summary of Contributions

The objectives of this thesis was to investigate sensor-based shared control techniques for wheelchair navigation assistance with an emphasis on user intention analysis. This in turn evolved into a characterization of assistive shared control, inspired in part from the proposed vision-based designs for corridor navigation assistance, as well as concepts from human-aware wheelchair navigation. Following a short preliminary introduction of the technical tools, we started with the first part on designing vision-based controllers for corridors navigation assistance wherein:

(i) We proposed asymptotically optimal monocular vision-based velocity controllers (Eqns. (3.14) and (3.30)) for realising the tasks of corridor following and passing through doorways. Easily extractable natural image features along with a visual servoing framework allowed us to easily adapt the controller to off-the-shelf wheelchair systems. We demonstrated analyses in simulation as well as experimental evidence on a robotized off-the-shelf wheelchair.

(ii) Owing to the vision-based autonomous controller for corridor following, it was possible to propose a wall collision avoidance task by *progressively* regulating the task only at specific intervals (Eqn. (4.6)). Therefore, one could fuse user teleoperation coming from a joystick so that the user has full control over the wheelchair motion, when not in danger of wall collisions, while following corridors. The resulting velocity controller (Eqn. (4.7)) turned out to be a linear control sharing policy owing to the continuous inverse of the task Jacobian (Eqn. (4.5)). We also demonstrated that haptic guidance in the form of joystick force feedback could be provided *in conjunction with the assistance scheme* (Eqn. (4.8)) for a more intuitive driving experience.

(iii) Based on the resulting linear control sharing formalism, we proposed an assistance scheme for passing through doorways using an intelligent wheelchair (Eqn. (4.13)). Most importantly, the assistance scheme integrated a very low-level form of user intention as in, the

system does not provide assistance unless the distance to a specific detected doorpost is less than a given threshold value. Furthermore, we provided experimental results for both assisted corridor following and assisted doorway passing scenarios.

From the design and especially the experiments conducted on vision-based assistance for wheelchair navigation, we inferred two important perspectives: firstly, a linear control sharing formalism is viable for providing efficient assistance for navigation tasks. Secondly, that it is important to consider the fact that human are indeed special objects while proposing solutions involving social robots such as intelligent wheelchairs. Therefore, in the second part of the thesis, we aimed to understand (in order to model) the spatial social considerations when social and service robots operate in human environments. We provided an overview of the proxemic rules related to human spatial arrangements, while also providing an introduction to a risk-based human-aware partial motion planner (RiskRRT) for autonomous navigation. In particular,

(iv) We designed a sensor-agnostic velocity controller (Eqn. (6.13)) that allows a robot operating in a human environment to equitably approach and join interacting groups. Extensive analyses in simulation demonstrated the feasibility of the controller to be deployed in real world environments. In addition, experiments using a mobile robot equipped with a single laser scanner also proved the success of the algorithm in a noisy real world scenario.

Evidently, based on the initially outlined human-aware navigation concepts, and owing to the motion planner RiskRRT, it was possible

(v) To design a semi-autonomous framework for human-aware navigation in an intelligent wheelchair. A generalized linear control sharing framework was proposed that was able to *progressively* correct the user teleoperation in order to avoid obstacles and in order to avoid disturbance to humans (Eqn. (7.7)). Meanwhile, we also proposed a Bayesian approach for user intention estimation (Eqn. (7.1)). The formulation was partly inferred from the design of the controller for assisted doorway passing, wherein we hypothesised that predicting short term goals is sufficient for eliminating user intention uncertainty. The hypothesis was validated in simulation along with the control sharing formalism. The theoretical claim was also supported experimentally using a robotized off-the-shelf wheelchair, equipped with a single laser scanner able to localize the wheelchair and detect humans.

Finally,

(vi) We laid out the foundations of a general framework for assistive shared control that can be applied to a variety of robotic assistance tasks. The algorithm was formalised as a two step process where we initially estimate the *short term* intention of the user (Eqn. (8.1)), that is sub-optimal but compatible with the user's long term goal. This allows us to eliminate user intention uncertainty that remains the bottleneck according to much of the related works in the domain. The second step is then to share control between the user who is manually

teleoperating the robot and the system itself, based on a linear control sharing formalism and a minimal set of guidelines for efficient control sharing.

Looking Forward

The results of this thesis are encouraging, but there still exists a variety of open issues that have to be resolved and some limitations do affect our proposed approaches.

Robustness is still a huge issue while proposing vision-based techniques for robot navigation (or navigation assistance). Especially considering that fact that such solutions would have to be utilized by users who are physically or mentally disadvantaged, it is essential to emphasise high accuracy and robustness for safety. We have to consider issues regarding visual feature extraction failure, camera field-of-view, extreme occlusions, etc. One solution for better robustness, would be to employ vision-sensors as a high-level perception and control medium (for example, for tasks like corridor following and doorway passing as proposed in this thesis) while using cheaper range sensors for low-level control (for example, in the form of obstacle avoidance). In fact, a *fully ultrasound-based* local obstacle avoidance scheme for semi-autonomous wheelchair navigation [**S.1**] is in advanced testing phase with target users at a rehabilitation center in Rennes, France.

In order to better model the effects of providing joystick force feedback to the user, rather than conducting test using the 3-D Phantom Omni haptic device, it is necessary to design a more intuitive teleoperation joystick that is able to actuate within a 2-D joystick space. A collaboration with the University College London is underway that focuses on designing a specially adapted haptic joystick for driving a wheelchair. Further user tests with force feedback also need to be performed in order to assess the overall user driving experience.

Moving onto the issue on human-aware designs for wheelchair navigation, a major drawback of our approach is the fact that we do not consider any gestural issues. Moreover, it would be interesting to perform user tests using a social robot such as Alderbaran's Pepper, in order to further study the influence of modelling the spatial social constraints, as well as the risk-based motion planner (RiskRRT). It would be also possible to integrate affective and gestural behaviours within such a robot, alongside the spatial social constraints.

With respect to the velocity controller for joining a group in interaction, apart from the assertion that the robot should initially turn towards a specific group in order to perform the approach, expressive and affective parameters were not modelled. In addition, real world user tests where a robotic wheelchair approaches a group would enhance the analysis of the algorithm. In fact, preliminary tests on the influence of powered (not robotic) wheelchairs on human walkers and human groups are being conducted at the moment.

But the main focus of this thesis is on how we characterize assistive shared control for wheelchair navigation, firstly using a vision-based framework and secondly on a human-aware constraint. A major issue in the proposed semi-autonomous framework in Chapter 7, is that we use a robotic wheelchair mounted with a single laser scanner on the wheelchair legs. This is impractical for people who especially suffer from disabilities in their lower limbs. A straightforward

way to solve this issue would be to use a distributed sensing system that communicates with the wheelchair wirelessly. Probably, this will be an inevitable future direction (atleast for indoor robotics navigation), not just for intelligent wheelchair research but also for service and social robot research. Another issue is the tuning of various parameters like the window of short term goal prediction, the size of the area within which the short term goal is predicted, as well as the distances that govern the assistance function $\mathbf{A}$. Other than empirically tuning the parameters, it would be beneficial to study the effects of variation in these parameters on the performance of the framework.

Evidently, to validate the proposed general framework for assistive shared control using short term goals, it is necessary to study the efficacy of the algorithm, not just for assisted wheelchair navigation (as shown in Chapter 7), but also on a variety of robotic assistance tasks. It is important also to question, *how short is too short*? Defining the interval of short term goal prediction must be quantified and well defined based on the application.

It is also possible to ask whether is it possible to tune the *short term interval* based on the user. Certainly from the sequence of user teleoperation data that is specified by $\mathcal{D}_{\mathcal{U}} = \{(\mathbf{X_1}, \mathbf{v}_{op_1}), (\mathbf{X_2}, \mathbf{v}_{op_2}).....(\mathbf{X_y}, \mathbf{v}_{op_y})\}$, it would be possible to tune the interval by reasoning over this data as well as the sequence of predicted short term goals. Finally, the proposition will be complete if the framework is able to integrate the idea of *providing assistance that is adapted to the user*. Based on the sequence of user outputs $\mathcal{V}_{op} = \{\mathbf{v}_{op_1}, \mathbf{v}_{op_2}....., \mathbf{v}_{op_y}\}$, the robot final control $\mathcal{V} = \{\mathbf{v}_1, \mathbf{v}_2....., \mathbf{v}_y\}$ and the assistance function $\mathcal{A} = \{\mathbf{A}_1, \mathbf{A}_2....., \mathbf{A}_y\}$, it is possible to optimise the assistance provided using adapted machine learning algorithms.

Supplementary Publication

S.1 Louise Devigne, **Vishnu K. Narayanan**, François Pasteau and Marie Babel. 'Low complex shared-control for power wheelchair navigation', *IEEE International Conference on Intelligent Robots and Systems (IROS)*, 2016.

Appendix A

Deriving the equations (3.23), (3.25) and (3.27)

We recall that (see Eqn. (3.22))

$$\dot{\phi_d} = \frac{z_d \dot{x_d} - x_d \dot{z_d}}{x_d^2 + z_d^2}, \tag{A.1}$$

From the well known kinematics equation $\dot{\boldsymbol{x}} = -\boldsymbol{v} - [\boldsymbol{\omega}]_\times \boldsymbol{x}$, we deduce $\dot{x_d}$ and $\dot{z_d}$ as

$$\begin{cases} \dot{x_d} = & -^{c_2}v_x - z_d^{c_2}\omega_y \\ \dot{z_d} = & -^{c_2}v_z + x_d^{c_2}\omega_y \end{cases} \tag{A.2}$$

which using Eqn. (3.5) leads to

$$\dot{x_d} = -\sin\theta_2 v + \omega(l_2 \cos\theta_2 + w_2 \sin\theta_2) + z_d\omega, \tag{A.3}$$

$$\dot{z_d} = -\cos\theta_2 v - \omega(l_2 \sin\theta_2 - w_2 \cos\theta_2) - x_d\omega. \tag{A.4}$$

Since $x_d = r\sin\phi_d$ and $z_d = r\cos\phi_d$, we obtain

$$\begin{aligned} \dot{\phi_d} = & \frac{\cos\phi_d[-\sin\theta_2 v + \omega(l_2\cos\theta_2 + w_2\sin\theta_2) + r\cos\phi_d\omega]}{r} \\ & - \frac{\sin\phi_d[-\cos\theta_2 v - \omega(l_2\sin\theta_2 - w_2\cos\theta_2) - r\sin\phi_d\omega]}{r}, \end{aligned} \tag{A.5}$$

which can be re-written as

$$\begin{aligned} \dot{\phi_d} = & \frac{1}{r}\left[(v(-\cos\phi_d\sin\theta_2 + \sin\phi_d\cos(\theta_2))\right] \\ & + \frac{1}{r}\left[\omega(l_2(\cos\phi_d\cos\theta_2 + \sin\phi_d\sin\theta_2) + w_2(\cos\phi_d\sin\theta_2 - \sin\phi_d\cos\theta_2)) + r\omega)\right]. \end{aligned} \tag{A.6}$$

Using trigonometric relations we finally get,

$$\boxed{\dot{\phi_d} = \omega + \frac{1}{r}\left[\sin(\phi_d - \theta_2)v + (l_2\cos(\phi_d - \theta_2) - w_2\sin(\phi_d - \theta_2))\omega\right].} \tag{A.7}$$

Similarly to obtain $\dot{r}$, in order to derive $\dot{\phi}_d^*$ (in Eqn. (3.24)), we deduce from Eqn. (3.15a)

$$\dot{r} = \frac{x_d\dot{x_d} + z_d\dot{z_d}}{\sqrt{x_d^2 + z_d^2}}. \tag{A.8}$$

Therefore using Eqn. (A.3) and Eqn. (A.4), we can write

$$\begin{aligned}\dot{r} = \sin\phi_d[-\sin\theta_2 v + \omega(l_2\cos\theta_2 + w_2\sin\theta_2) + r\cos\phi_d\omega] \\ + \cos\phi_d[-\cos\theta_2 v - \omega(l_2\sin\theta_2 - w_2\cos\theta_2) - r\sin\phi_d\omega].\end{aligned} \tag{A.9}$$

This gives,

$$\begin{aligned}\dot{r} = -v(\sin\phi_d\sin\theta_2 + \cos\phi_d\cos\theta_2) \\ + \omega[l_2(\sin\phi_d\cos\theta_2 - \cos\phi_d\sin\theta_2) + w_2(\sin\phi_d\sin\theta_2 + \cos\phi_d\cos\theta_2)]\end{aligned} \tag{A.10}$$

and using trigonometric formulae we finally have,

$$\dot{r} = -\cos(\phi_d - \theta_2)v + (l_2\sin(\phi_d - \theta_2) + w_2\cos(\phi_d - \theta_2))\omega. \tag{A.11}$$

Therefore $\dot{\phi}_d^*$ can be written as (from Eqn. (3.24))

$$\dot{\phi}_d^* = \frac{m\left[\cos(\phi_d - \theta_2)v - (l_2\sin(\phi_d - \theta_2) + w_2\cos(\phi_d - \theta_2))\omega\right]}{r\sqrt{r^2 - m^2}} \tag{A.12}$$

From Eqn. (3.18) and basic trigonometric relations, if we substitute $\frac{m}{r} = \sin(\phi_d^* - \theta_2)$ and $\frac{\sqrt{r^2-m^2}}{r} = \cos(\phi_d^* - \theta_2)$, we obtain

$$\boxed{\dot{\phi}_d^* = \frac{\sin(\phi_d^* - \theta_2)\left[\cos(\phi_d - \theta_2)v - (l_2\sin(\phi_d - \theta_2) + w_2\cos(\phi_d - \theta_2))\omega\right]}{r\cos(\phi_d^* - \theta_2)}} \tag{A.13}$$

Finally we derive the details to obtain Eqn. (3.27). From Eqn. (3.23) and Eqn. (A.13) we can write $\dot{\phi}_d - \dot{\phi}_d^*$ as

$$\begin{aligned}\dot{\phi}_d - \dot{\phi}_d^* = \omega + \frac{1}{r}\left[\sin(\phi_d - \theta_2)v + (l_2\cos(\phi_d - \theta_2) - w_2\sin(\phi_d - \theta_2))\omega\right] \\ - \frac{\sin(\phi_d^* - \theta_2)\left[\cos(\phi_d - \theta_2)v - (l_2\sin(\phi_d - \theta_2) + w_2\cos(\phi_d - \theta_2))\omega\right]}{r\cos(\phi_d^* - \theta_2)}.\end{aligned} \tag{A.14}$$

We can rearrange the above equation as,

$$\begin{aligned}\dot{\phi}_d - \dot{\phi}_d^* = \frac{v}{r}\left[\sin(\phi_d - \theta_2) - \frac{\sin(\phi_d^* - \theta_2)\cos(\phi_d - \theta_2)}{\cos(\phi_d^* - \theta_2)}\right] \\ +\omega\left[1 + \frac{l_2}{r}\left[\cos(\phi_d - \theta_2) + \frac{\sin(\phi_d - \theta_2)\sin(\phi_d^* - \theta_2)}{\cos(\phi_d^* - \theta_2)}\right] - \frac{w_2}{r}\left[\sin(\phi_d - \theta_2) - \frac{\sin(\phi_d^* - \theta_2)\cos(\phi_d - \theta_2)}{\cos(\phi_d^* - \theta_2)}\right]\right].\end{aligned} \tag{A.15}$$

and finally we can re-write the equation as

$$\dot{\phi_d} - \dot{\phi_d^*} = v\left[\frac{\sin(\phi_d - \phi_d^*)}{r\cos(\phi_d^* - \theta_2)}\right] + \omega\left[1 + \frac{l_2\cos(\phi_d - \phi_d^*) - w_2\sin(\phi_d - \phi_d^*)}{r\cos(\phi_d^* - \theta_2)}\right] \tag{A.16}$$

from which we deduce the form for $\dot{V}$ given in Eqn. (3.27).

Bibliography

[AIK+04] P. Althaus, H. Ishiguro, T. Kanda, T. Miyashita, and H.I. Christensen. Navigation for human-robot interaction tasks. *Proc. of IEEE International Conference on Robotics and Automation*, volume 2, 2004.

[AKPT04] D. Anguelov, D. Koller, E. Parker, and S. Thrun. Detecting and modeling doors with mobile robots. *Proc. of IEEE International Conference on Robotics and Automation*, volume 4, pages 3777–3784, 2004.

[AM97] P. Aigner and B. McCarragher. Human integration into robot control utilising potential fields. *Proc. of IEEE International Conference on Robotics and Automation*, volume 1, pages 291–296 vol.1, 1997.

[AR08] J. R. Azinheira and P. Rives. Image-based visual servoing for vanishing features and ground lines tracking: Application to a uav automatic landing. *International Journal of Optomechatronics*, 2(3), 2008.

[Arg16] Brenna D. Argall. Modular and Adaptive Wheelchair Automation. *Proc. of International Symposium on Experimental Robotics*, Springer International Publishing, 2016.

[Ark98] Ronald C. Arkin. Behavior-based Robotics. *MIT Press*, Cambridge, MA, USA, 1st edition, 1998.

[B. 14] B. D. Argall. Modular and Adaptive Wheelchair Automation. In *Proc. of the International Symposium on Experimental Robotics*, 2014.

[BA01] John Travis Butler and Arvin Agah. Psychological Effects of Behavior Patterns of a Mobile Personal Robot. *Autonomous Robots*, 10(2):185–202, 2001.

[Bar12] D. Barber. Bayesian Reasoning and Machine Learning. *Cambridge University Press*, 2012.

[BBCJ98] Samia Boukir, Patrick Bouthemy, FranÃ§ois Chaumette, and Didier Juvin. A local method for contour matching and its parallel implementation. *Machine Vision and Applications*, 10(5-6):321–330, 1998.

[BBP06] K. Boulanger, K. Bouatouch, and S. Pattanaik. ATIP: A Tool for 3D Navigation inside a Single Image with Automatic Camera Calibration. *Proc. of EG UK conference*, 2006.

[Bou89] P. Bouthemy. A maximum likelihood framework for determining moving edges. *IEEE Transactions on Pattern Analysis and Machine Intelligence*, 11(5):499–511, 1989.

[BPG+15] Marie Babel, François Pasteau, Sylvain Guégan, Philippe Gallien, Benoît Nicolas, Bastien Fraudet, Sophie Achille-Fauveau, and Daniel Guillard. HandiViz project: clinical validation of a driving assistance for electrical wheelchair. *Proc. of IEEE Workshop On Advanced Robotics And Its Social Impacts*, 2015.

[BPMR08] R A M Braga, M Petry, A P Moreira, and L P Reis. Intellwheels: A Development PlatForm for intelligent wheelchairs for disabled people. *Proc. of 5th International Conference on Informatics in Control, Automation and Robotics*, 1:115–121, 2008.

[Bra12] M. W. Brault. Americans with disability 2010. *United States Census Bureau*, 2012.

[Bro86] R. Brooks. A robust layered control system for a mobile robot. *IEEE Journal on Robotics and Automation*, 2(1):14–23, 1986.

[BS07] G. Bourhis and M. Sahnoun. Assisted Control Mode for a Smart Wheelchair. *Proc. of IEEE International Conference on Rehabilitation Robotics*, 158–163, 2007.

[BTK08] Cynthia Breazeal, Atsuo Takanishi, and Tetsunori Kobayashi. Social Robots that Interact with People. *Springer Handbook of Robotics*, 1349–1369, 2008.

[BWP07] J.C. Balasuriya, K. Watanabe, and A. Pallegedara. Giving robots some feelings towards interaction with humans in ubiquitous environment. *Proc. of International Conference on Industrial and Information Systems*, 529–534, 2007.

[CB08] Zhichao Chen and S.T. Birchfield. Visual detection of lintel-occluded doors from a single image. *Proc. of IEEE Computer Society Conference on Computer Vision and Pattern Recognition Workshops*, 1–8, 2008.

[CCO11] A. Cherubini, F. Chaumette, and G. Oriolo. Visual servoing for path reaching with nonholonomic robots. *Robotica*, 29(7):1037–1048, 2011.

[CD12] T. Carlson and Y. Demiris. Collaborative control for a robotic wheelchair: Evaluation of performance, attention, and workload. *IEEE Transactions on Systems, Man, and Cybernetics, Part B: Cybernetics*, 42(3):876–888, 2012.

[Cd13] Tom Carlson and Jose del R. Millan. Brain-Controlled Wheelchairs: A Robotic Architecture. *IEEE Robotics & Automation Magazine*, 20(1):65–73, 2013.

[CDRM13] T. Carlson and J. Del R Millan. Brain-controlled wheelchairs: A robotic architecture. *Robotics Automation Magazine, IEEE*, 20(1):65–73, 2013.

[Cen08] Andrea Censi. An ICP variant using a point-to-line metric. *Proc. of the IEEE International Conference on Robotics and Automation*, 2008.

[CG02] J. W. Crandall and M. A. Goodrich. Characterizing efficiency of human robot interaction: a case study of shared-control teleoperation. *Proc. of IEEE/RSJ International Conference on Intelligent Robots and Systems*, 1290–1295 vol.2, 2002.

[CH06] F. Chaumette and S. Hutchinson. Visual servo control, part i: Basic approaches. *IEEE Robotics and Automation Magazine*, 13(4):82–90, 2006.

[CH10] Shu-Yun Chung and Han-Pang Huang. A mobile robot that understands pedestrian spatial behaviors. *Proc. of IEEE/RSJ International Conference on Intelligent Robots and Systems*, 5861–5866, 2010.

[CK80] T. Matthew Ciolek and Adam Kendon. Environment and the Spatial Arrangement of Conversational Encounters. *Sociological Inquiry*, 50(3-4):237–271, 1980.

[CKC+09] Woojin Chung, Seokgyu Kim, Minki Choi, Jaesik Choi, Hoyeon Kim, Chang bae Moon, and Jae-Bok Song. Safe navigation of a mobile robot considering visibility of environment. *IEEE Transactions on Industrial Electronics*, 56(10):3941–3950, 2009.

[CPST02] Domenico Casadei, Francesco Profumo, Giovanni Serra, and Angelo Tani. Foc and dtc: two viable schemes for induction motors torque control. *IEEE Transactions on Power electronics*, 17(5):779–787, 2002.

[CSNF02] R. Carelli, C. Soria, O. Nasisi, and R. Freire. Stable agv corridor navigation with fused vision-based control signals. In *Proc. of Annual Conference of the Industrial Electronics Society*, volume 3, 2433–2438, 2002.

[DA11] G. Diego and T. K. O. Arras. Please do not disturb! minimum interference coverage for social robots. In *Proc. of IEEE/RSJ International Conference on Intelligent Robots and Systems*, 1968–1973, 2011.

[DEVPHDS12] Eric Demeester, Emmanuel EB Vander Poorten, Alexander Hüntemann, and Joris De Schutter. Wheelchair navigation assistance in the fp7 project radhar: Objectives and current state. *Proc. of IEEE/RSJ International Conference on Intelligent Robots and Systems, workshop on Navigation and Manipulation Assistance for Robotic Wheelchairs*, 2012.

[DH02] John Demiris and Gillian M. Hayes. Imitation in animals and artifacts. MIT Press, 327–361, 2002.

[DHV+06] E. Demeester, A. Huntemann, D. Vanhooydonck, G. Vanacker, A. Degeest, H. Van Brussel, and M. Nuttin. Bayesian estimation of wheelchair driver intents: Modeling intents as geometric paths tracked by the driver. In *Proc. of IEEE/RSJ International Conference on Intelligent Robots and Systems*, 5775–5780, 2006.

[DLN06] E. Delage, Honglak Lee, and A.Y. Ng. A dynamic bayesian network model for autonomous 3d reconstruction from a single indoor image. In *, Proc. of IEEE Conf. on Computer Vision and Pattern Recognition*, volume 2, 2418 – 2428, 2006.

[DS12] Anca Dragan and Siddhartha Srinivasa. Formalizing assistive teleoperation. *Robotics: Science and Systems*, 2012.

[DS13] Anca Dragan and Siddhartha Srinivasa. A policy blending formalism for shared control. *International Journal of Robotics Research*, 2013.

[DSHD01] Thomas Debus, Jeffrey Stoll, Robert D. Howe, and Pierre Dupont. Cooperative human and machine perception in teleoperated assembly. *Proc. of International Conference on Experimental Robotics*, 51–60, Springer-Verlag, 2001.

[DWW+06] K. Dautenhahn, M. Walters, S. Woods, K. L. Koay, C. L. Nehaniv, A. Sisbot, R. Alami, and T. Siméon. How may I serve you? *Proc. of the 1st ACM SIGCHI/SIGART conference on Human-robot interaction*, 2006.

[ECR92] B. Espiau, F. Chaumette, and P. Rives. A new approach to visual servoing in robotics. *IEEE Transactions on Robotics and Automation*, 8(3):313–326, 1992.

[Erv66] Erving Goffman. Behavior in Public Places: Notes on the Social Organization of Gatherings. *Free Press*, 1966.

[ESL13] Arturo Escobedo, Anne Spalanzani, and Christian Laugier. Multimodal control of a robotic wheelchair: Using contextual information for usability improvement. *Proc. of IEEE/RSJ International Conference on Intelligent Robots and Systems*, 4262–4267, 2013.

[ESL14] Arturo Escobedo, Anne Spalanzani, and Christian Laugier. Using social cues to estimate possible destinations when driving a robotic wheelchair. *Proc. of IEEE/RSJ International Conference on Intelligent Robots and Systems*, 3299–3304, 2014.

[FND03] Terrence Fong, Illah Nourbakhsh, and Kerstin Dautenhahn. A survey of socially interactive robots. *Robotics and Autonomous Systems*, 42(3-4):143 – 166, 2003.

[Fon01] Terrence W Fong. *Collaborative Control: A Robot-Centric Model for Vehicle Teleoperation*. PhD thesis, Robotics Institute, Carnegie Mellon University, 2001.

[FOPV13a] A. Faragasso, G. Oriolo, A. Paolillo, and M. Vendittelli. Vision-based corridor navigation for humanoid robots. *Proc. of IEEE International Conference on Robotics and Automation, *, 3190–3195, 2013.

[FOPV13b] Angela Faragasso, Giuseppe Oriolo, Antonio Paolillo, and Marilena Vendittelli. Vision-based corridor navigation for humanoid robots. *Proc. of IEEE International Conference on Robotics and Automation*, pages 3190–3195, 2013.

[FSB04] A. Fattouh, M. Sahnoun, and G. Bourhis. Force feedback joystick control of a powered wheelchair: preliminary study. *Proc. of IEEE International Conference on Systems, Man and Cybernetics*, volume 3, 2640–2645, 2004.

[FSLT10] Chiara Fulgenzi, Anne Spalanzani, Christian Laugier, and Christopher Tay. Risk based motion planning and navigation in uncertain dynamic environment. Research report, INRIA Grenoble, 2010.

[FTB03] Terrence Fong, Charles Thorpe, and Charles Baur. Multi-Robot Remote Driving With Collaborative Control. *IEEE Transactions on Industrial Electronics*, 2003.

[FvD03] Marcia Finlayson and Toni van Denend. Experiencing the loss of mobility: perspectives of older adults with multiple sclerosis. *Disability and Rehabilitation*, 25(20):1168–1180, 2003.

[GDA13] A. Goil, M. Derry, and B.D. Argall. Using machine learning to blend human and robot controls for assisted wheelchair navigation. *Proc. of IEEE International Conference on Rehabilitation Robotics*, 1–6, 2013.

[GFS07] R. Gockley, J. Forlizzi, and R. Simmons. Natural person-following behavior for social robots. *Proc. of 2nd ACM/IEEE International Conference on Human-Robot Interaction*, 17–24, 2007.

[GG04] P. Griffiths and R. B. Gillespie. Shared control between human and machine: haptic display of automation during manual control of vehicle heading. In *Proc. of 12th International Symposium on Haptics*, 358–366, 2004.

[GLRFM08] Martin Gerin-Lajoie, Carol L. Richards, Joyce Fung, and Bradford J. McFadyen. Characteristics of personal space during obstacle circumvention in physical and virtual environments. *Gait and Posture*, 27(2):239 – 247, 2008.

[GNL+08] F Galán, M Nuttin, E Lew, P W Ferrez, G Vanacker, J Philips, and J Del R Millán. A brain-actuated wheelchair: asynchronous and non-invasive Brain-computer interfaces for continuous control of robots. *Clinical Neurophysiology*, 119(9):2159–69, 2008.

[GSB07] G. Grisetti, C. Stachniss, and W. Burgard. Improved techniques for grid mapping with rao-blackwellized particle filters. *IEEE Transactions on Robotics*, 23(1):34–46, 2007.

[Hal66] E.T. Hall. The hidden dimension. *Doubleday publishsers*, 1966.

[HAMMCne08] H. Hadj-Abdelkader, Y. Mezouar, P. Martinet, and F. Chaumette. Catadioptric visual servoing from 3-d straight lines. *IEEE Transactions on Robotics*, 24(3):652–665, 2008.

[Hay78] Leslie A. Hayduk. Personal space: Where we now stand. *Psychological Bulletin*, Vol 94(2), 293-335, 1983.

[HM95] Dirk Helbing and Péter Molnár. Social force model for pedestrian dynamics. *Phys. Rev. E*, 51:4282–4286, 1995.

[HSK00] Mitchell P. LaPlante H. Stephen Kaye, Taewoon Kang. Mobility device use in the united states. *Disability Statistics Report*, 14, 2000.

[IMDS01] LisaI. Iezzoni, EllenP. McCarthy, RogerB. Davis, and Hilary Siebens. Mobility difficulties are not only a problem of old age. *Journal of General Internal Medicine*, 16(4):235–243, 2001.

[KBCG+12] Bernd Krieg-Brückner, David Crombie, Bernd Gersdorf, Alexander Jüptner, Michael Lawo, Christian Mandel, Antonio B Martínez, Thomas Röfer, and Christoph Stahl. Challenges for indoor and outdoor mobility assistance. *Technik für ein selbstbestimmtes Leben*, 2012.

[KBS+06] H. K. Kim, J. Biggs, W. Schloerb, M. Carmena, M. A. Lebedev, M. A. L. Nicolelis, and M. A. Srinivasan. Continuous shared control for stabilizing reaching and grasping with brain-machine interfaces. *IEEE Transactions on Biomedical Engineering*, 53(6):1164–1173, 2006.

[KC11] O. Kermorgant and F. Chaumette. Combining ibvs and pbvs to ensure the visibility constraint. *Proc. of IEEE/RSJ International Conference on Intelligent Robots and Systems*, 2849–2854, 2011.

[Ken10] Adam Kendon. Development of Multimodal Interfaces: Active Listening and Synchrony. *Lecture Notes in Computer Science*, Springer Berlin Heidelberg, 2010.

[KFH+12] A. Kokosy, T. Floquet, G. Howells, H. Hu, M. Pepper, and C. DonzÃ©. SYSIASS : An Intelligent Powered Wheelchair. *Proc. of International Conference on Systems and Computer Science*, 2012.

[KHKCG+12] D. J. Kim, R. Hazlett-Knudsen, H. Culver-Godfrey, G. Rucks, T. Cunningham, D. Portee, J. Bricout, Z. Wang, and A. Behal. How autonomy impacts performance and satisfaction: Results from a study with spinal cord injured subjects using an assistive robot. *IEEE Transactions on Systems, Man, and Cybernetics - Part A: Systems and Humans*, 42(1):2–14, 2012.

[KKBT01] L. Kitagawa, T. Kobayashi, T. Beppu, and K. Terashima. Semi-autonomous obstacle avoidance of omnidirectional wheelchair by joystick impedance control. In *Proc. of IEEE/RSJ International Conference on Intelligent Robots and Systems*, 2148–2153, 2001.

[KKMN91] Y. Kanayama, Y. Kimura, F. Miyazaki, and T. Noguchi. A stable tracking control method for a non-holonomic mobile robot. *Proc. of IEEE/RSJ International Conference on Intelligent Robots and Systems (Workshop Intelligence for Mechanical Systems)*, 1236–1241 vol.3, 1991.

[KKSB12] Markus Kuderer, Henrik Kretzschmar, Christoph Sprunk, and Wolfram Burgard. Feature-based prediction of trajectories for socially compliant navigation. *Proc. of Robotics: Science and Systems (RSS)*, 2012.

[KP15] Beomjoon Kim and Joelle Pineau. Socially adaptive path planning in human environments using inverse reinforcement learning. *International Journal of Social Robotics*, 8(1):51–66, 2015.

[KPAK13] Thibault Kruse, Amit Kumar Pandey, Rachid Alami, and Alexandra Kirsch. Human-aware robot navigation: A survey. *Robotics and Autonomous Systems*, 61(12):1726–1743, 2013.

[KSF09] Rachel Kirby, Reid Simmons , and Jodi Forlizzi. Companion: A constraint optimizing method for person-acceptable navigation. In *Proc. of IEEE International Symposium on Robot and Human Interactive Communication*, 607–612, 2009.

[KUJ+14] Daphne Karreman, Lex Utama, Michiel Joosse, Manja Lohse, Betsy van Dijk, and Vanessa Evers. Robot etiquette: How to approach a pair of people? *Proc. of the ACM/IEEE International Conference on Human-robot Interaction*, 196–197, 2014.

[KWLV05] J. Kofman, Xianghai Wu, T. J. Luu, and S. Verma. Teleoperation of a robot manipulator using a vision-based human-robot interface. *IEEE Transactions on Industrial Electronics*, 52(5):1206–1219, 2005.

[LBJ+99] Simon P. Levine, David A. Bell, Lincoln A. Jaros, Richard C. Simpson, Yoram Koren, and Johann Borenstein. The navchair assistive wheelchair navigation system. *IEEE Transactions on Rehabilitation Engineering*, 7:443–451, 1999.

[LKK12] T. Li, O. Kermorgant, and A. Krupa. Maintaining visibility constraints during tele-echography with ultrasound visual servoing. *Proc. of IEEE International Conference on Robotics and Automation*, 4856–4861, 2012.

[LO03] Ming Li and A. M. Okamura. Recognition of operator motions for real-time assistance using virtual fixtures. *Proc. of 11th Symposium on Haptics*, 125–131, 2003.

[Luo99] R.C. Luo. Force reflective feedback control for intelligent wheelchairs. In *Proc. of IEEE/RSJ International Conference on Intelligent Robots and Systems*, volume 2, 918–923, 1999.

[LWG+13] R. Li, L. Wei, D. Gu, H. Hu, and K. D. McDonald-Maier. Multi-layered map based navigation and interaction for an intelligent wheelchair. *Proc. of IEEE International Conference on Robotics and Biomimetics* , 115–120, 2013.

[Mar12] Jorge-Rois Martinez. Socially-Aware Robot Navigation: combining Risk Assessment and Social Conventions. *Thesis, University of Grenoble*, 2012.

[MC07] N Mansard and F Chaumette. Task Sequencing for High-Level Sensor-Based Control. *IEEE Transactions on Robotics*, 23(1):60–72, 2007.

[MGBK09] Aniket Murarka, Shilpa Gulati, Patrick Beeson, and Benjamin Kuipers. Towards a safe, low-cost, intelligent wheelchair. *Proc. of IEEE IROS, Workshop on Planning, Perception and Navigation for Intelligent Vehicles (PPNIV)*, 42–50, 2009.

[MMAM06] L. Montesano, J. Minguez, J. M. Alcubierre, and L. Montano. Towards the adaptation of a robotic wheelchair for cognitive disabled children. *Proc. of IEEE/RSJ International Conference on Intelligent Robots and Systems*, 710–716, 2006.

[MRC09] N. Mansard, A. Remazeilles, and F. Chaumette. Continuity of Varying-Feature-Set Control Laws. *IEEE Transactions on Automatic Control*, 54(11):2493–2505, 2009.

[MS95] David P Miller and Marc G Slack. Design and testing of a low-cost robotic wheelchair prototype. *Autonomous robots*, 2(1):77–88, 1995.

[MS12] Marc Mehu and Klaus R. Scherer. A psycho-ethological approach to social signal processing. *Cognitive Processing*, 13(2):397–414, 2012.

[MSC05] E. Marchand, F. Spindler, and François Chaumette. ViSP for visual servoing: a generic software platform with a wide class of robot control skills. *IEEE Robotics and Automation Magazine*, 12(4):40–52, 2005.

[NAS95] NASA. Human performance capabilities, *Technical Report*, 1995.

[NMO+15] Ippei Nishitani, Tetsuya Matsumura, Mayumi Ozawa, Ayanori Yorozu, and Masaki Takahashi. Human-centered space path planning for mobile robot in dynamic environments. *Robotics and Autonomous Systems*, 66:18 – 26, 2015.

[NR00] Andrew Y. Ng and Stuart J. Russell. Algorithms for inverse reinforcement learning. *Proc. of the International Conference on Machine Learning*, 663–670, 2000.

[OTD12] K. Ok, D.-N. Ta, and F. Dellaert. Vistas and wall-floor intersection features - enabling autonomous flight in man-made environments. *Proc. of IEEE IROS Workshop on Visual Control of Mobile Robots*, 2012.

[PBS13] Francois Pasteau, Marie Babel, and Rafiq Sekkal. Corridor following wheelchair by visual servoing. *Proc. of IEEE/RSJ International Conference on Intelligent Robots and Systems*, 590–595, 2013.

[PCJ06] Elena Pacchierotti, Henrik Christensen, and Patric Jensfelt. Design of an Office-Guide Robot for Social Interaction Studies. *Proc. of IEEE/RSJ International Conference on Intelligent Robots and Systems*, 4965–4970, 2006.

[PdV+07] Johan Philips, Jose del R. Millan, Gerolf Vanacker, Eileen Lew, Ferran Galan, Pierre W. Ferrez, Hendrik Van Brussel, and Marnix Nuttin. Adaptive Shared Control of a Brain-Actuated Simulated Wheelchair. *Proc. of IEEE 10th International Conference on Rehabilitation Robotics*, 408–414, 2007.

[pf12] Raspberry pi fundation. Raspberry Pi An ARM GNU/Linux box for $25. Take a byte! *http://www.raspberrypi.org/*, 2012.

[PJO+02] S. Patel, Sang-Hack Jung, J.P. Ostrowski, R. Rao, and C.J. Taylor. Sensor based door navigation for a nonholonomic vehicle. *Proc. of IEEE International Conference on Robotics and Automation*, volume 3, 3081–3086, 2002.

[PKB14] François Pasteau, Alexandre Krupa, and Marie Babel. Vision-based assistance for wheelchair navigation along corridors. *Proc. of IEEE International Conference on Robotics and Automation*, 2014.

[PKay11] Jong Jin Park and B. Kuipers. A smooth control law for graceful motion of differential wheeled mobile robots in 2d environment. *Proc. of IEEE International Conference on Robotics and Automation*,4896–4902, 2011.

[PKNBC15] F. Pasteau, V. Karakkat-Narayanan, M. Babel, and F. Chaumette. A visual servoing approach for autonomous corridor following and doorway passing in a wheelchair. *Robotics and Autonomous Systems*, 2015.

[QCG+09a] Morgan Quigley, Ken Conley, Brian Gerkey, Josh Faust, Tully Foote, Jeremy Leibs, Rob Wheeler, and Andrew Y Ng. Ros: an open-source robot operating system. *Proc. of IEEE ICRA workshop on open source software*, 3(3.2):5, 2009.

[QCG+09b] Morgan Quigley, Ken Conley, Brian P. Gerkey, Josh Faust, Tully Foote, Jeremy Leibs, Rob Wheeler, and Andrew Y. Ng. Ros: an open-source robot operating system. In *ICRA Workshop on Open Source Software*, 2009.

[R. 12] R. Grompone von Gioi, J. Jakubowicz, J.-M. Morel, G. Randall. LSD: a Line Segment Detector. *Image Processing On Line*, 2012.

[RBZ06] Nathan D. Ratliff, J. Andrew Bagnell, and Martin A. Zinkevich. Maximum margin planning. In *Proc. of the 23rd International Conference on Machine Learning*, 729–736, 2006.

[RMSL11] J. Rios-Martinez, A. Spalanzani, and C. Laugier. Understanding human interaction for probabilistic autonomous navigation using Risk-RRT approach. *Proc. of IEEE/RSJ International Conference on Intelligent Robots and Systems*, 2014–2019, 2011.

[RMSL14] Jorge Rios-Martinez, Anne Spalanzani, and Christian Laugier. From Proxemics Theory to Socially-Aware Navigation: A Survey. *International Journal of Social Robotics*, 2014.

[RMSL15] J. Rios-Martinez, A. Spalanzani, and C. Laugier. From proxemics theory to socially-aware navigation: A survey. *International Journal of Social Robotics*, 7(2):137–153, 2015.

[Rot00] C. Rother. A new approach for vanishing point detection in architectural environments. *Proc. of 11th British Machine Vision Conference*, 382–391, 2000.

[SAS+05] E.A. Sisbot, R. Alami, T. Simeon, K. Dautenhahn, M. Walters, and S. Woods. Navigation in the presence of humans. *Proc. of 5th IEEE-RAS International Conference on Humanoid Robots, 2005.*, 181–188, 2005.

[SCAR08] E.A. Sisbot, A. Clodic, R. Alami, and M. Ransan. Supervision and motion planning for a mobile manipulator interacting with humans. In *Proc. of 3rd ACM/IEEE International Conference on Human-Robot Interaction*, 327–334, 2008.

[SCM+06] E. Sisbot, Aurelie Clodic, Luis Marin U., Mathias Fontmarty, Ludovic Brethes, and Rachid Alami. Implementing a Human-Aware Robot System. In *Proc. of 15th IEEE International Symposium on Robot and Human Interactive Communication*, 727–732, 2006.

[SEB91] Claude Samson, Bernard Espiau, and Michel Le Borgne. Robot Control: The Task Function Approach. *Oxford University Press*, 1991.

[Sim04] Richard C Simpson. Smart wheelchairs: A literature review. *Journal of rehabilitation research and development*, 42(4):423–436, 2004.

[SKD10] S. Sehestedt, S. Kodagoda, and G. Dissanayake. Robot path planning in a social context. *Proc. of IEEE Conference on Robotics, Automation and Mechatronics*, 206–211, 2010.

[SKG+09] S. Satake, T. Kanda, D.F. Glas, M. Imai, H. Ishiguro, and N. Hagita. How to approach humans?-strategies for social robots to initiate interaction. *Proc. of 4th ACM/IEEE International Conference on Human-Robot Interaction* , 2009.

[SL97] R.C. Simpson and S.P. Levine. Adaptive shared control of a smart wheelchair operated by voice control. *Proc. of the IEEE/RSJ International Conference on Intelligent Robot and Systems*, volume 2, 622–626, 1997.

[SLD+13] Kyle Wayne Strabala, Min Kyung Lee, Anca Diana Dragan, Jodi Lee Forlizzi, Siddhartha Srinivasa, Maya Cakmak, and Vincenzo Micelli. Towards Seamless Human-Robot Handovers. *Journal of Human-Robot Interaction*, 2(1):112–132, 2013.

[SPB02] Richard C Simpson, Daniel Poirot, and Francie Baxter. The hephaestus smart wheelchair system. *IEEE Transactions on Neural Systems and Rehabilitation Engineering*, 10(2):118–122, 2002.

[SPB+13] Rafik Sekkal, François Pasteau, Marie Babel, Baptiste Brun, and Ivan Leplumey. Simple Monocular door detection and tracking. *Proc. of IEEE Internatioanl Conference on Image Processing*, 2013.

[SSSL16] Procopio Stein, Anne Spalanzani, Vitor Santos, and Christian Laugier. Leader following: A study on classification and selection. *Robotics and Autonomous Systems*, 75, Part A:79 – 95, 2016.

[SSVO08] Bruno Siciliano, Lorenzo Sciavicco, Luigi Villani, and Giuseppe Oriolo. Robotics: Modelling, Planning and Control. *Springer Publishing Company*, 1st edition, 2008.

[SVSL15] P. Salaris, C. Vassallo, P. SouÃ¨res, and J. P. Laumond. The geometry of confocal curves for passing through a door. *IEEE Transactions on Robotics*, 31(5):1180–1193, 2015.

[Tak98] Developing intelligent wheelchairs for the handicapped. *Assistive Technology and Artificial Intelligence, Applications in Robotics, User Interfaces and Natural Language Processing*, 1998.

[TBF05] Sebastian Thrun, Wolfram Burgard, and Dieter Fox. Probabilistic Robotics. *The MIT Press*, 2005.

[TMD08] T. Taha, J.V. Miro, and G. Dissanayake. Pomdp-based long-term user intention prediction for wheelchair navigation. *Proc. of IEEE International Conference on Robotics and Automation*, 3920–3925, 2008.

[Tra15] P. Trautman. Assistive planning in complex, dynamic environments: A probabilistic approach. *Proc. of IEEE International Conference on Systems, Man, and Cybernetics*, 3072–3078, 2015.

[TSR+ne09] J.M. Toibero, C.M. Soria, F. Roberti, R. Carelliz, and P. Fiorini. Switching visual servoing approach for stable corridor navigation. *Proc. of International Conference on Advanced Robotics*, 1–6, 2009.

[VDR+12] E.B. Vander Poorten, E. Demeester, E. Reekmans, J. Philips, A. Huntemann, and J. De Schutter. Powered wheelchair navigation assistance through kinematically correct environmental haptic feedback. *Proc. of IEEE International Conference on Robotics and Automation*, 3706–3712, 2012.

[VSRM+13] Dizan Vasquez, Procópio Stein, Jorge Rios-Martinez, Arturo Escobedo, Anne Spalanzani, and Christian Laugier. Human Aware Navigation for Assistive Robotics. *Springer Tracts in Advanced Robotics*, vol. 88, 2013.

[WDWK07] M.L. Walters, K. Dautenhahn, S.N. Woods, and K.L. Koay. Robotic etiquette: Results from user studies involving a fetch and carry task. *Proc. of 2nd ACM/IEEE International Conference on Human-Robot Interaction* , 317–324, 2007.

[WGLSV00] N. Winters, J. Gaspar, G. Lacey, and J. Santos-Victor. Omni-directional vision for robot navigation. *Proc. of IEEE Workshop on Omnidirectional Vision*, 2000.

[WL14] Huanran Wang and X.P. Liu. Adaptive shared control for a novel mobile assistive robot. *IEEE/ASME Transactions on Mechatronics*, 19(6):1725–1736, 2014.

[YADP05] Wentao Yu, R. Alqasemi, R. Dubey, and N. Pernalete. Telemanipulation assistance based on motion intention recognition. *Proc. of the IEEE International Conference on Robotics and Automation*, 1121–1126, 2005.

[Yan98a] Holly Yanco. Integrating robotic research: A survey of robotic wheelchair development. *AAAI Spring Symposium on Integrating Robotic Research*, 1998.

[Yan98b] Holly A. Yanco. Wheelesley: A robotic wheelchair system: Indoor navigation and user interface. *Springer Berlin Heidelberg: Assistive Robotics issue*, 256–268, 1998.

[YH12] Erkang You and Kris Hauser. Assisted Teleoperation Strategies for Aggressively Controlling a Robot Arm with 2D Input, *Proc. of Robotics: Science and Systems*, 354–361, 2012.

[ZJK07] H. Zender, P. Jensfelt, and G. J. M. Kruijff. Human- and situation-aware people following. *Proc. of 16th IEEE International Symposium on Robot and Human Interactive Communication*, 1131–1136, 2007.

[ZJX+14] Y. Zhou, G. Jiang, G. Xu, X. Wu, and L. Krundel. Kinect depth image based door detection for autonomous indoor navigation. *Proc. of 23rd IEEE International Symposium on Robot and Human Interactive Communication*, 147–152, 2014.

[ZMBD08] Brian D. Ziebart, Andrew Maas, J. Andrew Bagnell, and Anind K. Dey. Maximum entropy inverse reinforcement learning. *Proc. of AAAI Conference on Artificial Intelligence*, 1433–1438, 2008.

List of Figures

Résumé

Les premiers documents attestant l'utilisation d'une chaise à roues utilisée pour transporter une personne avec un handicap datent du 6ème siècle en Chine. À l'exception des fauteuils roulants pliables X-frame inventés en 1933, 1400 ans d'évolution de la science humaine n'ont pas changé radicalement la conception initiale des fauteuils roulants. Pendant ce temps, les progrès de l'informatique et le développement de l'intelligence artificielle depuis le milieu des années 1980 ont conduit inévitablement à la conduite de recherches sur des fauteuils roulants intelligents. Plutôt que de se concentrer sur l'amélioration de la conception sous-jacente, l'objectif principal de faire un fauteuil roulant intelligent est de le rendre le plus accessible. Même si l'invention des fauteuils roulants motorisés ont partiellement atténué la dépendance d'un utilisateur à d'autres personnes pour la réalisation de leurs actes quotidiens, certains handicaps qui affectent les mouvements des membres, le moteur ou la coordination visuelle, rendent impossible l'utilisation d'un fauteuil roulant électrique classique. L'accessibilité peut donc être interprétée comme l'idée d'un fauteuil roulant adaptée à la pathologie de l'utilisateur de telle sorte que il / elle soit capable d'utiliser les outils d'assistance.

S'il est certain que les robots intelligents sont prêts à répondre à un nombre croissant de problèmes dans les industries de services et de santé, il est important de comprendre la façon dont les humains et les utilisateurs interagissent avec des robots afin d'atteindre des objectifs communs. En particulier dans le domaine des fauteuils roulants intelligents d'assistance, la préservation du sentiment d'autonomie de l'utilisateur est nécessaire, dans la mesure où la liberté individuelle est essentielle pour le bien-être physique et social. De façon globale, ce travail vise donc à caractériser l'idée d'une assistance par contrôle partagé, et se concentre tout particulièrement sur deux problématiques relatives au domaine de la robotique d'assistance appliquée au fauteuil roulant intelligent, à savoir une assistance basée sur la vision et la navigation en présence d'humains.

En ciblant les tâches fondamentales qu'un utilisateur de fauteuil roulant peut avoir à exécuter lors d'une navigation en intérieur, une solution d'assistance à bas coût, basée vision, est conçue pour la navigation dans un couloir. Le système fournit une assistance progressive pour les tâches de suivi de couloir et de passage de porte en toute sécurité. L'évaluation du système est réalisée à partir d'un fauteuil roulant électrique de série et robotisé. A partir de la solution plug and play imaginée, une formulation adaptative pour le contrôle partagé entre l'utilisateur et le robot est déduite. De plus, dans la mesure où les fauteuils roulants sont des dispositifs fonctionnels qui opèrent en présence d'humains, il est important de considérer la question des environnements peuplés d'humains pour répondre de façon complète à la problématique de la mobilité en fauteuil roulant. En s'appuyant sur les concepts issus de l'anthropologie, et notamment sur les conventions sociales spatiales, une modélisation de la navigation en fauteuil roulant en présence d'humains est donc proposée. De plus, une stratégie de navigation, qui peut être intégrée sur un robot social (comme un fauteuil roulant intelligent), permet d'aborder un groupe d'humains en interaction de façon équitable et de se joindre à eux de façon socialement acceptable.

Enfin, à partir des enseignements tirés des solutions proposées d'aide à la mobilité en fauteuil roulant, nous pouvons formaliser mathématiquement un contrôle adaptatif partagé pour la planification de mouvement relatif à l'assistance à la navigation. La validation de ce formalisme permet de proposer une structure générale pour les solutions de navigation assistée en fauteuil roulant et en présence d'humains.

Abstract

Earliest records of a wheeled chair used to transport a person with disability dates back to the 6th century in China. With the exception of the collapsible X-frame wheelchairs invented in 1933, 1400 years of human scientific evolution has not radically changed the initial wheelchair design. Meanwhile, advancements in computing and the development of artificial intelligence since the mid-1980s has inevitably led to research on *Intelligent Wheelchairs*.

Rather than focusing on improving the underlying design, the core objective of making a wheelchair intelligent is to make it more *accessible*. Even though the invention of the powered wheelchairs have partially mitigated a user's dependence on other people for their daily routines, some disabilities that affect limb movements, motor or visual coordination, make it impossible for a user to operate a common powered wheelchair. Accessibility can also thus be thought of as the idea, where the wheelchair *adapts* to the user malady such that he/she is able to utilize its assistive capabilities.

While it is certain that intelligent robots are poised to address a growing number of issues in the service and medical care industries, it is important to resolve how humans and users interact with robots in order to accomplish common objectives. Particularly in the assistive intelligent wheelchair domain, preserving a sense of autonomy with the user is required, as individual agency is essential for his/her physical and social well-being. This work thus aims to globally characterize the idea of *assistive* shared control while particularly devoting the attention to two issues within the intelligent assistive wheelchair domain viz. vision-based assistance and human-aware navigation.

Recognizing the fundamental tasks that a wheelchair user may have to execute in indoor environments, we design low-cost vision-based assistance framework for corridor navigation. The framework provides progressive assistance for the tasks of safe corridor following and doorway passing. Evaluation of the framework is carried out on a robotized off-the-shelf wheelchair. From the proposed plug and play design, we infer an adaptive formulation for sharing control between user and robot.

Furthermore, keeping in mind that wheelchairs are assistive devices that operate in human environments, it is important to consider the issue of human-awareness within wheelchair mobility. We leverage spatial social conventions from anthropology to surmise wheelchair navigation in human environments. Moreover, we propose a motion strategy that can be embedded on a social robot (such as an intelligent wheelchair) that allows it to equitably approach and join a group of humans in interaction. Based on the lessons learnt from the proposed designs for wheelchair mobility assistance, we can finally mathematically formalize adaptive shared control for assistive motion planning.

In closing, we demonstrate this formalism in order to design a general framework for assistive wheelchair navigation in human environments.

INSA RENNES

N° d'ordre :

Institut National des Sciences Appliquées de Rennes

20, Avenue des Buttes de Coësmes - CS 14315 - F-35043 Rennes Cedex

Tél : 02 23 23 82 00 – Fax : 02 23 23 83 96